



THE HONG KONG  
POLYTECHNIC UNIVERSITY

香港理工大學

Pao Yue-kong Library  
包玉剛圖書館

---

## Copyright Undertaking

This thesis is protected by copyright, with all rights reserved.

**By reading and using the thesis, the reader understands and agrees to the following terms:**

1. The reader will abide by the rules and legal ordinances governing copyright regarding the use of the thesis.
2. The reader will use the thesis for the purpose of research or private study only and not for distribution or further reproduction or any other purpose.
3. The reader agrees to indemnify and hold the University harmless from and against any loss, damage, cost, liability or expenses arising from copyright infringement or unauthorized usage.

If you have reasons to believe that any materials in this thesis are deemed not suitable to be distributed in this form, or a copyright owner having difficulty with the material being included in our database, please contact [lbsys@polyu.edu.hk](mailto:lbsys@polyu.edu.hk) providing details. The Library will look into your claim and consider taking remedial action upon receipt of the written requests.

**Intermolecular and Intramolecular Ru-H $\cdots$ H-X  
Dihydrogen-Bonding Interaction in Some  
Ruthenium Complexes**

A Thesis submitted to

The Department of Applied Biology and Chemical Technology

for the degree of Master of Philosophy

at

The Hong Kong Polytechnic University

By

**Yat Fai Lam**

November 2001



## **Declaration**

I hereby declare that this thesis summarized my own work carried out since my registration for the Degree of Master of Philosophy in September, 1998; and that has not been previously included in a thesis, dissertation or report submitted to this or any other institution for a degree, diploma or other qualification.

---

Yat-Fai Lam

November, 2001.

## *Acknowledgements*

I would like to express my deepest gratitude to my supervisor Dr. C. P. Lau for his advice and patience throughout the course of my study. His guidance, encouragement and devoted attitude in research in research has made my study a truly rewarding experience. Without his generous guidance and suggestion, this thesis would not be possible.

Thanks are also expressed to my co-supervisor Dr. C. H. Yeung for his valuable discussions and suggestions, Ms. Laura Chan for grammatical corrections for my thesis.

I also want to thank all my postgraduate colleagues in Dr. Lau's group, Mr. C. C. Mak, Mr. M. L. Man, Mr. W. K. Fung, Mr. T. C. Chan and Mr. H. N. Zhang, all of whom have made my study in FG 703 more pleasant. Special thanks are expressed to Mr. C. Q. Yin and Mr. S. M. Ng for their valuable discussions and assistance.

I am obliged to the staff and the technical service crew of the Chemical Technology section of the Department of Applied Biology and Chemical Technology, The Hong Kong Polytechnic University for their assistance throughout my postgraduate study, especially thanks to Mr. Y. K. Au, Mrs. P. S. Chan and Mr. W. K. Kwan and for their assistance in running the MS and NMR spectra respectively.

I would like to thank my family and friends for their love and continual support in various ways, especially thanks to Ms. O. P. Chung for her support, patience and concern.

Finally, I would like to acknowledge the Research Degree Committee of The Hong Kong Polytechnic University for the awarding of a studentship.

Abstract of thesis entitled "Intermolecular and Intramolecular Ru-H...H-X  
Dihydrogen-Bonding Interaction in Some Ruthenium Complexes"

Submitted by Yat-Fai Lam

for the degree of Master of Philosophy

at the Hong Kong Polytechnic University

in November, 2001.

## Abstract

The Tp and Tpm (Tp = hydridotris(pyrazole)borate, Tpm = trispyrazolylmethane) supported ruthenium hydride complexes,  $\text{TpRu}(\text{PPh}_3)_2\text{H}$  (**34**) and  $[\text{TpmRu}(\text{PPh}_3)_2\text{H}](\text{BF}_4)$  (**35**), have been examined for their abilities to form intermolecular hydrogen bonding. Acidic alcohols such as TFE, HFIP and PFTB (TFE = trifluoroethanol, HFIP = hexafluoroisopropyl alcohol and PFTB = perfluoro-*tert*-butyl alcohol) have been chosen to react with the complexes in order to investigate the existence of hydrogen-bonding interaction of the type  $\text{ROH}\cdots\text{H-M}$ . The interaction is monitored by variable-temperature NMR spectroscopy and  $T_1$  measurement of the hydride and  $\eta^2$ -dihydrogen ligands.

My work shows the presence of equilibria between the intermolecular hydrogen-bonded intermediate and  $\eta^2$ -dihydrogen complexes at different temperatures. The  $^1\text{H}$  NMR hydride signal of  $\text{TpRu}(\text{PPh}_3)_2\text{H}$  disappeared as excess HFIP was added at 228K while an upfield broad signal assignable to a  $\eta^2$ - $\text{H}_2$  ligand was observed. After the temperature was raised to 263K, an upfield signal assignable to the hydrogen-bonded intermediate became observable and its intensity increased with increase in temperature. This phenomenon is in line with other complexes containing dihydrogen bonds which show enhanced  $\text{M-H}\cdots\text{H-X}$  interaction as the temperature is lowered. Since the acidity of the acidic alcohol increase from TFE, HFIP, PFTB; equilibria between the hydrogen bonded intermediate and the dihydrogen complex is observed with the addition of HFIP to **34** in variable temperature NMR (VT-NMR) spectroscopy. There are no interaction detected for **35** with any acidic alcohol in the  $^1\text{H}$  NMR spectra.

The second part of my research concerns the chemistry of intramolecular hydrogen bonding between the pendent amino group and the hydride ligand in the aminocyclopentadienyl ruthenium complexes, and studies of their reactivities. The starting aminocyclopentadienyl ruthenium phosphite complex  $\text{CpNRu}[\text{P}(\text{OPh})_3]_2\text{Cl}$  (**40**) ( $\text{CpN} = [2\text{-}(\text{N,N}\text{-dimethylamino})\text{ethyl}]\text{cyclopentadienyl}$ ) was obtained by reflux of  $\text{CpNRu}(\text{PPh}_3)_2\text{Cl}$  with triphenylphosphite in toluene solution.

The ortho-metalated complexes  $[\text{CpNRu}(\text{P}(\text{OPh})_3)(\text{P}(\text{OC}_6\text{H}_4)(\text{OPh})_2)]$  (**41**) was prepared by reactions of **40** with excess silver triflate in THF solution and followed by column chromatography using neutral alumina. Acidification of **41** with  $\text{HBF}_4 \cdot \text{Et}_2\text{O}$  yielded the protonated ortho-metalated complex  $[\text{CpNH}^+\text{Ru}(\text{P}(\text{OPh})_3)(\text{P}(\text{OC}_6\text{H}_4)(\text{OPh})_2)]$  (**42**). Application of 25 bar of hydrogen pressure to **41** and **42** in chlorobenzene yielded different results. Complex **42** gave the corresponding hydride complex  $[\text{CpNH}^+\text{Ru}((\text{P}(\text{OPh})_3))_2\text{H}]$  (**43**) but no reaction for **41** was observed even with prolonged heating at elevated temperature. The complex  $\text{CpNRu}(\text{P}(\text{OPh})_3)_2\text{H}$  (**44**) was prepared by reacting **43** with KOH in ethanol solution. However, 2D-NOESY experiments show that there is no hydride-proton interaction between the Ru-H and N-H<sup>+</sup> moieties in **43**.

The catalytic activity of the CpN complex **43**, toward hydrogenation of carbon dioxide was also studied. It was found that, although similar in structure to previously reported dppm analogue  $[\text{CpNH}^+\text{Ru}(\text{dppm})\text{H}](\text{BF}_4)$  which catalyzes  $\text{CO}_2$  hydrogenation albeit in low rate, **43** showed no catalytic activity. We attribute the lack of activity of **43** to decreased hydricity of the hydride ligand in the complex due to the presence of the low donating phosphite ligand.



# Table of Contents

Abstract	i
Table of Content	iii
List of Figures	v
List of Schemes	vii
Abbreviations	viii
Chapter One	
Introduction	1
1.1 Review of hydrogen bonding in organometallic compounds	1
1.1.1 Hydrogen bonding to transition metals atoms - the XH...M type	4
1.1.1.1 Intermolecular hydrogen bonding	4
1.1.1.2 Intramolecular hydrogen bonding	5
1.1.2 Hydrogen bond of the [ML]...HX type	6
1.1.3 Hydrogen bonding of the MH...HX type	8
1.1.3.1 Intermolecular hydrogen bonding	8
1.1.3.2 Intramolecular hydrogen bonding	11
1.2 Introduction of cyclopentadienyl complexes containing amino side-arms	15
Chapter Two	
Intermolecular M-H...H-OR hydrogen bonding of ruthenium hydride complexes with acidic alcohols	24
2.1 Introduction	24
2.2 Experimental	25
2.2.1 Materials and instrumentation	25
2.2.2 General procedure of reaction of a ruthenium hydride with an acidic alcohol	26
2.3 Results and Discussion	27
2.3.1 Reaction of TpRu(PPh <sub>3</sub> ) <sub>2</sub> H with trifluoroethanol (TFE)	27
2.3.2 Reaction of TpRu(PPh <sub>3</sub> ) <sub>2</sub> H with hexafluoroisopropanol (HFIP)	28
2.3.3 Reaction of TpRu(PPh <sub>3</sub> ) <sub>2</sub> H with perfluoro- <i>tert</i> -butanol (PFTB)	33
2.3.4 Reaction of [TpmRu(PPh <sub>3</sub> ) <sub>2</sub> H](BF <sub>4</sub> ) towards hexafluoroisopropanol (HFIP)	35
2.3.5 Reaction of [TpmRu(PPh <sub>3</sub> ) <sub>2</sub> H](BF <sub>4</sub> ) towards perfluoro- <i>tert</i> -butanol (PFTB)	37
Chapter Three	
Synthesis, characterization and study on the intramolecular hydrogen bonding of tethered cyclopentadienyl ruthenium complexes	39
3.1 Introduction	39

3.2 Experimental	40
3.2.1 Materials and instrumentation	40
3.2.2 Synthesis and characterization	41
3.2.2.1 $(\eta^5\text{-C}_5\text{H}_4(\text{CH}_2)_2\text{NMe}_2)\text{Ru}(\text{P}(\text{OPh})_3)_2\text{Cl}$ (40)	41
3.2.2.2 $(\eta^5\text{-C}_5\text{H}_4(\text{CH}_2)_2\text{NMe}_2)\text{Ru}(\text{P}(\text{OPh})_3)(\text{P}(\text{OPh})_2\text{OC}_6\text{H}_4)$ (41)	42
3.2.2.3 $[(\eta^5\text{-C}_5\text{H}_4(\text{CH}_2)_2\text{NMe}_2\text{H}^+)\text{Ru}(\text{P}(\text{OPh})_3)-$ $(\text{P}(\text{OPh})_2\text{OC}_6\text{H}_4)](\text{BF}_4)$ (42)	43
3.2.2.4 $[(\eta^5\text{-C}_5\text{H}_4(\text{CH}_2)_2\text{NMe}_2\text{H}^+)\text{Ru}(\text{P}(\text{OPh})_3)_2\text{H}](\text{BF}_4)$ (43)	43
3.2.2.5 $(\eta^5\text{-C}_5\text{H}_4(\text{CH}_2)_2\text{NMe}_2)\text{Ru}(\text{P}(\text{OPh})_3)_2\text{H}$ (44)	44
3.3 Results and Discussion	45
3.3.1 Synthesis and characterization of ortho-metalated amino- cyclopentadienyl ruthenium complexes	45
3.3.2 Synthesis and characterization of hydrido amino-cyclopentadienyl ruthenium complexes	49
3.3.3 Reactivities of $[(\eta^5\text{-C}_5\text{H}_4(\text{CH}_2)_2\text{NMe}_2\text{H})\text{Ru}(\text{P}(\text{OPh})_3)_2\text{H}]^+$ towards $\text{H}_2/\text{CO}_2$	53
Chapter Four	
Conclusion	55
Reference	58
Appendix	72
Publication	85

## List of figures

Figure 1.1	Different modes of hydrogen bonding	3
Figure 1.2	The first dihydrogen complexes discovered by Kubas <i>et al.</i> [W( $\eta^2$ -H <sub>2</sub> )(CO) <sub>3</sub> (P- <i>i</i> -Pr <sub>3</sub> ) <sub>2</sub> ].	3
Figure 1.3	XH $\cdots$ M type hydrogen bonding	4
Figure 1.4	Intramolecular hydrogen bonded carbinols complexes studied by Epstein and co-workers	6
Figure 1.5	Metal complexes having ML $\cdots$ HX type hydrogen bond	7
Figure 1.6	The detailed structure of the NH $\cdots$ H <sub>2</sub> Re in [ReH <sub>5</sub> (PPh <sub>3</sub> ) <sub>3</sub> ] $\cdot$ C <sub>8</sub> H <sub>6</sub> NH $\cdot$ C <sub>6</sub> H <sub>6</sub>	10
Figure 1.7	Proton-hydride interaction in [K(1,10-diaza-18-crown-6)][RuH <sub>5</sub> (P <sup><i>i</i></sup> Pr <sub>3</sub> ) <sub>2</sub> ]	11
Figure 1.8	Linear and bifurcated MH $\cdots$ HX type hydrogen bonds	13
Figure 1.9	Relationship of intermolecular and intramolecular coordination affected by ring strain and solubility	15
Figure 1.10	Hemilabile behavior of the side-chain donor complexes	16
Figure 1.11	Representative selection of dialkylaminoalkyl-substituted Cp complexes	18
Figure 2.1	Variable temperature <sup>1</sup> H NMR spectra (upfield region) of TpRu(PPh <sub>3</sub> ) <sub>2</sub> H + HFIP in CD <sub>2</sub> Cl <sub>2</sub>	30
Figure 2.2	Various temperature <sup>31</sup> P NMR spectrum of TpRu(PPh <sub>3</sub> ) <sub>2</sub> H react with excess HFIP in CD <sub>2</sub> Cl <sub>2</sub>	33
Figure 3.1	400 MHz <sup>1</sup> H NMR spectrum of CpNRu[P(OPh) <sub>3</sub> ] <sub>2</sub> Cl ( <b>40</b> )	71
Figure 3.2	161.7 MHz <sup>31</sup> P { <sup>1</sup> H} NMR spectrum of CpNRu[P(OPh) <sub>3</sub> ] <sub>2</sub> Cl ( <b>40</b> )	72
Figure 3.3	400 MHz <sup>1</sup> H NMR spectrum of CpNRu[P(OPh) <sub>3</sub> ][(OPh) <sub>2</sub> P(OC <sub>6</sub> H <sub>4</sub> )] ( <b>41</b> )	73
Figure 3.4	161.7 MHz <sup>31</sup> P { <sup>1</sup> H} NMR spectrum of CpNRu[P(OPh) <sub>3</sub> ][(OPh) <sub>2</sub> P(OC <sub>6</sub> H <sub>4</sub> )] ( <b>41</b> )	74
Figure 3.5	100.6 MHz <sup>13</sup> C { <sup>1</sup> H} NMR spectrum of CpNRu[P(OPh) <sub>3</sub> ][(OPh) <sub>2</sub> P(OC <sub>6</sub> H <sub>4</sub> )] ( <b>41</b> )	75

Figure 3.6	400 MHz $^1\text{H}$ NMR spectrum of $\{\text{CpNH}^+\text{Ru}[\text{P}(\text{OPh})_3][(\text{OPh})_2\text{P}(\text{OC}_6\text{H}_4)]\}(\text{BF}_4)$ ( <b>42</b> )	76
Figure 3.7	161.7 MHz $^{31}\text{P}\{^1\text{H}\}$ NMR spectrum of $\{\text{CpNH}^+\text{Ru}[\text{P}(\text{OPh})_3][(\text{OPh})_2\text{P}(\text{OC}_6\text{H}_4)]\}(\text{BF}_4)$ ( <b>42</b> )	77
Figure 3.8	100.6 MHz $^{13}\text{C}\{^1\text{H}\}$ NMR spectrum of $\{\text{CpNH}^+\text{Ru}[\text{P}(\text{OPh})_3][(\text{OPh})_2\text{P}(\text{OC}_6\text{H}_4)]\}(\text{BF}_4)$ ( <b>42</b> )	78
Figure 3.9	400 MHz $^1\text{H}$ NMR spectrum of $\{\text{CpNH}^+\text{Ru}[\text{P}(\text{OPh})_3]_2\text{H}\}(\text{BF}_4)$ ( <b>43</b> )	79
Figure 3.10	161.7 MHz $^{31}\text{P}\{^1\text{H}\}$ NMR spectrum of $\{\text{CpNH}^+\text{Ru}[\text{P}(\text{OPh})_3]_2\text{H}\}(\text{BF}_4)$ ( <b>43</b> )	80
Figure 3.11	400 MHz $^1\text{H}$ NMR spectrum of $\text{CpNRu}[\text{P}(\text{OPh})_3]_2\text{H}$ ( <b>44</b> )	81
Figure 3.12	161.7 MHz $^{31}\text{P}\{^1\text{H}\}$ NMR spectrum of $\text{CpNRu}[\text{P}(\text{OPh})_3]_2\text{H}$ ( <b>44</b> )	82

## List of Schemes

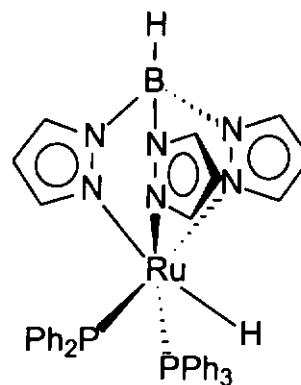
Scheme 1.1	Proposed mechanism for the formation of the spiro-metalloocene	20
Scheme 1.2	Proposed mechanism of hydrogenation of CO <sub>2</sub> to formic acid by $[(\eta^5:\eta^1\text{-C}_5\text{H}_4(\text{CH}_2)_2\text{NMe}_2)\text{Ru}(\text{dppm})](\text{BF}_4)$	22
Scheme 3.1	Proposed mechanism of the reactivity of $[(\eta^5:\eta^1\text{-C}_5\text{H}_4(\text{CH}_2)_2\text{N}(\text{Me}_2))\text{Ru}[\text{P}(\text{OPh})_3]_2]$ towards H <sub>2</sub>	45
Scheme 3.2	Reaction pathways for the preparation of ortho-metalated aminocyclopentadienyl ruthenium complexes	48
Scheme 3.3	Proposed mechanism for the rapid and reversible hydride proton exchange via $\eta^2$ -tautomer in $[(\eta^5:\eta^1\text{-C}_5\text{H}_4(\text{CH}_2)_2\text{NMe}_2)\text{Ru}(\text{dppm})]^+$	50
Scheme 3.4	Proposed reaction pathway of the deuterium labeling experiment	53
Scheme 3.5	Proposed mechanism for the hydrogenation of carbon dioxide by $[(\eta^5:\eta^1\text{-C}_5\text{H}_4(\text{CH}_2)_2\text{NMe}_2)\text{Ru}(\text{dppm})]^+$	54

## Abbreviations

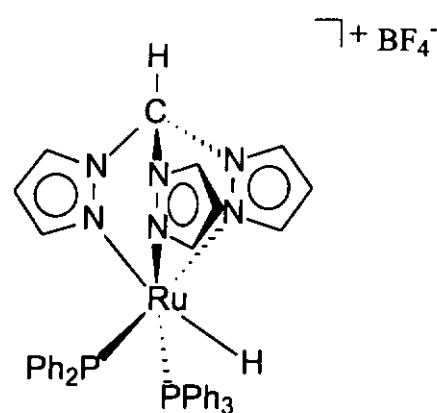
$\delta$ :	Chemical shift (NMR)
$\eta$ :	Descriptor for hapticity
L :	Generalized ligand, in particular a 2e ligand
$L_nM$ :	Generalized metal fragment with n ligands
Tp :	Hydrotris(1-pyrazolyl)borate
Tpm :	Hydrotris(1-pyrazolyl)methane
Cp :	Cyclopentadienyl
CpN :	(2-(Dimethylamino)ethyl)cyclopentadienyl
PPh <sub>3</sub> :	Triphenylphosphine
P(OPh) <sub>3</sub> :	Triphenylphosphite
OTf :	Trifluoromethane sulfonate
BF <sub>4</sub> :	Tetrafluoroborate
Me :	Methyl
EtOH :	Ethanol
Et <sub>2</sub> O :	Diethyl ether
THF :	Tetrahydrofuran
TFE :	Trifluoroethanol
HFIP :	Hexafluoroisopropanol
PFTB :	Perfluoro- <i>tert</i> -butanol

NMR :	Nuclear magnetic resonance spectroscopy
VT-NMR :	Variable temperature nuclear magnetic resonance spectroscopy
TMS :	Tetramethylsilane
br :	Broad
s:	Singlet
d :	Doublet
t :	Triplet
m :	Multiplet

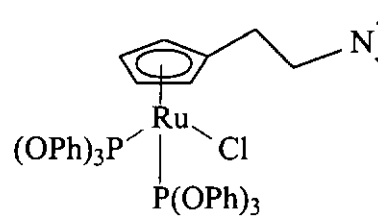
(34) :  $\text{TpRu}(\text{PPh}_3)_2\text{H}$



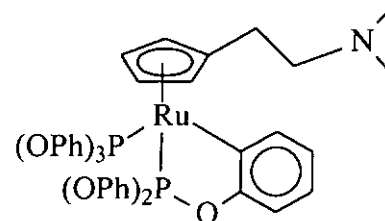
(35) :  $[\text{TpmRu}(\text{PPh}_3)_2\text{H}](\text{BF}_4)$



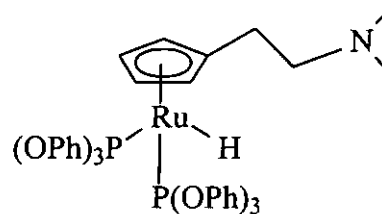
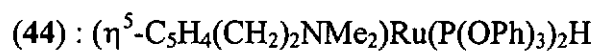
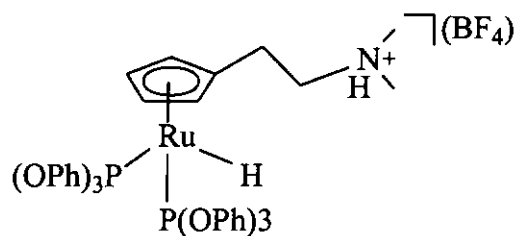
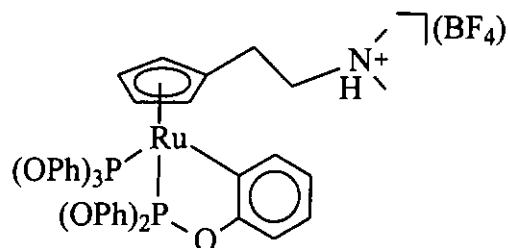
(40) :  $(\eta^5\text{-C}_5\text{H}_4(\text{CH}_2)_2\text{NMe}_2)\text{Ru}(\text{P}(\text{OPh})_3)_2\text{Cl}$



(41) :  $(\eta^5\text{-C}_5\text{H}_4(\text{CH}_2)_2\text{NMe}_2)\text{Ru}(\text{P}(\text{OPh})_3)(\text{P}(\text{OPh})_2\text{OC}_6\text{H}_4)$







# **1. Introduction**

## **1.1 Review of hydrogen bonding in organometallic compounds**

Proton transfer reactions proceeding through hydrogen bonding are widespread and fundamental in chemistry and biochemistry [1]. The modern concepts of the nature and the structural and spectral manifestations of hydrogen bonds were formed on the basis of the large data on the interaction between organic acids and bases. Tremendous success was achieved in determining the structure of intra- and intermolecular hydrogen bonds, the energetics of ion-molecular hydrogen bonded complex formation in the gas phase, as well as in the determination of correlations between hydrogen bond characteristics and acid-basic properties [2].

In recent years, much attention has been paid to the investigation of hydrogen bonding with transition metal complexes or hydrides and its participation in proton transfer reactions. It is therefore extremely important to find out whether the numerous catalytic processes involving transition metal complexes can proceed through intermediate hydrogen-bonded complexes to explicate the reaction mechanism. Hydrogen bonds with different ligands have been examined extensively. For example, hydrogen bonds with  $\pi$ -ligands have been investigated since the 1970s. The large series of works by Lokshin and co-workers concerned the study of the interaction of fluorinated alcohols [3] and HCl with carbonyl and nitrosyl containing half-sandwich transition metal  $\pi$ -complexes was continued by Poliakoff and co-workers. These low temperature IR investigations in

liquid xenon solution enabled the detection and study of previously unknown hydrogen bonding with the oxygen atom of terminal CO- and NO- groups. Fairly strong H-bonds of proton donors with alkoxy and phenoxy ligands were studied in solutions and in the solid state. The nature of hydrogen bonds with the oxygen atom of terminal CO- and NO- groups is similar to the hydrogen bonds typical of organic bases, since lone pairs of sp-electrons of heteratoms or p-electrons of unsaturated and aromatic fragments are acting as proton acceptors [4]. Braga and co-workers, concluded that hydrogen bonded in organometallic complexes through the oxygen atom of terminal carbonyl group with proton donors have structural properties that are similar to those of related organic solids after an analysis of the structural data in the Cambridge database [5, 6].

Recently, new types of hydrogen bonds which are characteristic only of organometallic compounds were found and investigated. (Figure 1.1) These are hydrogen bonding to transition metal atoms ( $XH \cdots M$ ) (1). In contrast to organic bases, in this case d-electrons are proton acceptors. In ( $ML \cdots HX$ ) (2), the ligand of the metal complexes, which act as the proton acceptor, is the bonding site. Another surprise presented by organometallic chemistry in recent years is hydrogen bonds formed with transition metal hydrides. The particular characteristic of transition metal hydrides is their dual reactivity, i.e. they can be the source of both protons and hydride ions. Two extreme cases of hydride ligand participation in hydrogen bonding were found: acting as a proton donor ( $[MH]^+ \cdots B$ ) (3), in the case of cationic hydrides, and as an acceptor of protons ( $MH \cdots HX$ ) (4). Since hydrogen has no lone pair, the hydrogen bond in 4, is exceptional. Moreover, these new

types of hydrogen bonds are in a head-on manner, not the side-on manner of agostic interactions.

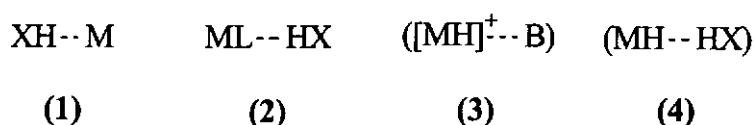


**Figure 1.1 Different modes of hydrogen bonding.**

Since the discovery of the first dihydrogen complex by Kubas in 1984 [7] (Figure 1.2), great effort has been put into investigating the chemical, structural, thermodynamics, kinetics, acidity, and computational studies as well as characterization of this type of complexes. Dihydrogen complexes are important intermediates in a number of hydrogenation processes. This type of complexes have been extensively investigated by Kubas [8], Heinekey [9], Morris [10], Crabtree's [11] and other research groups including ours.

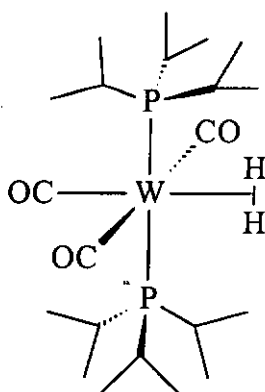


**Figure 1.2 The first dihydrogen complexes discovered by Kubas *et al.*.  $[\text{W}(\eta^2\text{-H}_2)(\text{CO})_3(\text{P-}i\text{-Pr}_3)_2]$ .**

## 1.1.1 Hydrogen bonding to transition metals atoms - the $\text{XH}\cdots\text{M}$ type

### 1.1.1.1 Intermolecular hydrogen bonding

Formation of the  $\text{XH}\cdots\text{M}$  hydrogen bonding has frequently been postulated as a key-step in reaction pathways in organometallic chemistry. This type of hydrogen bonding has been observed by Calderazzo *et al.* [12] and Brammer and co-workers in crystal structures [13-15].

Calderazzo *et al.* found that reaction of trialkylamines and  $\text{HCo}(\text{CO})_4$  forms 1:1 adducts, intermolecular hydrogen bonding was observed between the protonated amine and the cobalt metal [12] (Fig 1.3a). Recently, many examples of complexes having this type of hydrogen bond have been found. Poliakoff *et al.* found spectroscopic evidence for  $\text{O-H}\cdots\text{Ir}$  bonding between cyclopentadienyl complexes  $(\eta^5\text{-C}_5\text{R}_5)\text{ML}_2$  and fluoroalcohols in solution at room temperature by infrared spectroscopy [16] (Fig 1.3b).

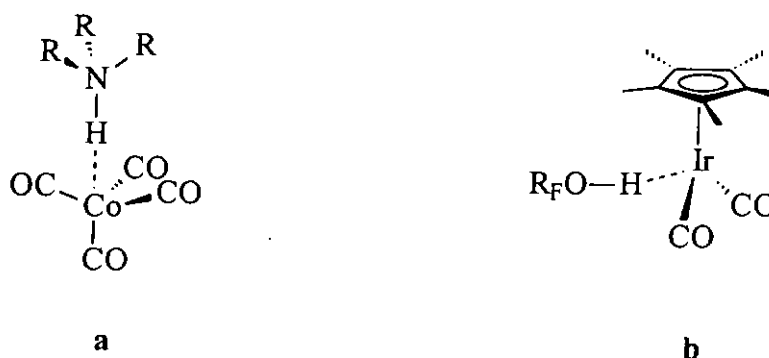
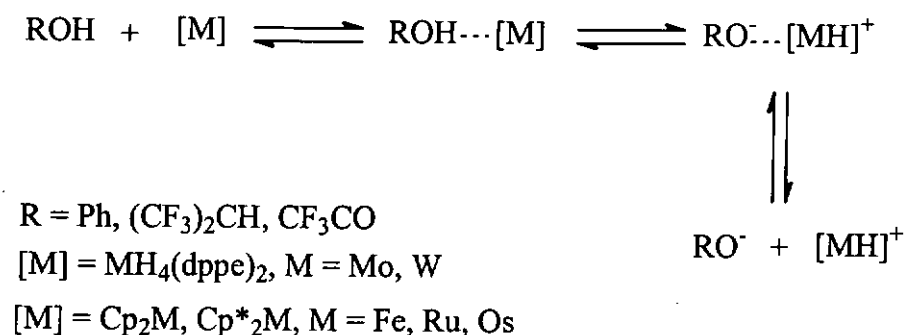


Figure 1.3  $\text{XH}\cdots\text{M}$  type hydrogen bonding

Epstein's group found that the intermolecular hydrogen-bonding initially formed by interaction of metallocenes and metal polyhydrides  $MH_4(dppe)_2$  with proton donors is the first stage of protonation. An ionic hydrogen bonded complex of the type  $MH^+ \cdots O^-$  was formed as a result of proton transfer [17],[18]. The following equilibrium involving the first type hydrogen bond after proton transfer appears for all compounds investigated by Epstein's group.



Eq. 1.1

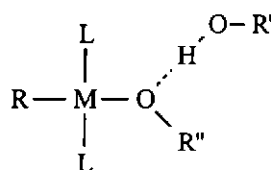
### 1.1.1.2 Intramolecular hydrogen bonding

Intramolecular hydrogen bonding of the  $XH \cdots M$  type has been observed since the 1970's. In 1986, Roundhill *et al.* found an intramolecular hydrogen bond between an amido N-H and a platinum center with a bond length in crystal structure of 2.318(22) Å. The Pt-H bond was not observed in  $^1H$  NMR spectroscopy due to chemical shift anisotropy broadening [19].



existed between the metal and the oxygen atom in the rhodium complex  $(\text{PMe}_3)_3\text{Rh-OR}$  and ROH [21]. The hydrogen bond is rather strong ( $\Delta H = -9.7 \pm 0.5$  kcal/mol in benzene).

Similar hydrogen-bonding was found to be present in *trans*- $\text{PdR}_2\text{L}_2$  ( $\text{R} = \text{CH}_3, \text{C}_2\text{H}_5$ ;  $\text{L} = \text{PMe}_3, \text{PEt}_3$ ) and *trans*- $\text{NiR}_2\text{L}_2$  complexes by IR, NMR spectroscopy and X-ray diffraction study. The distance between the oxygen atom of the associated alcohol or phenol and the phenoxide ligand were in the range of 2.59-2.61 Å. The OH hydrogen atoms were located in difference Fourier maps at distances of 1.61-1.62 Å from the oxygen atom of the phenoxide ligand and at distances of 1.00-1.01 Å from that of the associated phenol and alcohol. The O-H...O angles in these complexes were in the range of 165-170°, indicating that the hydrogen is close to the line connecting the two oxygen atoms [22] (Figure 1.5). Van Koten and co-workers also detected this type of hydrogen bonding between platinum, palladium phenoxide and associated phenol [23].



1.  $\text{M} = \text{Ni}$ ;  $\text{R} = \text{Me}$ ,  $\text{R}' = \text{R}'' = \text{Ph}$ ,  $\text{L} = \text{PMe}_3$
2.  $\text{M} = \text{Pd}$ ;  $\text{R} = \text{Me}$ ,  $\text{R}' = \text{R}'' = \text{Ph}$ ,  $\text{L} = \text{PMe}_3$
3.  $\text{M} = \text{Pd}$ ,  $\text{R} = \text{Ph}$ ,  $\text{R}'' = \text{CH}(\text{CF}_3)\text{Ph}$ ,  $\text{L} = \text{PMe}_3$

**Figure 1.5 Metal complexes having  $\text{ML}\cdots\text{HX}$  type hydrogen bond.**

Hydrogen bond between the bridged carbon monoxide in  $[\text{CpRu}(\text{CO})_2]_2$  and perfluorinated alcohol have been observed by Lokshin and co-workers in liquid Xe



solution [3]. Poliakoff *et al.* also investigated the hydrogen bonding in permethylated cyclopentadienyl metal carbonyls with perfluoro-*tert*-butyl alcohol (PFTB) in liquid xenon and found evidence for its existence between the metal carbonyl and the perfluorinated alcohol [4]. It is however, different from the hydrogen-bonding interactions in the solid phase.

Epstein, Caulton and co-workers had carried out theoretical calculation for the hydrogen-bond that existed between an acidic alcohol and the chloride ligand of the osmium complex  $\text{OsHCl}(\text{CO})(\text{PtBu}_2\text{Me})_2$ . The steric hindrance of the bulky ligands prevented the hydroxy group from approaching either the hydride or the metal ion and favoured its approach to the chloride [24].

### 1.1.3 Hydrogen bonding of the $\text{MH}\cdots\text{HX}$ type

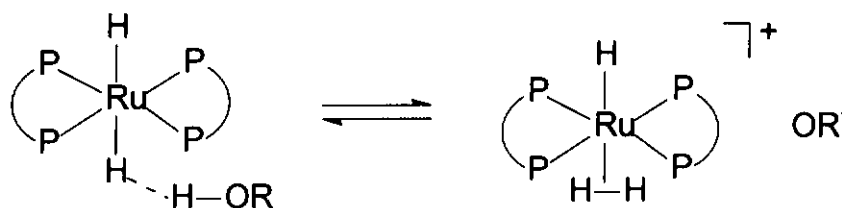
#### 1.1.3.1 Intermolecular hydrogen bonding

Epstein and Berke reported spectroscopic evidence for intermolecular hydrogen-bonding of the type  $\text{M-H}\cdots\text{H-OR}$  in a series of tungsten hydride complexes in acidic alcohol solutions. The tungsten hydride complex,  $\text{WH}(\text{CO})_2(\text{NO})\text{L}_2$  ( $\text{L} = \text{PMe}_3, \text{PEt}_3, \text{P}(\text{O}^i\text{Pr})_3, \text{PPh}_3$ ) was used as the proton acceptor, while acidic alcohols  $\text{PhOH}$ ,  $(\text{CF}_3)_2\text{CHOH}$  (HFIP), and  $(\text{CF}_3)_3\text{COH}$  (PFTB) function as the proton donors. Hydrogen bonds formed between the acidic alcohol and the metal hydride in hexane, toluene- $d_8$ , and  $\text{CD}_2\text{Cl}_2$

solutions [25]. Similar hydrogen-bonding interaction was found in rhenium hydrides  $\text{ReH}_2(\text{CO})_2(\text{NO})\text{L}_2$  ( $\text{L} = \text{PMe}_3, \text{PEt}_3, \text{P}(\text{O}^i\text{Pr})_3$ ) within acidic alcohols but the interaction is weaker than those in the tungsten complexes[26].

Recently, Berke, Epstein and co-workers have found that other than the hydrides in  $\text{ReH}_2(\text{CO})_2(\text{NO})\text{L}_2$  and  $\text{ReHCl}(\text{CO})(\text{NO})(\text{PMe}_3)_2$  ( $\text{L} = \text{PMe}_3, \text{PEt}_3, \text{P}(\text{O}^i\text{Pr})_3$ ), ligands such as NO, CO, Cl are also potential hydrogen-bonding sites [27, 28]. Very recently, the same group has also discovered M-H $\cdots$ H-OR type of hydrogen bond in complexes with facial ligands. Evidence from in situ IR and low temperature variable-temperature NMR spectroscopies show that interaction of the hydride ligand with various proton donors is the first step of the protonation reaction [29-31].

Chaudret *et al.* have conducted similar experiments by adding the metal hydride  $\text{Ru}(\text{dppm})_2\text{H}_2$  to acidic alcohols. They found that a dynamic equilibrium was established between the hydrogen-bonded species and a  $\eta^2$ -dihydrogen complex [32] (Eq. 1.2). The same group carried out experiments to measure quantum mechanical exchange couplings, which provide evidence for the formation of hydrogen bonds between the hydride and different proton donors by adding different proton donors to  $\text{Cp}^*\text{RuH}_3(\text{PCy}_3)$  in deuterated toluene [33]. Recently, protonations of  $\text{Cp}^*\text{RuH}_3(\text{PCy}_3)$  with different acidic alcohols in freon mixture  $\text{CDCl}_2\text{F}/\text{CDF}_3$  (2:1) have been carried out. The novel cationic complex  $[\text{Cp}^*\text{RuH}_4(\text{PCy}_3)]^+[\text{A}\cdots\text{H}\cdots\text{A}]^-$  had been observed at low temperatures as the intermediate species, but it was too unstable to be isolated at room temperature [34].



Eq. 1.2

Crabtree *et al.* detected the presence of three-centered hydrogen-bond between indole and metal polyhydrides ( $[\text{ReH}_5(\text{PPh}_3)_3]$ ,  $[\text{ReH}_7(\text{dppe})]$ , and  $[\text{WH}_4(\text{PMePh}_2)_4]$ ) in solid crystalline structures and solid films. They found that the bond angles of the  $\text{ReH}_2\cdots\text{HN}$  ( $97.2(3)$  and  $118.9(4)$ ) are strongly bent (Fig. 1.6). Therefore, it was suggested that the hydrogen-bonding is in a side-on manner [35], not the usual linear  $\text{A-H}\cdots\text{B}$  type [36, 37]. Very recently, it was discovered that hydrogen-bond exists between the N-H of imidazole and a hydride ligand of  $\text{ReH}_7(\text{PPh}_3)_2$  [38].

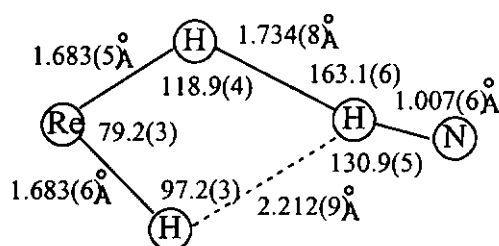
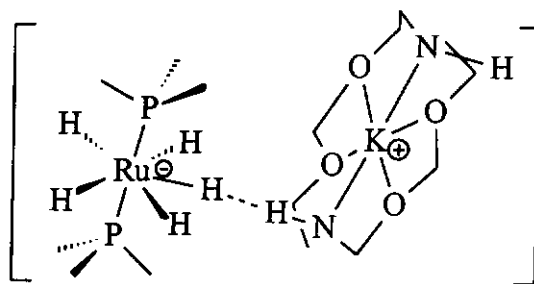


Figure 1.6 The detailed structure of the  $\text{NH}\cdots\text{H}_2\text{Re}$  in  $[\text{ReH}_5(\text{PPh}_3)_3]\cdot\text{C}_8\text{H}_6\text{NH}\cdot\text{C}_6\text{H}_6$ .

Morris and co-workers have identified intermolecular hydride-proton interaction in metal polyhydrides and crown ether as ion pairs:  $[\text{K}(\text{Q})][\text{MH}_5(\text{P}^i\text{Pr}_3)_2]$  ( $\text{M} = \text{Os}, \text{Ru}$ ;  $\text{Q} = 18\text{-crown-6}, 1\text{-aza-18-crown-6}, 1,10\text{-diaz-18-crown-6}$ ). Intermolecular proton-hydride interactions between the hydrides of the anions and the NH moieties of the cation (Fig. 1.7) cause the self assembly of one-dimensional networks of pentagonal

bipyramidal  $[\text{MH}_5(\text{P}^i\text{Pr}_3)_2]^-$  anions and  $[\text{K}(\text{diaza-18-crown-6})]^+$  cations. For complexes containing cation with one aza-group, one-dimensional chains formed with hydrogen-bonding interactions presented in  $\text{MH}\cdots\text{HN}$  and weak  $\text{MH}\cdots\text{HC}$  manner [39].



**Figure 1.7 Proton-hydride interaction in  $[\text{K}(\text{1,10-diaza-18-crown-6})][\text{RuH}_5(\text{P}^i\text{Pr}_3)_2]$**

Lau *et al.* found interesting results when acidifying  $[\text{tpmRu}(\text{PPh}_3)_2\text{H}]\text{BF}_4$  with excess aqueous  $\text{HBF}_4$  or aqueous triflic acid in  $\text{THF-d}_8$ . Variable temperature  $^1\text{H}$ - and  $^{31}\text{P}$ -NMR studies revealed that the aqueous acid did not fully protonate the metal hydride to form the dihydrogen complex, but a hydrogen bonded species was formed. The special feature of this species is that the strength of its  $\text{Ru-H}\cdots\text{H}-(\text{H}_2\text{O})_m$  interaction decreases with temperature; this phenomenon is unusual because other complexes containing dihydrogen bonds usually show enhanced  $\text{M-H}\cdots\text{H-X}$  interaction as the temperature is lowered. Decrease of the dihydrogen-bond strength with temperature in the present case can be attributed to the decline of acidity that results from the formation of larger  $\text{H}^+(\text{H}_2\text{O})_n$  ( $n > m$ ) clusters at lower temperature; steric hindrance of these large clusters also contributes to the weakening of the dihydrogen bonding interactions [40].

### 1.1.3.2 Intramolecular hydrogen bonding

In 1990, an early example of weak intramolecular M-H...XH interaction was confirmed in  $[\text{IrH}(\text{OH})(\text{PMe}_3)_4]^+$  [41]. The hydroxy ligand is having a bent conformation close to the metal hydride. The comparatively small bond angle of Ir-O-H ( $104.4^\circ$ ) indicates an attractive interaction between the hydridic Ir-H and the electron-deficient OH proton, in effect an  $\text{H}(\delta^+)\cdots\text{H}(\delta^-)$  interaction.

Crabtree's group described intramolecular hydrogen-bonding in transition metal hydrides with a pendant side-arm ligands [42]. A series of iridium complexes containing pendant amino ligands were synthesized and crystallographic data suggested that hydrogen bonding existed between hydride ligands and the pendant amino and aldehyde groups [43, 44] [45] (Chart 1.1). Core potential ab initio studies were carried out for  $\text{IrH}_2\text{Y}(\text{pyNH}_2)(\text{PPh}_3)_2$  and it was found that the N-H...H-Ir hydrogen bond strength is in the range of 5.7-7.1 kcal/mol, assuming that the intrinsic C-N rotation barrier is the same in free and coordinated 2- $\text{C}_5\text{H}_4\text{NH}_2$ . Factors causing such strong hydrogen bonds are (i) a favorable geometry which allows NH and IrH to approach very close to one another and (ii) the facility with which Ir-H may be polarized in the sense  $\text{Ir}^{\delta+}\text{-H}^{\delta-}$  on the approach of the N-H bond [46]. The same group also found that the formation of the N-H...H-Ir interaction depends on the basicity of the surrounding ligands of the metal complexes as well [47]. The pendent arm in the complexes studied above not only acts as proton donor but also stabilizes other ligands such as fluoride ions and ketones [48, 49].

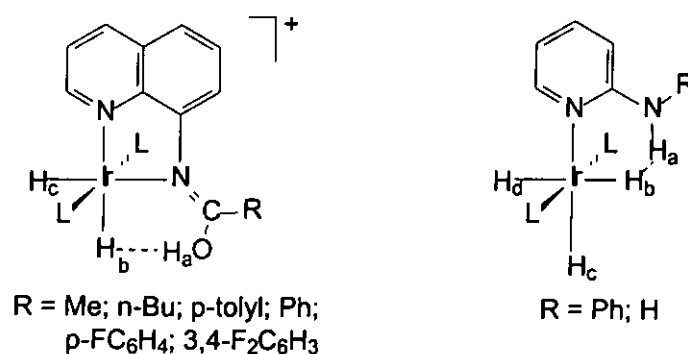


**Chart 1.1** Examples of intramolecular hydrogen bonding complexes.

Morris *et al.* reported intramolecular hydrogen bonding in iridium complexes with 2-pyridiniumthiolate ligands coordinated in a monodentate fashion via the sulfur atom [50, 51]. Hoffmann and co-workers used this complex for the study of the intramolecular hydrogen-hydrogen interaction with extended Huckel method and found that the interaction is weakly attractive [52]. Recently, Morris's group identified linear and bifurcated hydrogen bonds between iridium complexes and tetrafluoroborate ions in crystal structures and in  $\text{CD}_2\text{Cl}_2$  solutions [53, 54] (Fig. 1.8).

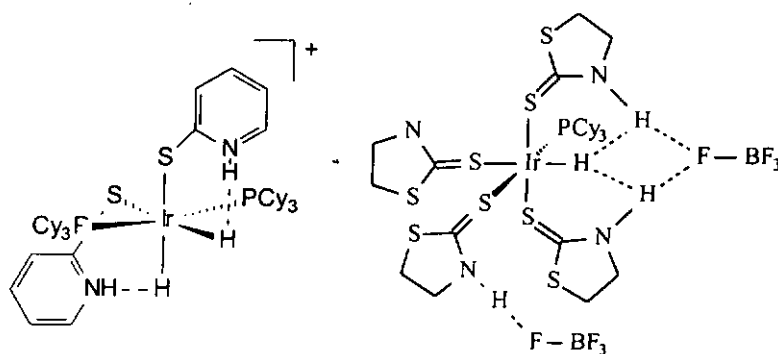


**Figure 1.8** Linear and bifurcated  $\text{MH}\cdots\text{HX}$  type hydrogen bonds.

Lau *et al.* have synthesized intramolecularly Ru-H...H-N dihydrogen-bonded ruthenium complexes with pendant (2-(dimethylamino)ethyl)cyclopentadienyl and (3-(dimethylamino)propyl)cyclopentadienyl ligands [55]. When the complexes were exposed to H<sub>2</sub>/CO<sub>2</sub> (40 atm /40 atm) at 80°C for 16h, formic acid was formed in low yield. The formation of formic acid is best explained by a mechanism which involves intramolecular heterolytic cleavage of the bound H<sub>2</sub> to generate [(η<sup>5</sup>-C<sub>5</sub>H<sub>4</sub>(CH<sub>2</sub>)<sub>n</sub>NMe<sub>2</sub>H<sup>+</sup>)RuH(dppm)]BF<sub>4</sub>, followed by CO<sub>2</sub> insertion into the Ru-H and then N-H protonation of the formato ligand.

Chaudret *et al.* have synthesized similar ruthenium complexes with the η<sup>5</sup>-cyclopentadienyl-amino ligand [56]. They found that addition of 1 equiv of HBF<sub>4</sub>.Et<sub>2</sub>O to (Cp-N)RuH(PPh<sub>3</sub>)<sub>2</sub> (Cp-N = C<sub>5</sub>H<sub>4</sub>CH<sub>2</sub>CH<sub>2</sub>NMe<sub>2</sub>) yielded, after the elimination of H<sub>2</sub>, [(η<sup>5</sup>:η<sup>1</sup>-Cp-N)Ru(PPh<sub>3</sub>)<sub>2</sub>](BF<sub>4</sub>) containing a chelating amino-cyclopentadienyl ligand. Addition of excess HPF<sub>6</sub> leads to the dicationic derivative [(Cp-NH)RuH<sub>2</sub>(PPh<sub>3</sub>)<sub>2</sub>](PF<sub>6</sub>)<sub>2</sub> in which both the metal and the amino substituent are protonated. Intramolecular hydrogen bonds were suggested between the hydride and the protonated pendant amino side arm.

Not only mononuclear species contain XH...HM hydrogen bonding, metal cluster may also have intramolecular hydrogen bonding. Aime *et al.* have found this type of interaction between osmium hydride and coordinated imine ligand in H(μ-H)Os<sub>3</sub>(CO)<sub>10</sub>(HN=CHCH<sub>3</sub>) [57].

## 1.2 Introduction to cyclopentadienyl complexes containing amino side-arms

Cyclopentadienyl complexes have been intensively studied during the past 40 years. During the last decade, the introduction of functional groups at the C<sub>5</sub> perimeter of a cyclopentadienyl (Cp) fragment has become an interesting tool to modify drastically the chemical and physical properties of classical Cp complexes of s-, p-, d- and f- block elements. The coordination of a tethered donor fragment to a metal center is thermodynamically favored when compared with the coordination of a free donor molecule. Furthermore, intramolecular coordination is generally preferred to intermolecular coordination. However, increase in ring strain of the chelating ligand and decrease in solubility might enforce the formation of coordination polymers (Fig. 1.9).

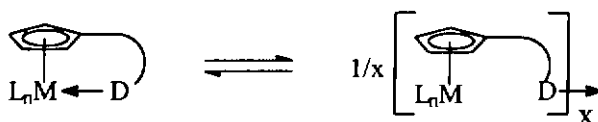
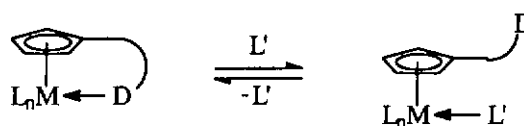


Figure 1.9 Relationship of intermolecular and intramolecular coordination affected by ring strain and solubility

In cyclopentadienyl complexes of transition metals, the Cp ligand is known to stabilize metal fragments in both low and high oxidation states and is usually regarded as substitutionally inert. The effect of an additional donor group, however, strongly depends on the nature of the metal and of the donor group. The strength of the interaction can be estimated on the basis of Pearson's HSAB concept that 'hard' ligands combine preferentially with 'hard' metal centers, and 'soft' ligands favor the interaction with 'soft' metal centers. Interesting reactivity due to change of electronic effect at the metal center is achieved when unfavored 'hard-soft' combinations are used. These unfavored



combinations are stabilized to a certain extent by the chelate effect. Of course, the side-chain donor can be easily substituted in such types of complexes. This results in a hemilabile behavior [58], where the side-chain functionally can either act as donor or as a spectator ligand (Figure 1.10).



**Figure 1.10 Hemilabile behavior of the side-chain donor complexes**

The hemilabile situation is expected in compounds where a ‘hard’ donor, such as an amino or alkoxy group, coordinates to a ‘soft’ metal center, as present in complexes with a late transition metal in low oxidation states. Vice versa, hemilability is anticipated when a ‘soft’ donor, such as phosphino, thio, or alkenyl group, interacts with a ‘hard’ center, as present in complexes with early transition metals in high oxidation states. Of course, there exist many ‘borderline’ bonding situations, where the donor-acceptor interaction is difficult to predict. A substitutionally labile group is capable of temporarily blocking a coordination site and therefore allows turning-on of the reactivity of the metal center. The fluxional ‘opening and closing’ character provides interesting perspectives in terms of stabilization of reactive, unsaturated species, of substrate activation, of chemical sensing, and of homogenous catalysis.

Many examples of dialkylaminoalkyl-substituted Cp complexes with s-, p-, d-, and f-block elements have been described in the literature [59, 60]. A representative selective is collected in Figure 1.11.

Jutzi's group has synthesized the metallocenes **1** and **2**. The coordination of the amino side-chain prevents association to oligomers. In a similar manner, compounds **3** and **4**, achieved intramolecular stabilization and were prevented from association into oligomers. The monomeric lanthanum complex **3**, reported by Herrmann and co-workers, contains three dimethylaminoethyl substituted cyclopentadienyl groups; two of the amino groups coordinate to the metal center and thus circumventing the formation of oligomers. Lanthanoid complexes of type **4**, reported by Schumann *et al.*, are more stable towards air and moisture than the parent compounds; unfortunately, they do not catalyze ethylene polymerization reaction [61].

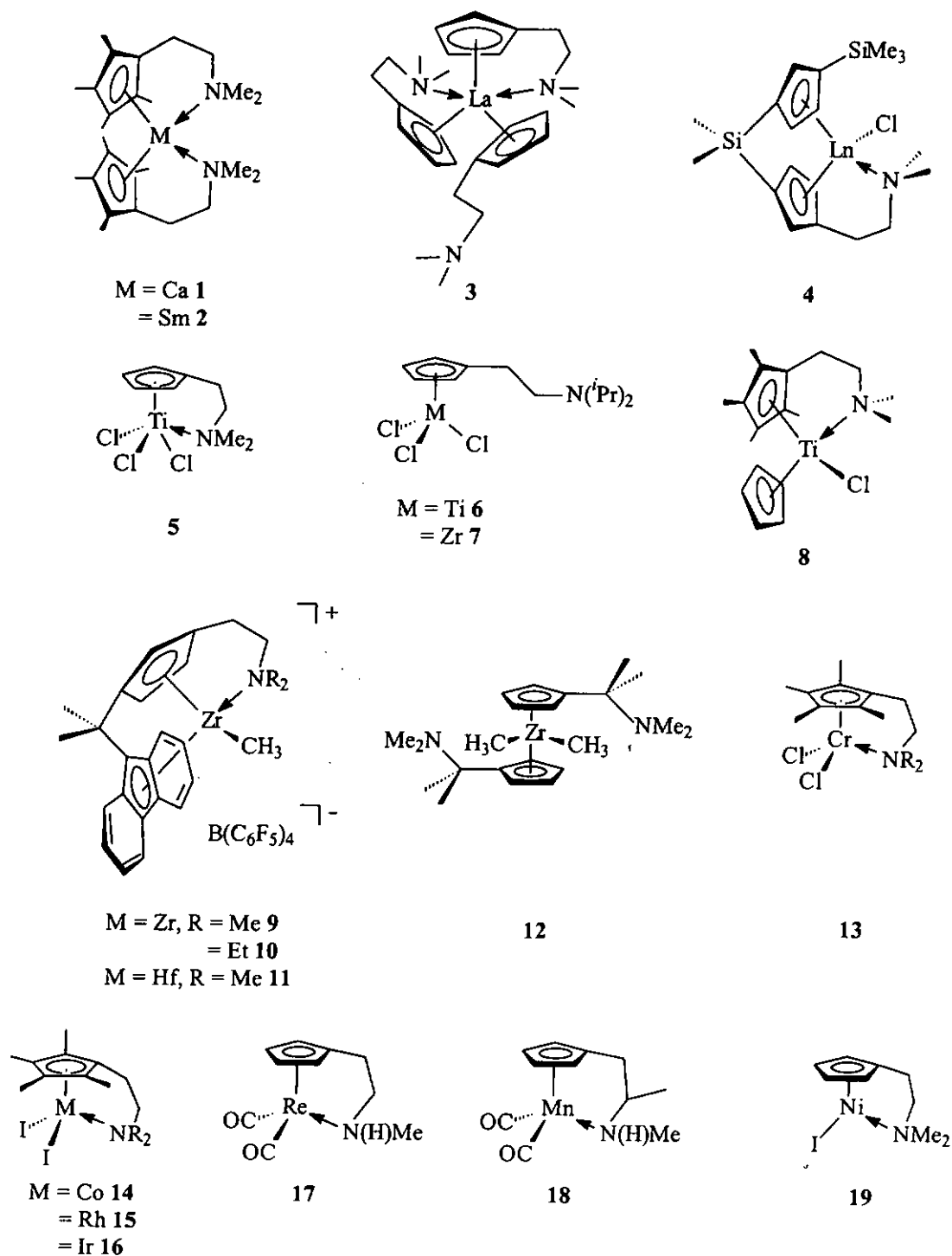
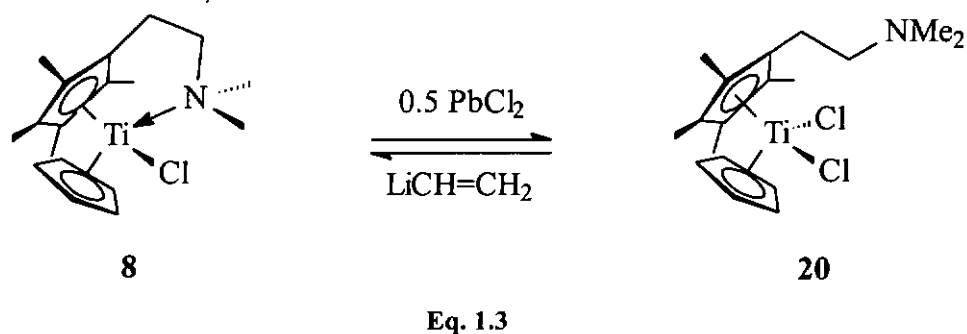


Figure 1.11 Representative selection of dialkylaminoalkyl-substituted Cp complexes

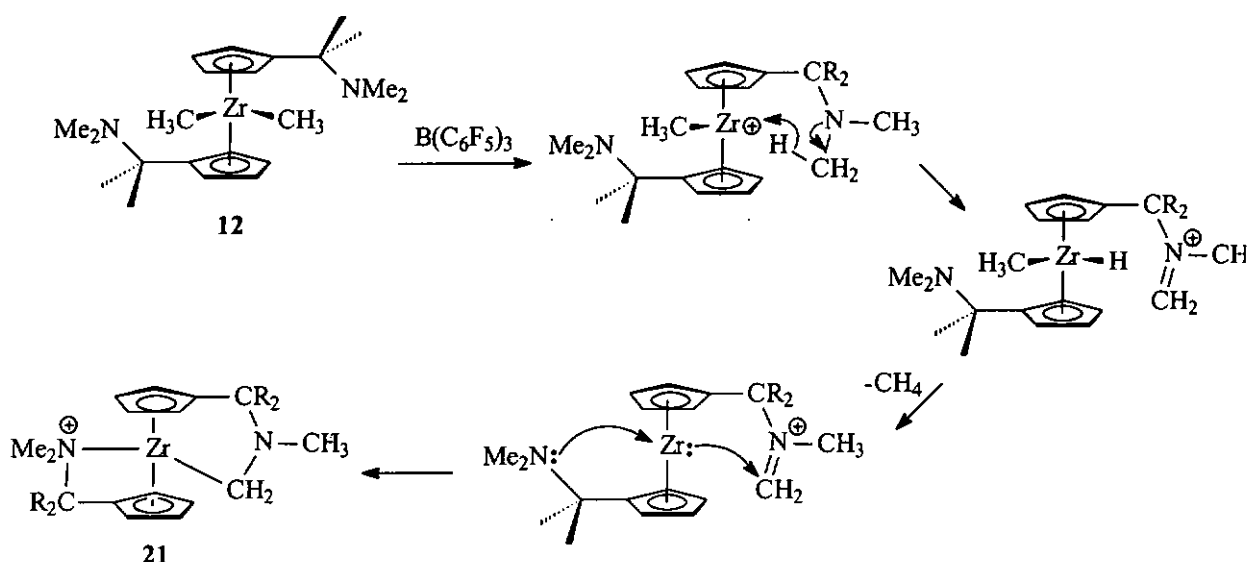
The alkyl substituents at the amino groups in complex 5-7 are different. The titanium half-sandwich complex 5, as described by Rausch and co-workers, is monomeric

in the solid state and in solution [62]. Analogous to the parent compound  $\text{CpTiCl}_3$ , **5** in combination with methylaluminoxane (MAO) is a very active catalyst for the polymerization of ethylene; the role of the dimethylamino group in the polymerization process has not been elucidated yet. Jutzi's group has prepared complexes **6** and **7** [63], with diisopropylamino groups on the side chain. These compounds prefer an intermolecular coordination, which resulted in the formation of coordination polymers. Influence of the oxidation state of the central metal on the coordination behavior was studied by Beckhaus *et al.* [64]. Experimental result showed that oxidation of **8** to **20** (Eq. 1.3) is accompanied by decomplexation. Although **20** is a 16-valence-electron early transition metal complex, intramolecular coordinations of the amino-side arm to obtain an 18 electron species has not been reported. But, addition of  $\text{LiCH}=\text{CH}_2$  to **20** yields the starting compound **8** with the amino group coordinated at the metal center.



Very recently, Jutzi's group have synthesized compounds **9-11**, NMR spectral studies showed those complexes to have the amino groups coordinated to the metal centers [65]. Surprisingly, the amino group is bonded to the metal center rather strongly, therefore preventing hemilability. Upon addition of aluminum trialkyl to **9** and **10**, active catalysts for the polymerization of ethylene was obtained. It is probably due to the coordination of the Lewis acidic aluminum alkyl to the amino group and the activation of

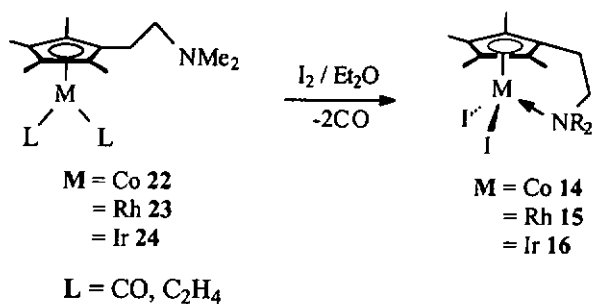
the dormant catalytically active site [66]. An interesting aspect concerning the effect of space length has been reported by Erker and co-workers [67]. Treatment of **12**, in which the Cp rings are substituted by dimethylaminomethyl groups, with the strong Lewis acidic tris(pentafluorophenyl)-borane leads to an ionic intermediate, which undergoes a surprising reaction sequence: C-H activation under loss of methane instead of coordination of the second dimethylamino group, yields the spiro-metalocene **21** (Scheme 1.1).



**Scheme 1.1** Proposed mechanism for the formation of the spiro-metalocene, **21**

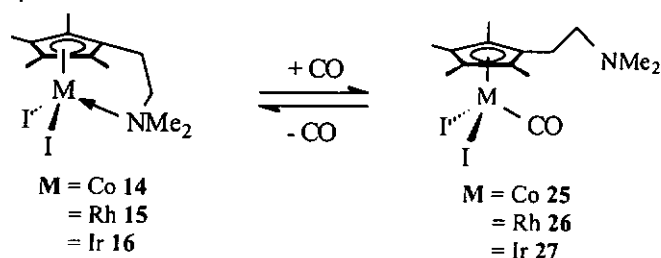
Jolly *et al.* reported the chromium half-sandwich complex **13**. It is a highly active catalyst when combined with MAO for the polymerization of ethylene. Unfortunately, the reaction mechanism remains unknown. Late transition metal complexes bearing functionalized cyclopentadienyl ligands have been extensively studied by Jutzi *et al.* [68, 69]. The amino side-chains do not coordinate in complexes **22-24** (L = CO, C<sub>2</sub>H<sub>4</sub>; M = Co, Rh, Ir). However, oxidation of the complexes with I<sub>2</sub> leads to the formation of

complexes **14-16**, each having the amino group coordinated to metal center in the oxidation state of +III (Eq. 1.4).



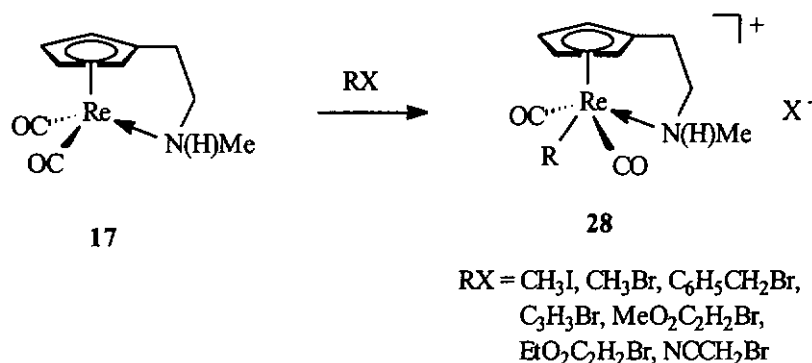
Eq. 1.4

Moreover, application of CO pressure to **14-16** gives the unarmed complexes **25-27** (Eq. 1.5).



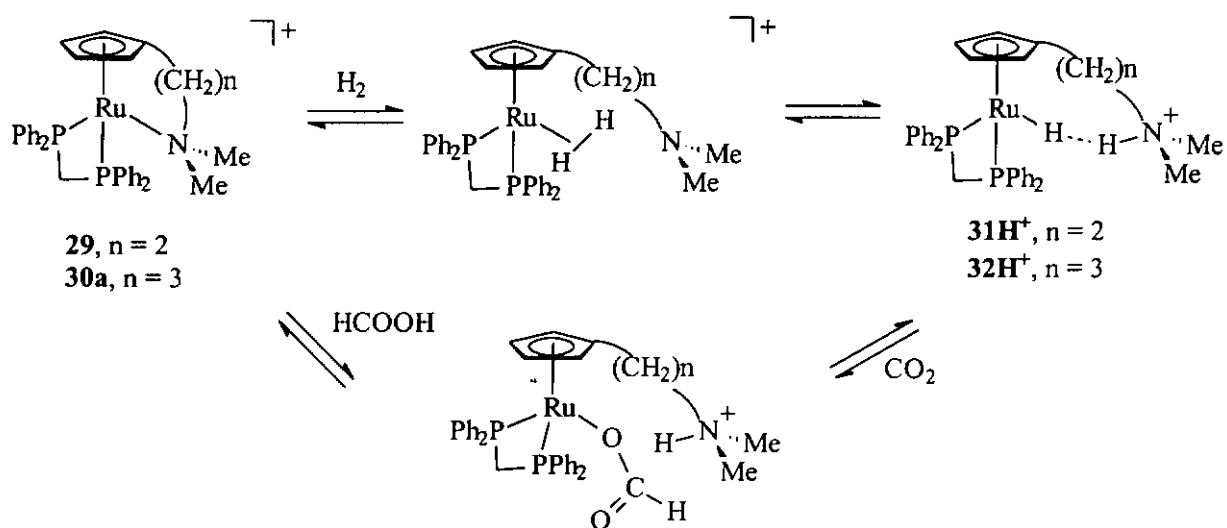
Eq. 1.5

Wang *et al.* have contributed significantly to the area of amino-substituted Cp ligands [70-72], for example, they have synthesized compound **17**, in which the 'hard' amino group is coordinated to a 'soft' Re(I) center. The enhanced nucleophilicity of the metal now enables alkylation with substrates RX (Eq. 1.6) [73]. The same group also presented complex **18**, in which chelating effect supported N-donor coordination to the mono-valent metal center.



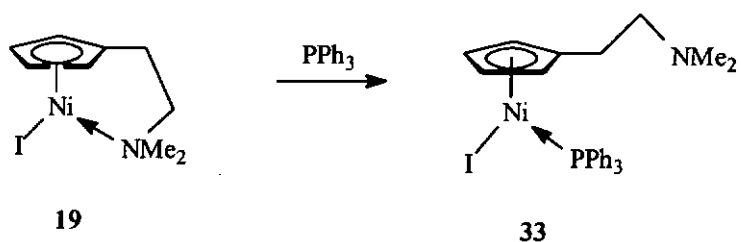
Eq. 1.6

Lau *et al.* synthesized ruthenium complexes **29**, **30** containing cyclopentadienyl ligand with amino sidearms, and found that **29** and **30** catalyzed hydrogenation of  $CO_2$  to formic acid, albeit in low yields [55]. The formation of formic acid can be explained by intramolecular heterolytic cleavage of the bound  $H_2$  to generate  $[(\eta^5-C_5H_4(CH_2)_nNMe_2H^+)RuH(dppm)]BF_4$  ( $n = 2$ , **31H<sup>+</sup>**;  $n = 3$ , **32H<sup>+</sup>**), followed by  $CO_2$  insertion into the Ru-H and then N-H protonation of the formato ligand (Scheme 1.2).



Scheme 1.2 Proposed mechanism of hydrogenation of  $CO_2$  to formic acid by  $[(\eta^5:\eta^1-C_5H_4(CH_2)_2NMe_2)Ru(dppm)](BF_4)$

Another example consisting of intramolecular coordination of amino sidearm to a Group 10 element has been reported by Fischer and co-workers [74]. The labile dimethylaminoethyl group in the nickel (II) complex **19** can easily be displaced by a triphenylphosphine ligand (Eq. 1.7).



Eq. 1.7

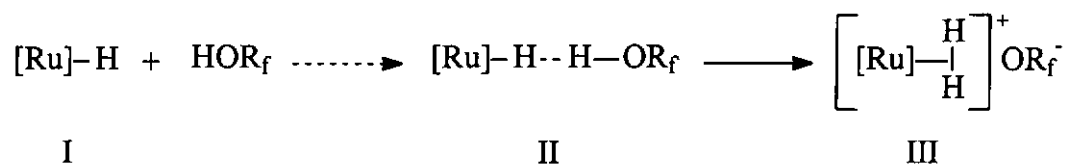


## 2 Intermolecular M-H...H-OR Hydrogen bonding of Ruthenium hydride complexes with acidic alcohols

### 2.1 Introduction

The protonation reaction of transition metal hydrides with acids to yield the corresponding  $\eta^2$ -H<sub>2</sub> complexes is well known and common. [8-11, 75] It has recently been reported that protonation may proceed via intermediate species containing unusual intramolecular [42, 44, 46, 50, 51] or intermolecular [25, 26, 36, 37] dihydrogen bonds M-H...H-X, a special kind of hydrogen bond in which the proton acceptor is a metal hydride. Shubina et al [25] reported that intermolecular W-H...H-OR dihydrogen bonding was formed between acidic alcohols and the tungsten hydride complex WH(CO)<sub>2</sub>(NO)L<sub>2</sub>; hydricity of the metal hydride and the proton donating ability of the acidic alcohol are factors affecting the strength of the intermolecular dihydrogen bonding.

In this work, reactions of various proton donors (trifluoroethanol, TFE; hexafluoroisopropanol, HFIP and perfluoro-*tert*-butanol, PFTB) with ruthenium hydride complexes [TpRu(PPh<sub>3</sub>)<sub>2</sub>H (34) and [TpmRu(PPh<sub>3</sub>)<sub>2</sub>H](BF<sub>4</sub>) (35)] have been studied in deuterated dichloromethane solution by in-situ NMR spectroscopy. The aim of this work is to show that the intermediate in the protonation reaction is the dihydrogen-bonded species **II**.



**Eq. 2.1**

## 2.2 *Experimental*

### 2.2.1 **Materials and instrumentation**

Ruthenium trichloride,  $\text{RuCl}_3 \cdot x\text{H}_2\text{O}$  was obtained from Johnson Matthey and Pressure Chemical Co. Pyrazole, triphenylphosphine, sodium tetrafluoroborate, potassium borohydride were purchased from Aldrich. Fluorinated alcohols were purchased from ACROS and used without further purification. The complexes,  $\text{Ru}(\text{PPh}_3)_3\text{Cl}_2$  [76],  $\text{RuHCl}(\text{PPh}_3)_3$  [77],  $\text{TpRu}(\text{PPh}_3)_2\text{H}$  [78] and  $[\text{TpmRu}(\text{PPh}_3)_2\text{H}](\text{BF}_4)$  [79] were prepared according to literature methods.

NMR spectra were recorded with a Bruker DPX-400 spectrometer.  $^1\text{H}$  NMR spectra were measured at 400.13 MHz, chemical shifts were reported relative to residual protons of deuterated solvents.  $^{31}\text{P}\{^1\text{H}\}$  NMR spectra were measured at 161.70 MHz, chemical shifts were relative to 85%  $\text{H}_3\text{PO}_4$  in  $\text{D}_2\text{O}$  (0 ppm) as an external reference. Standard Bruker software was used for measuring the longitudinal relaxation times,  $T_1$ ,

using the 180° inversion recovery method. The reactions of acidic alcohol with the various ruthenium hydride complexes were carried out in CD<sub>2</sub>Cl<sub>2</sub> solutions at 223 K in 5 mm NMR tubes. The NMR spectra were first measured at low temperature with pre-cooled probe-heads (223K), and then measured at increasing temperature.

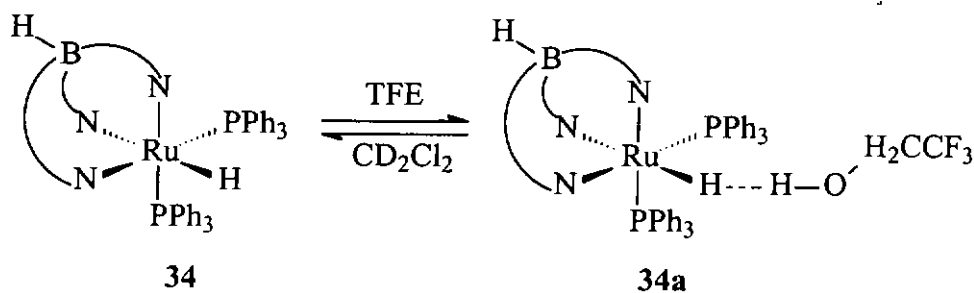
### **2.2.2 General procedure of reaction of a ruthenium hydride with an acidic alcohol**

A sample of 15 mg of ruthenium hydride complex was weighed into a 5 mm NMR tube which was then sealed with a rubber septum. The tube was purged and filled with nitrogen. Degassed deuterated dichloromethane (0.35 ml) was added. The tube was then placed in the pre-cooled probe and was allowed to stand for 5 minutes. The pre-cooled NMR tube was then lifted up for the addition of 10 equiv of an acidic alcohol by a micro-syringe. The mixture was allowed to stand for 15 minutes for the reaction to proceed. The <sup>1</sup>H, <sup>31</sup>P NMR spectra and T<sub>1</sub> relaxation time were then measured. The temperature was increased by 10 degree and the solution was allowed to equilibrate for 10 minutes before taking the measurements. These NMR measurements were taken for the temperature range of 223K to 293K.

## 2.3 Results and Discussion

### 2.3.1 Reaction of $\text{TpRu}(\text{PPh}_3)_2\text{H}$ with trifluoroethanol (TFE)

After 10 equiv of TFE was added to  $\text{TpRu}(\text{PPh}_3)_2\text{H}$  (**34**) in  $\text{CD}_2\text{Cl}_2$  solution at 223K, the  $^1\text{H}$  NMR spectrum showed a small upfield shift ( $\Delta\delta = 0.27$  ppm) of the hydride signal. The  $^{31}\text{P}$  NMR signal of the equivalent phosphine ligands also showed a similar shift from  $\delta$  74.83 ppm to  $\delta$  73.72 ppm. Moreover, decrease of the longitudinal relaxation time  $T_1(\text{min})$  of the hydride signal was observed. For the hydride complex in  $\text{CD}_2\text{Cl}_2$  solution, the  $T_1(\text{min})$  is 304 ms (400 MHz) at 246 K, and after addition of 10 equiv. of TFE, the  $T_1(\text{min})$  dropped to 266 ms at 238 K. The decrease in  $T_1(\text{min})$  was caused by weak interaction between the metal hydride **34** and the proton of TFE (Eq. 2.2). Similar observation was made by Chaudret *et al* when excess phenol was added to a solution of  $\text{Ru}(\text{dppm})_2\text{H}_2$  in  $\text{C}_7\text{D}_8$  at room temperature. The  $^1\text{H}$  NMR signals of both the hydrogen-bonded adducts of the *cis*- and *trans*- isomers of  $\text{Ru}(\text{dppm})_2\text{H}_2$  were found shifted upfield and the  $T_1(\text{min})$  were shortened [32].

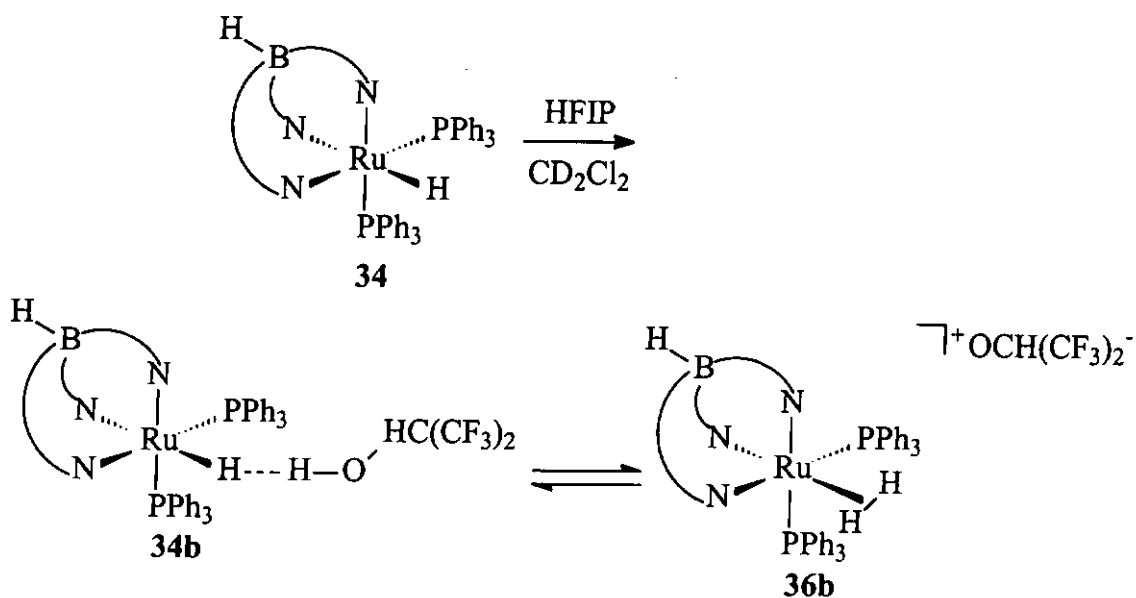


Eq. 2.2

Proton NMR monitoring of the reaction of **34** with TFE shows no sign of formation of the dihydrogen complex  $[\text{TpRu}(\text{PPh}_3)_2(\text{H}_2)]^+$ , indicating that complete proton transfer for TFE to the complex has not occurred; it may be due to the fact that acidity of trifluoroethanol (TFE) is lower than that of  $[\text{TpRu}(\text{PPh}_3)_2(\text{H}_2)]^+$ . In view of this, a more acidic alcohol was then employed for the study of intermolecular dihydrogen bonding between **34** and the alcohol.

### 2.3.2 Reaction of $\text{TpRu}(\text{PPh}_3)_2\text{H}$ with hexafluoroisopropanol (HFIP)

Since little reaction was observed between **34** and TFE, a more acidic alcohol, hexafluoroisopropanol (HFIP) was then employed for the study. Addition of 10 equiv of HFIP to a solution of **34** in  $\text{CD}_2\text{Cl}_2$  at 223 K led to the immediate disappearance of the hydride signal in  $^1\text{H}$  NMR spectroscopy. A new broad singlet at  $\delta -8.44$  ppm, integrating to two hydrogens and assignable to the  $\text{Ru}(\eta^2\text{-H}_2)$  was observed. The assignment was based on comparison to the  $\eta^2$ -dihydrogen NMR signal of  $[\text{TpRu}(\text{PPh}_3)_2(\text{H}_2)]^+(\text{BF}_4)^-$  formed by acidification of **34** with  $\text{HBF}_4\cdot\text{Et}_2\text{O}$  in dichloromethane [78]. The literature values of the chemical shift of the  $\eta^2\text{-H}_2$  peak and  $T_1(\text{min})$  of  $[\text{TpRu}(\text{PPh}_3)_2(\text{H}_2)]^+(\text{BF}_4)^-$  are  $-8.20$  ppm and 21 ms (240 K) in  $\text{CD}_2\text{Cl}_2$ , respectively. In the reaction of **34** with HFIP, the chemical shift of the  $\eta^2\text{-H}_2$  peak and  $T_1(\text{min})$  were found to be  $-8.44$  ppm and 18 ms (242 K), respectively.



Eq. 2.3

When the temperature was increased from 223 K to 293 K, the signal of  $\eta^2$ -H<sub>2</sub> ligand shifted slightly upfield ( $\Delta\delta = 47$  ppb). At 263 K, in addition to the  $\eta^2$ -H<sub>2</sub> signal, a small peak was observed at  $-14.08$  ppm, the intensity of which increased with temperature, and eventually it became clearly visible and appeared as a broad triplet with  $^2J(\text{HP})$  of 26.4 Hz. This triplet was attributable to the hydrogen bonded intermediate, **34b**. The formation of **34b** resulted from weakening of the H-H bond of **36b** as temperature increased. Apparently, increase in temperature shifted the equilibrium to the left. The assignment of **34b** is supported by upfield shift of the hydride signal to  $\delta -14.06$  ppm relative to that of **34** at  $\delta -13.96$  ppm in the absence of alcohol at 293 K. The intermolecularly-hydrogen bonded complex **34b** was formed as temperature increased at the expense of the  $\eta^2$ -dihydrogen complex **36b**. The variable temperature <sup>1</sup>H NMR measurements are totally reversible (Figure 2.1).

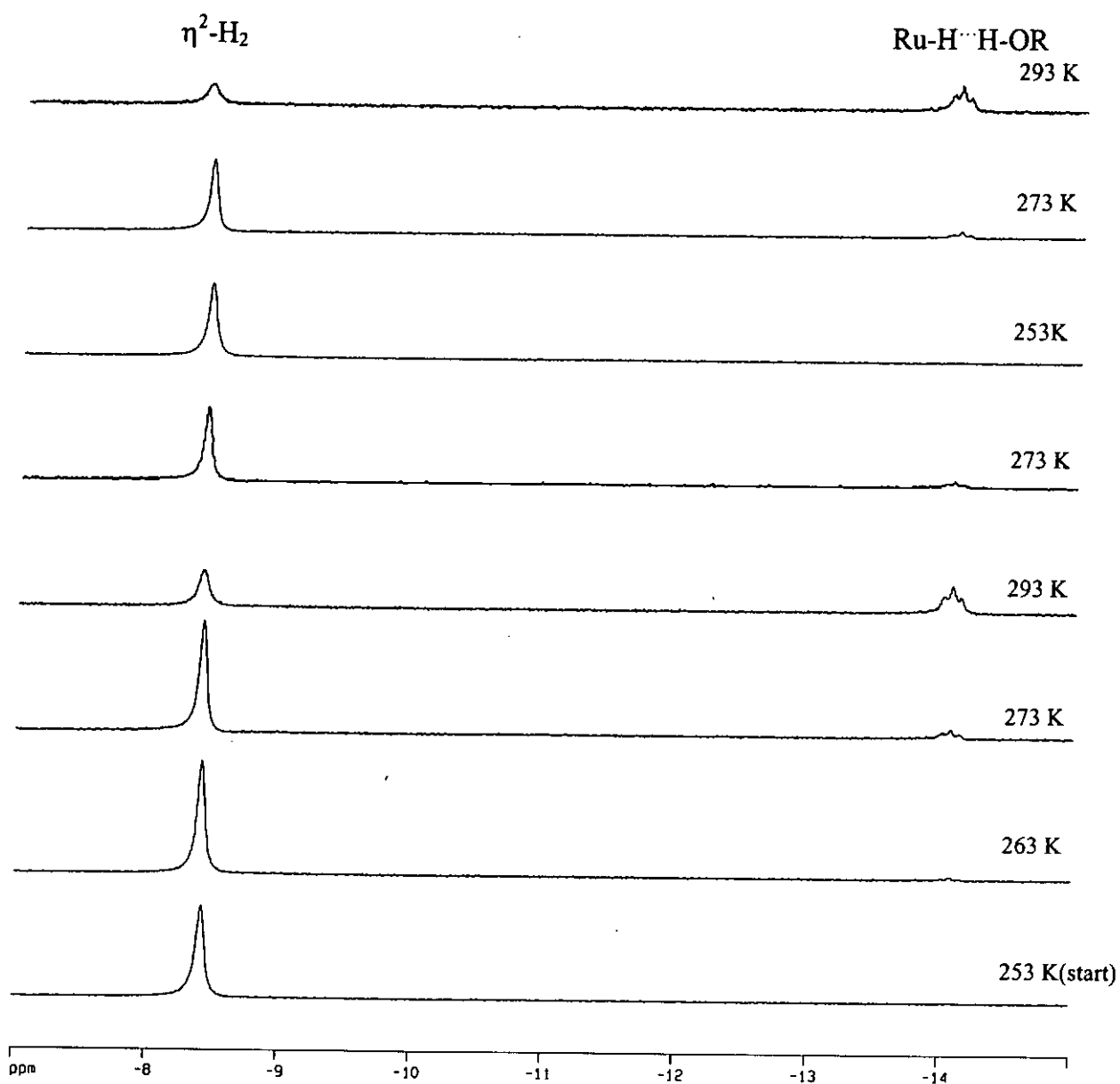


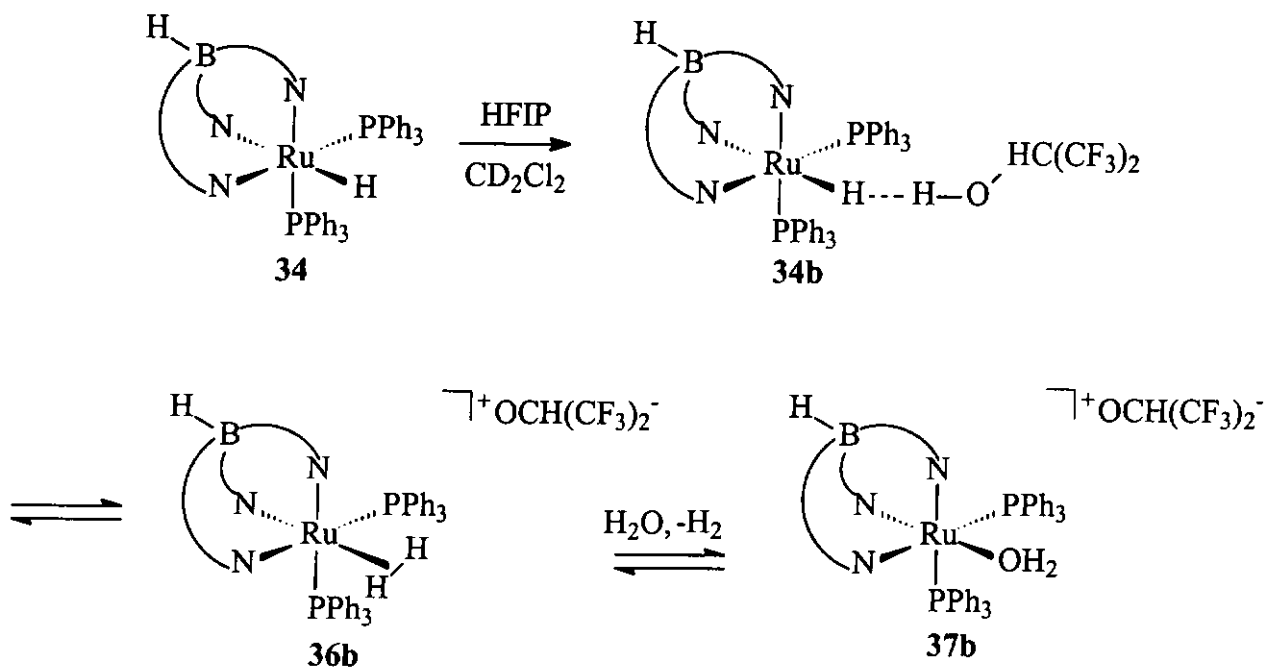
**Figure 2.1** Variable temperature  $^1\text{H}$  NMR spectra (upfield region) of  $\text{TpRu}(\text{PPh}_3)_2\text{H} + \text{HFIP}$  in  $\text{CD}_2\text{Cl}_2$

The variable temperature  $^1\text{H}$  NMR study showed that an equilibrium existed between **34b** and **36b**. The upfield hydride signal of **34b** was broad when compared to that

of **34**; broadening of the hydride signal indicates that hydrogen bond interaction is present between the hydride ligand of **34** and the proton of HFIP. Measurement of the  $T_1(\text{min})$  of **34b** was attempted, but it was thwarted by the shifting of the equilibrium (Eq. 2.3) to the far right at lower temperatures, at which **34b** was no longer detectable.

$^{31}\text{P}$  NMR study showed that after addition of 10 equiv of HFIP at 223 K to **34** in  $\text{CD}_2\text{Cl}_2$ , the phosphine signal at  $\delta$  74.8 ppm disappeared, and new peaks were found at  $\delta$  51.9 and 42.9 ppm, with integral ratio of about 9:1. The peak at  $\delta$  51.9 ppm was assignable to the product of complete proton transfer, **36b** while the other peak at  $\delta$  42.9 ppm was due to the chloro-complex,  $\text{TpRu}(\text{PPh}_3)_2\text{Cl}$ , which was formed by reaction of **34** with the dichloromethane. When the temperature was increased to 263 K, two more new signals appeared at  $\delta$  74.6 and 48.8 ppm. The peak at  $\delta$  74.6 ppm was due to the dihydrogen-bonded intermediate, **34b**. The other signal at  $\delta$  48.8 ppm was assigned to be the aquo complex,  $[\text{TpRu}(\text{PPh}_3)_2(\text{H}_2\text{O})](\text{OCH}(\text{CF}_3)_2)$ , **37b** (Eq. 2.4); similar signal was assignable to the  $[\text{TpRu}(\text{PPh}_3)_2(\text{H}_2\text{O})]\text{BF}_4$  in  $\text{CDCl}_3$  by reacting  $\text{TpRu}(\text{PPh}_3)_2\text{H}$  with  $\text{HBF}_4 \cdot \text{Et}_2\text{O}$  in dichloromethane followed by addition of  $\text{H}_2\text{O}$  [78].





Eq. 2.4

The formation of **37b** resulted from cleavage of the labile dihydrogen ligand and coordination of adventitious water. The intensities of the two new peaks at  $\delta$  74.6 and 48.8 ppm further increased with increased temperature, while the intensity of the signal of the dihydrogen complex at 51.9 ppm decreased. This observation is reversible when temperature was decreased. The intensities of the signals corresponded to **37b** and **34b** decreased when the temperature decreased while the signal of the dihydrogen complex, **36b**, increased. The signal for the intermolecular hydrogen bonded intermediate, **34b** disappeared completely at 253 K or below, it became detectable again as temperature was raised to 263 K or above.

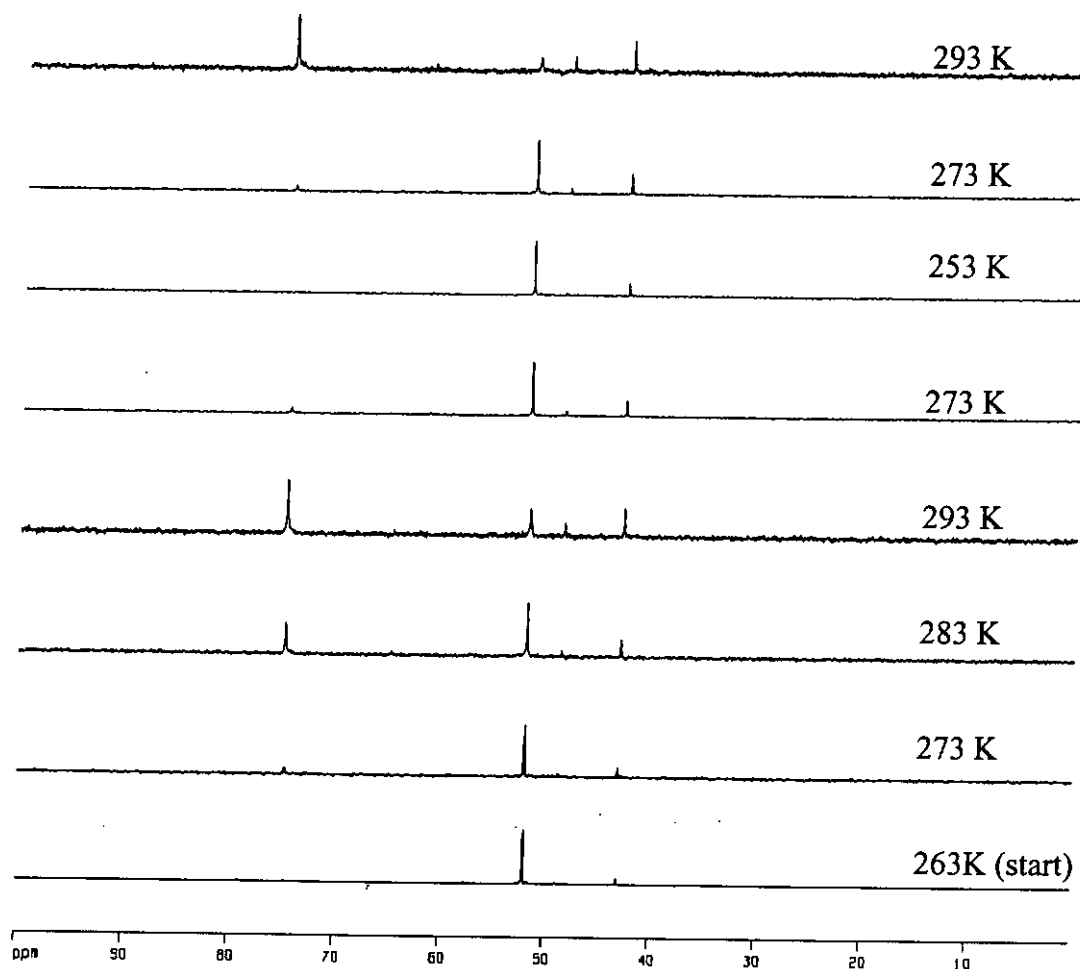


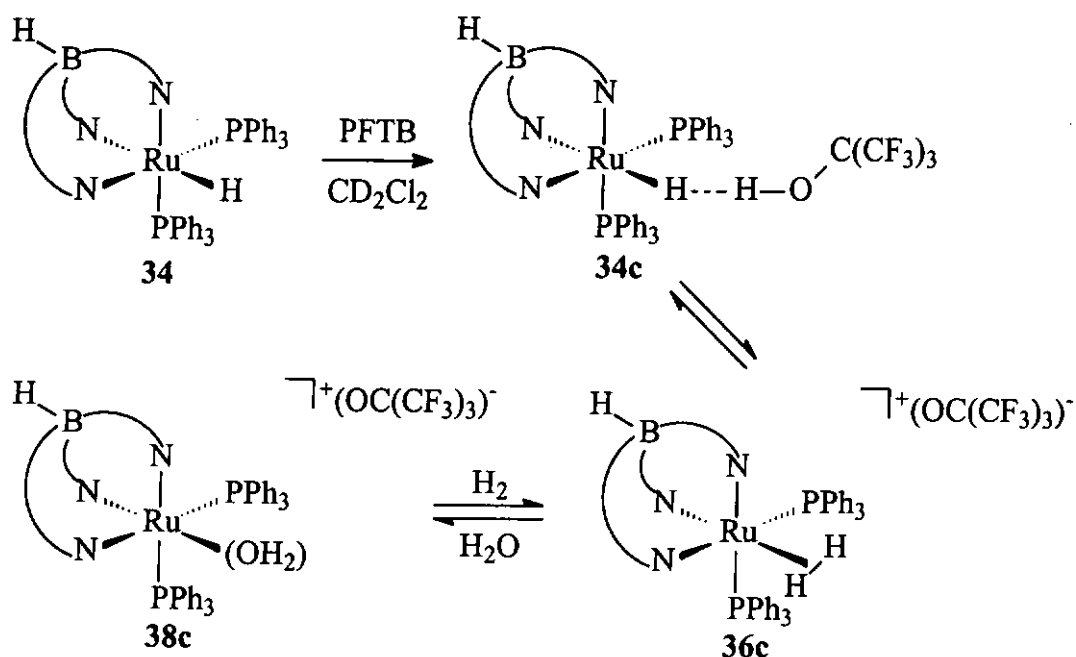
**Figure 2.2** Variable temperature  $^{31}\text{P}$  NMR spectrum of mixture of  $\text{TpRu}(\text{PPh}_3)_2\text{H}$  and excess HFIP in  $\text{CD}_2\text{Cl}_2$

### 2.3.3 Reaction of $\text{TpRu}(\text{PPh}_3)_2\text{H}$ with perfluoro-*tert*-butanol (PFTB)

The interaction of ruthenium hydride with the more acidic proton donor, PFTB was monitored by  $^1\text{H}$  NMR spectroscopy. When ten equivalents of PFTB were added to a solution of **34** in  $\text{CD}_2\text{Cl}_2$  at 223K, the hydride signal at  $\delta -13.76$  ppm

disappeared immediately and a broad peak at  $\delta -8.2$  ppm appeared. This peak was attributed to the  $\eta^2\text{-H}_2$  of the product of proton transfer, **36c** (Eq. 2.5). Since the acidity of PFTB was the strongest among the three acidic alcohols chosen, net proton transfer was expected. Variable temperature NMR measurement monitored between 223 K and 293 K did not show signal of the intermolecular hydrogen bonded intermediate, **34c**. The  $T_1(\text{min})$  of the dihydrogen peak ( $\delta -8.2$  ppm) was measured to be 20 ms(400 MHz) at 245 K.

Other than the broad peak found at the upfield region, free  $\text{H}_2$  was also observed as a small peak at 4.57 ppm in  $^1\text{H}$  NMR spectrum after the addition of PFTB. The free dihydrogen at  $\delta 4.57$  ppm can be explained, in terms of the cleavage of the labile  $\eta^2\text{-H}_2$  ligand and its replacement by adventitious water. For example, Epstein and Berke showed that cleavage of  $\eta^2\text{-H}_2$  followed by coordination of the alkoxo group of acidic alcohol gave the final product of the reaction between  $\text{WH}(\text{CO})_2(\text{NO})\text{L}_2$  ( $\text{L} = \text{PMe}_3, \text{PEt}_3, \text{P}(\text{O}^i\text{Pr})_3, \text{PPh}_3$ ) and HFIP [25]. Moreover, the same group observed the cleavage of  $\text{H}_2$  when  $[(\text{triphos})\text{Re}(\text{CO})_2\text{H}]$  reacted with excess PFTB and eventually forming the alkoxo complex [29].



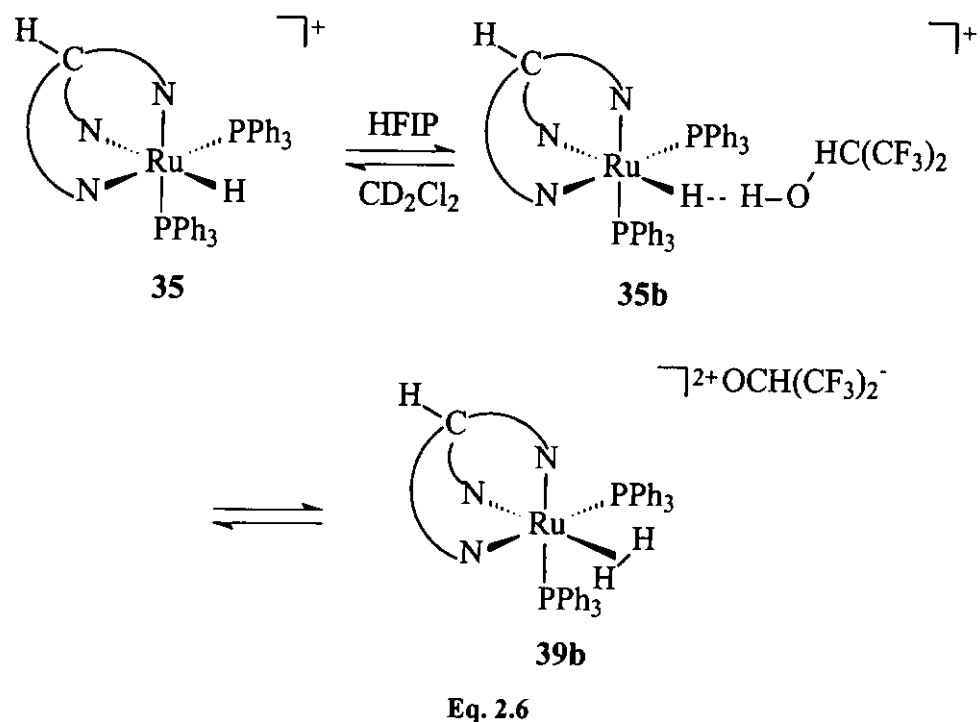
Eq. 2.5

### 2.3.4 Reaction of [TpmRu(PPh<sub>3</sub>)<sub>2</sub>H](BF<sub>4</sub>) towards hexafluoroisopropanol (HFIP)

The strength of intermolecular hydrogen bonding between the metal hydride and the acidic alcohol depends on the proton donating ability of the alcohol and also the hydricity of the metal hydride. After studying the effect of variation of proton donating ability of the acidic alcohols on the strength of proton-hydride interaction between 34 and different alcohols, we turn our attention to the effect of changing hydricity of the metal hydride on the strength of the dihydrogen bond.

Ten equiv of HFIP was added to a CD<sub>2</sub>Cl<sub>2</sub> solution of [TpmRu(PPh<sub>3</sub>)<sub>2</sub>H](BF<sub>4</sub>) (**35**) and the reaction was monitored by low-temperature <sup>1</sup>H NMR spectroscopy. The hydride region in the <sup>1</sup>H NMR spectrum, recorded at 223 K (400 MHz), showed no significant change. As the temperature was increased from 223 K to 293 K, no new peaks were observed in the upfield region. This implied that there was no evidence for interaction between **35** and HFIP in the <sup>1</sup>H NMR spectrum. However, very weak interaction between **35** and HFIP was supported by the *T*<sub>1</sub>(min) measurements. *T*<sub>1</sub>(min) measured for the hydride peak at -13.76 ppm in the reaction of **35** to HFIP from 223 K to 293 K was found to be 302 ms at 257 K, in comparison to a solution of **35** in CD<sub>2</sub>Cl<sub>2</sub> without alcohol gave a *T*<sub>1</sub>(min) of 319 ms at 253 K for the hydride signal.

In the <sup>31</sup>P NMR spectrum, there were no other signals observed except the singlet at δ 73.61 ppm of **35** from 223 K to 297 K. The very weak interaction between **35** and HFIP may be due to the high acidity of the product of the proton transfer reaction, [TpmRu(PPh<sub>3</sub>)<sub>2</sub>(H<sub>2</sub>)]<sup>2+</sup>, **39b**, (p*K*<sub>a</sub> = 2.8) [40] (Eq. 2.6). Such high acidity of the dihydrogen complex shifted the equilibrium to the far left. As a result, very little reaction of **35** with HFIP was observed. Alternatively, lack of dihydrogen bonding between **35** and HFIP may be explained in terms of the low hydricity of the hydride ligand in the former. Lower hydricity of the hydride ligand in **35** relative to that of the hydride ligand in the Tp analogue **34** is due to the extra charge of the metal center in the former.



### 2.3.5 Reaction of $[\text{TpmRu}(\text{PPh}_3)_2\text{H}](\text{BF}_4)$ towards perfluoro-*tert*-butanol (PFTB)

Since experimental result implied very weak interaction between **35** and HFIP, the more acidic proton donor PFTB was employed to see if proton-hydride interaction between **35** and the alcohol would become detectable. Upon addition of 10 equiv of PFTB to **35** in  $\text{CD}_2\text{Cl}_2$  at 223 K, the  $^1\text{H}$  NMR spectrum of the mixture again showed no noticeable change, no new peaks were observed as the temperature was increased from 223 K to 293 K.

The very weak interaction between PFTB and **35** was also supported by the  $T_1(\text{min})$  measurement. The  $T_1(\text{min})$  for the hydride signal at  $-13.76$  ppm of the mixture of

PFTB and **35** was measured to be 309 ms at 263 K. This  $T_1(\text{min})$  was very close to that of the hydride ligand of **35** in  $\text{CD}_2\text{Cl}_2$  (319 ms at 253 K). Although a more powerful proton donating alcohol was used, still no dihydrogen-bonding interaction has observable between **35** and the alcohol.

### 3 Synthesis, Characterization and Study on the Intramolecular Hydrogen Bonding of Tethered Cyclopentadienyl Ruthenium Complexes

#### 3.1 Introduction

Cyclopentadienyls are one of the most widely used classes of ligands in organometallic chemistry and homogeneous catalysis [80]. Many studies concerning functionalized cyclopentadienyl have also been reported. Cyclopentadienyls with tethered amino groups (CpN) have been used for coordination with various transition metals. Surprisingly, ruthenium complexes bearing these ligands are not too many. In view of the fact that intramolecular hydrogen bonding was found in the complex  $\text{CpNH}^+\text{Ru}(\text{PPh}_3)_2\text{H}$  [55], studies of dihydrogen bonding in aminocyclopentadienyl ruthenium hydride complexes and the catalytic activity of these complexes in  $\text{CO}_2$  hydrogenation were continued. We choose to study the influence of decreased basicity of the metal center on the strength of the  $\text{Ru-H}\cdots\text{H-N}$  dihydrogen bond and the efficiency of  $\text{CO}_2$  hydrogenation. Thus, it is the purpose of this chapter to fine-tune the intramolecular dihydrogen bond by changing ligands from electron donating to electron withdrawing, viz. from triphenylphosphine to triphenylphosphite.



## 3.2 *Experimental*

### 3.2.1 **Materials and instrumentation**

Ruthenium trichloride,  $\text{RuCl}_3 \cdot x\text{H}_2\text{O}$  was obtained from Johnson Matthey and Pressure Chemical Co. All other chemicals were obtained from Aldrich except dicyclopentadiene and deuterated NMR solvents, which were purchased from BDH and Armar, respectively. The ligand  $\text{C}_5\text{H}_5(\text{CH}_2)_2\text{NMe}_2$  [81], the complexes  $\text{Ru}(\text{PPh}_3)_3\text{Cl}_2$  [76] and  $(\eta^5\text{-C}_5\text{H}_4(\text{CH}_2)_2\text{NMe}_2)\text{Ru}(\text{PPh}_3)_2\text{Cl}$  [55] were prepared according to literature methods.

Solvents were distilled under dry nitrogen atmosphere with the appropriate drying agents: (solvent/ drying agent) methanol/  $\text{Mg-I}_2$ , ethanol/  $\text{Mg-I}_2$ , tetrahydrofuran/ Na benzophenone ketyl, diethyl ether/ Na, n-hexane/ Na, toluene/ Na, chlorobenzene/  $\text{P}_2\text{O}_5$ . All reactions were performed under an atmosphere of dry nitrogen using standard Schlenk techniques. High-purity hydrogen gas was supplied by Hong Kong Oxygen.

Elemental analyses were performed by M-H-W laboratories, Phoenix, Arizona, USA. NMR spectra were recorded with a Bruker DPX-400 spectrometer.  $^1\text{H}$  NMR spectra were measured at 400.13 MHz, chemical shifts were reported relative to residual protons of deuterated solvents.  $^{31}\text{P}\{^1\text{H}\}$  NMR spectra were measured at 161.70 MHz, chemical shifts of these spectra were relative to 85%  $\text{H}_3\text{PO}_4$  in  $\text{D}_2\text{O}$  (0 ppm) as an external reference.  $^{13}\text{C}\{^1\text{H}\}$  NMR spectra were measured at 100.63 MHz, the chemical shifts of these spectra were referenced to the solvent peaks of the deuterated solvent.

Relaxation time  $T_1$  measurements were carried out at 400 MHz by the inversion-recovery method using the standard  $180^\circ\text{-}\tau\text{-}90^\circ$  pulse sequence. High-pressure studies were carried out in a commercial 5mm Wilmad pressure-valved NMR tube.

### 3.3 Syntheses and Characterization

#### 3.3.1 $(\eta^5\text{-C}_5\text{H}_4(\text{CH}_2)_2\text{NMe}_2)\text{Ru}(\text{P}(\text{OPh})_3)_2\text{Cl}$ (**40**)

A solution containing  $(\eta^5\text{-C}_5\text{H}_4(\text{CH}_2)_2\text{NMe}_2)\text{Ru}(\text{PPh}_3)_2\text{Cl}$  (1.00 g, 1.12 mmol) and triphenylphosphite (1.02 mL, 3.92 mmol) in toluene (50 mL) was refluxed for 48 h. Upon removal of the solvent under vacuum, 20 mL of ether was added to the residual paste with vigorously stirring to produce a yellow sticky solid which was then washed with hexane (2 x 20 mL) and dried in *vacuo*. Yield 0.87 g, (86%).

Anal. Calcd. for  $\text{C}_{45}\text{H}_{44}\text{ClNO}_6\text{P}_2\text{Ru}$ : C, 60.50; H, 4.96; N 1.58; Found: C, 59.36; H, 5.01; N 1.61.

$^1\text{H}$  NMR ( $\text{CDCl}_3$ , 400 MHz,  $20^\circ\text{C}$ ):  $\delta$ 1.84(2H, br s,  $-\text{CH}_2\text{-N}$ ), 2.21(2H, m, Cp- $\text{CH}_2$ ), 2.28(6H, s,  $\text{NMe}_2$ ), 3.54(2H, br s, Cp ring), 3.93(2H, br s, Cp ring), 6.81-7.33(30H, m,  $\text{P}(\text{OPh})_3$ ),  $^{31}\text{P}\{^1\text{H}\}$ NMR:  $\delta$ 138.3 (s).

### 3.3.2 $(\eta^5\text{-C}_5\text{H}_4(\text{CH}_2)_2\text{NMe}_2)\text{Ru}(\text{P}(\text{OPh})_3)(\text{P}(\text{OPh})_2\text{OC}_6\text{H}_4)$ (41)

A sample of 40 (0.25g, 0.28 mmol) was added to excess  $\text{AgSO}_3\text{CF}_3$  in THF (20 mL), the resulting solution was stirred at room temperature for 2 days. The solution was filtered to remove the silver chloride, and the solvent of the filtrate was removed by vacuum to yield a brown oily liquid. Elution of this oily compound through a neutral alumina column (1 cm x 10 cm) with toluene followed by ethanol gave, after evaporation of solvent, the pure complex as a tacky yellow solid. Yield 0.12 g, (50%).

The complex can also be prepared by an alternative method: a sample of 40 (0.12 g, 0.13 mmol) was added to a solution of sodium methoxide (1.25 g, 23.10 mmol) in methanol (30 mL), the resulting solution was allowed to reflux for 24 h. It was then filtered and the solvent was removed by vacuum to yield a yellow oil. The oily product was purified by elution through neutral alumina column (1 cm x 10 cm) with toluene followed by ethanol. Removal of solvent by vacuo yielded the product as sticky yellow solid. Yield 0.08 g, (33%).

Anal. Calcd. for  $\text{C}_{45}\text{H}_{43}\text{NO}_6\text{P}_2\text{Ru}$ : C, 63.08; H, 5.06; N, 1.63 ; Found: C, 62.06; H, 5.84; N, 1.67.

$^1\text{H}$  NMR (acetone- $d_6$ , 400 MHz, 20°C):  $\delta$ 1.86(2H, m,  $-\text{CH}_2\text{-N}$ ), 2.03(6H, s,  $\text{NMe}_2$ ), 2.06(2H, m,  $\text{Cp-CH}_2$ ), 4.08(1H, br s, Cp ring), 4.09(1H, br s, Cp ring), 4.37(1H, br s, Cp ring), 4.86(1H, br s, Cp ring), 6.89-7.52(29H, m,  $\text{P}(\text{OPh})_3$ ),  $^{31}\text{P}\{^1\text{H}\}$ NMR: 144.3(d,  $\text{P}(\text{OPh})_3$ ,  $^2\text{J}(\text{PP})=100\text{Hz}$ ), 170.9(d,  $\text{P}(\text{OPh})_2(\text{OC}_6\text{H}_4)$ ,  $^2\text{J}(\text{PP})=100\text{Hz}$ ).  $^{13}\text{C}\{^1\text{H}\}$ NMR: 111.10(d, Ru-C,  $^2\text{J}(\text{PC})=16.0\text{ Hz}$ ).

### 3.3.3 $[(\eta^5\text{-C}_5\text{H}_4(\text{CH}_2)_2\text{NMe}_2\text{H}^+)\text{Ru}(\text{P}(\text{OPh})_3)(\text{P}(\text{OPh})_2\text{OC}_6\text{H}_4)](\text{BF}_4)$ (**42**)

To a sample of **41** (0.10 g, 0.12 mmol) in 15 mL of tetrahydrofuran was added 1.2 equiv of tetrafluoroboric acid in ethereal solution ( $\text{HBF}_4\cdot\text{Et}_2\text{O}$  54%) (19  $\mu\text{L}$ , 0.14 mmol), the resulting solution was allowed to stir for 1 h. It was then concentrated to 1-2 mL, and 20 mL of hexane was added to precipitate the product. The solution was filtered and the product was washed with diethyl ether (2 x 15 mL) and dried in *vacuo* to yield a sticky yellowish brown solid. Yield 0.08 g, (73%).

Anal. Calcd. for  $\text{C}_{45}\text{H}_{44}\text{BF}_4\text{NO}_6\text{P}_2\text{Ru}$ : C, 57.22; H, 4.69; N, 1.48 ; Found: C, 57.54; H, 4.59; N, 1.57.

$^1\text{H}$  NMR ( $\text{CDCl}_3$ , 400 MHz, 20°C):  $\delta$ 2.39(2H, m,  $-\text{CH}_2\text{-N}$ ), 2.60(3H, d,  $\text{NH}^+\text{Me}_2$ ,  $J=4.3\text{Hz}$ ), 2.70(3H, d,  $\text{NH}^+\text{Me}_2$ ,  $J=4.3\text{Hz}$ ), 2.87(2H, m, Cp- $\text{CH}_2$ -), 5.04(1H, br s, Cp ring), 5.20(1H, br s, Cp ring), 5.45(1H, br s, Cp ring), 5.66(1H, br s, Cp ring), 6.95-7.38(29H, m,  $\text{P}(\text{OPh})_3$ ), 8.17 (1H, br,  $\text{HN}^+\text{Me}$ ).  $^{31}\text{P}\{^1\text{H}\}$ NMR: 144.2 (d,  $\text{P}(\text{OPh})_3$ ,  $^2\text{J}(\text{PP})=89\text{Hz}$ ), 172.9(d,  $\text{P}(\text{OPh})_2(\text{OC}_6\text{H}_4)$ ,  $^2\text{J}(\text{PP})=89\text{Hz}$ ).  $^{13}\text{C}\{^1\text{H}\}$ NMR: 111.21(d, Ru-C,  $^2\text{J}(\text{PC})=16.1\text{ Hz}$ ).

### 3.3.4 $[(\eta^5\text{-C}_5\text{H}_4(\text{CH}_2)_2\text{NMe}_2\text{H}^+)\text{Ru}(\text{P}(\text{OPh})_3)_2\text{H}](\text{BF}_4)$ (**43**)

A solution of **42** (0.20 g, 0.21 mmol) in chlorobenzene (15 mL) was stirred at room temperature under 25 bar of  $\text{H}_2$  in a stainless steel autoclave for 16 h. The reactor was carefully vented and the solvent of the resulting solution was removed by vacuum. The product was washed with 3 x 20 mL portions of hexane and 20 mL of diethyl ether to yield a sticky pale brown solid. Yield 0.15 g, (75%).

Anal. Calcd. for  $C_{45}H_{46}BF_4NO_6P_2Ru$ : C, 57.09; H, 4.90; N, 1.48 ; Found: C, 57.64; H, 5.04; N, 1.53.

$^1H$  NMR (benzene- $d_6$ , 400 MHz, 20°C):  $\delta$  -11.83 (1H, t,  $^2J(HP)$ =26.0 Hz, RuH), 2.33 (2H, br s,  $-CH_2-N$ ), 2.55 (6H, d,  $J$ =4.8 Hz,  $-NMe_2$ ), 2.89 (2H, br s, Cp- $CH_2$ -), 4.48(2H, s, Cp ring), 5.49(2H, s, Cp ring), 7.23-7.60(30H, m, P(OPh) $_3$ ), 8.43(1H, br s,  $Me_2N^+H$ ).  $^{31}P\{^1H\}$ NMR: 149.7 (s).

### 3.3.5 ( $\eta^5-C_5H_4(CH_2)_2NMe_2$ )Ru(P(OPh) $_3$ ) $_2$ H (44)

A sample of **43** (0.15g, 0.16 mmol) was added to a suspension of excess powdered potassium hydroxide in ethanol (20 mL). The mixture was allowed to stir overnight at room temperature. It was filtered to remove the unreacted KOH, and the solvent of the filtrate was removed in *vacuo* to yield a black oily liquid, which was extracted with 4 x 20mL portions of hexane. The solvent of the extract was removed by vacuum, and a very sticky brown solid was obtained. Yield 0.09 g, (65%).

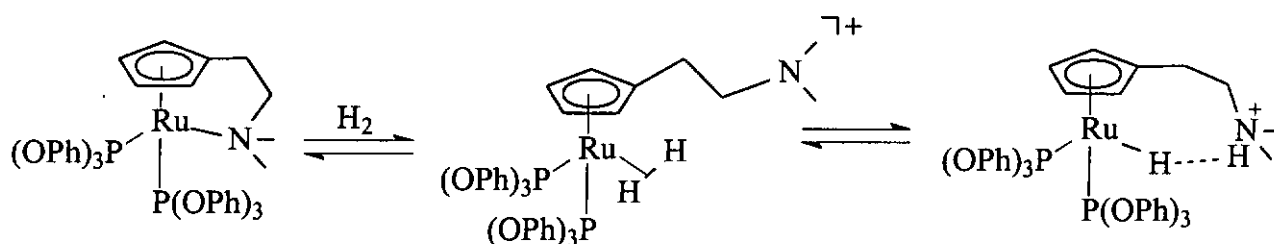
Anal. Calcd. for  $C_{45}H_{45}NO_6P_2Ru$ : C, 62.93; H, 5.28; N, 1.63; Found: C, 62.91; H, 5.25; N, 1.43.

$^1H$  NMR (benzene- $d_6$ , 400 MHz, 20°C):  $\delta$  -11.54 (1H, t,  $^2J(HP)$ =36.0 Hz, RuH), 2.21 (2H, br s,  $-CH_2-N$ ), 2.29(8H, br s, Cp- $CH_2$ - overlapped with  $-NMe_2$ ), 4.44(2H, s, Cp ring), 4.50(2H, s, Cp ring), 7.10-7.63(30H, m, P(OPh) $_3$ ).  $^{31}P\{^1H\}$ NMR: 143.7 (s).

### 3.4 Results and Discussion

#### 3.4.1 Synthesis and characterization of ortho-metalated amino-cyclopentadienyl ruthenium complexes

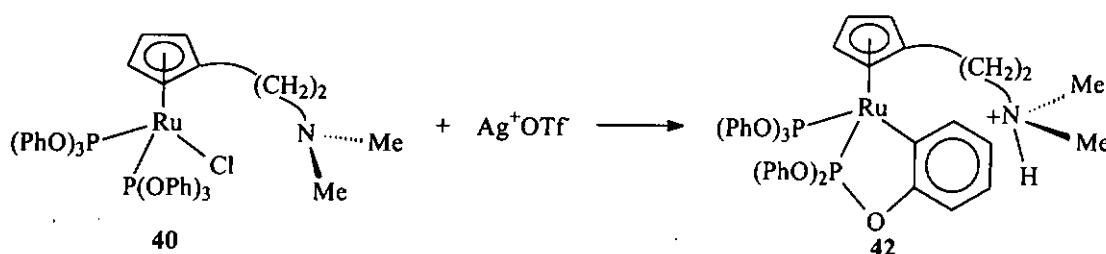
We intended to prepare the triphenylphosphite analogue of  $[(\eta^5:\eta^1\text{-C}_5\text{H}_4(\text{CH}_2)_2\text{NMe}_2)\text{Ru}(\text{dppm})]^+$ , **29** and then react the complex with pressurized  $\text{H}_2$  to obtain  $(\eta^5\text{-C}_5\text{H}_4(\text{CH}_2)_n\text{NMe}_2\text{H}^+)\text{Ru}(\text{P}(\text{OPh})_3)_2\text{H}$ , the phosphite analogue of  $[(\eta^5\text{-C}_5\text{H}_4(\text{CH}_2)_2\text{NMe}_2\text{H}^+)\text{Ru}(\text{dppm})\text{H}]$  (**31**), with which we would study the strength of its  $\text{Ru-H}\cdots\text{H-N}$  interaction. Comparisons in terms of H-bond strength and reactivity of this complex with those of **31** could then be made. (Scheme 3.1)



Scheme 3.1 Proposed mechanism of the reaction of  $[(\eta^5:\eta^1\text{-C}_5\text{H}_4(\text{CH}_2)_2\text{N}(\text{Me}_2))\text{Ru}[\text{P}(\text{OPh})_3]_2]$  towards  $\text{H}_2$

The chloro precursor  $(\eta^5\text{-C}_5\text{H}_4(\text{CH}_2)_2\text{NMe}_2)\text{Ru}(\text{P}(\text{OPh})_3)_2\text{Cl}$  (**40**) was prepared by refluxing a solution of  $(\eta^5\text{-C}_5\text{H}_4(\text{CH}_2)_2\text{NMe}_2)\text{Ru}(\text{PPh}_3)_2\text{Cl}$  with triphenylphosphite in toluene. We reacted the chloro complex **40** with  $\text{AgOTf}$ , anticipating

that removal of the chloro ligand would create a vacant site, which would be occupied by the amine sidearm, thus producing the desired complex. But apparently, instead of sidearm coordination, proximal generation of a vacant coordination site at the cationic ruthenium center induced cyclometalation of one of the triphenylphosphite ligands and produced the ortho-metalated complex  $[(\eta^5\text{-C}_5\text{H}_4(\text{CH}_2)_2\text{NMe}_2\text{H}^+)\text{Ru}(\text{P}(\text{OPh})_3)(\text{P}(\text{OPh})_2\text{OC}_6\text{H}_4)]^+\text{OTf}^-$  (**42-OTf**) (Eq 3.1).



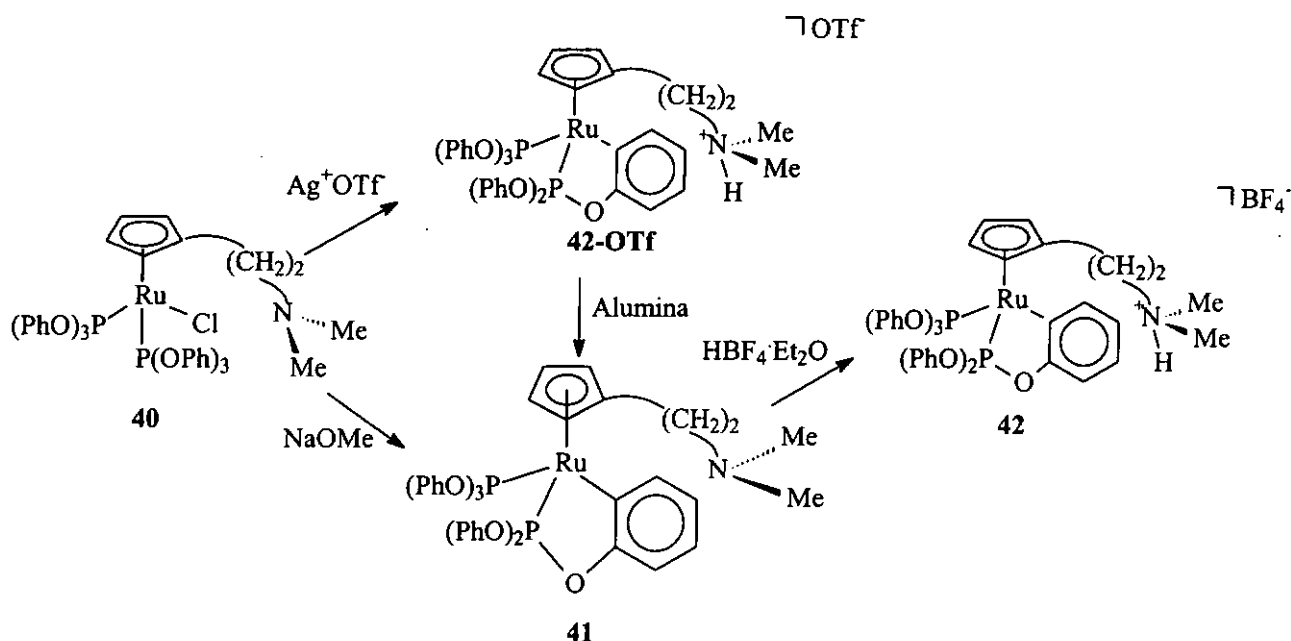
Formation of **42** is not surprising, since it is known that the unsubstituted Cp complex  $(\eta^5\text{-C}_5\text{H}_5)\text{Ru}(\text{PPh}_3)(\text{P}(\text{OPh})_3)\text{Cl}$  reacts with  $\text{AgOTf}$  in the presence of piperidine at room temperature to give the ortho-metalated complex  $(\eta^5\text{-C}_5\text{H}_5)(\text{PPh}_3)(\eta^2\text{-P}(\text{OPh})_2\text{OC}_6\text{H}_4)$  [82]. Ortho-metalated Cp ruthenium and osmium complexes are well-documented [70, 71], [82]. Complex **42** was characterized by NMR spectroscopy. The  $^{31}\text{P}\{^1\text{H}\}$  NMR spectrum showed two doublets corresponding to the two inequivalent phosphites at  $\delta$  144.2 and 172.9 ppm ( $J(\text{PP}) = 89$  Hz). The sharp AX pattern indicates that there is no interconversion of the two phosphites at room temperature by reversible metalation/demetalation of ortho-hydrogens on the two different phosphites. Exchange of the two phosphines has been observed in the ortho-metalated iridium complex  $\text{IrH}(\text{C}_2\text{Ph})(\text{P}'\text{Bu}_2\text{Ph})(\eta^2\text{-C}_6\text{H}_4\text{P}'\text{Bu}_2)$  [83]. The doublet signal at  $\delta$  111.2 ppm ( $J(\text{CP}) = 16.1$

Hz) in the  $^{13}\text{C}$  NMR spectrum of **42** is diagnostic of metalated ortho-carbon atom Ru-C. Signals with similar chemical shifts and P-C coupling constants also appear in  $^{13}\text{C}$  NMR spectra of similar ortho-metalated Ru(II) complexes [70],[82]. The amine group in the sidearm was protonated. Evidence for amine protonation was provided by  $^1\text{H}$  NMR spectrum of **42**, it showed the N-methyl protons as two doublets at  $\delta$  2.60 ( $J(\text{HH}) = 4.4$  Hz) and 2.70 ( $J(\text{HH}) = 4.3$  Hz) ppm, which were downfield-shifted from the N-methyl proton signal of the free ligand  $\text{C}_5\text{H}_5(\text{CH}_2)_2\text{NMe}_2$  ( $\delta$  2.27 ppm). Similar downfield shifts of the N-methyl protons have been observed in **31** and its chloro analogue [79], in molybdenum [70, 71] and rhodium [83] complexes containing similar ligands. Protonation of the amine group in **42** was also supported by observation of the broad singlet signal of N-H at  $\delta$  8.20 ppm. It is also noteworthy that the N-methyl groups are inequivalent, probably due to restricted rotation of the C-N bond.

It is difficult to obtain analytically pure sample of **42** by the silver triflate reaction (Eq. 3.1), probably due to difficulty in completely removing the silver salts from the product, which is a sticky semi-solid. We attempted to purify **42** by column chromatography using neutral alumina, but the product collected was the deprotonated form of **42**, i.e.  $(\eta^5\text{-C}_5\text{H}_4(\text{CH}_2)_2\text{NMe}_2)\text{Ru}(\text{P}(\text{OPh})_3)(\eta^2\text{-P}(\text{OPh})_2\text{OC}_6\text{H}_4)$  (**41**). The  $^{31}\text{P}\{^1\text{H}\}$  NMR spectrum of **41** is similar to that of **42**, showing two doublets at  $\delta$  144.3 ( $J(\text{PP}) = 99.9$  Hz) and 170.9 ( $J(\text{PP}) = 99.9$  Hz) ppm. The  $^{13}\text{C}$  NMR spectrum of **41**, similar to that of **42**, also contains a doublet in the downfield region at  $\delta$  111.1 ppm ( $J(\text{CP}) = 16.0$  Hz), due to Ru-C. However, the  $^1\text{H}$  NMR spectrum of **41**, shows, instead of a pair of downfield-shifted doublets for the N-methyl protons, a relatively upfield singlet, which integrates to 6



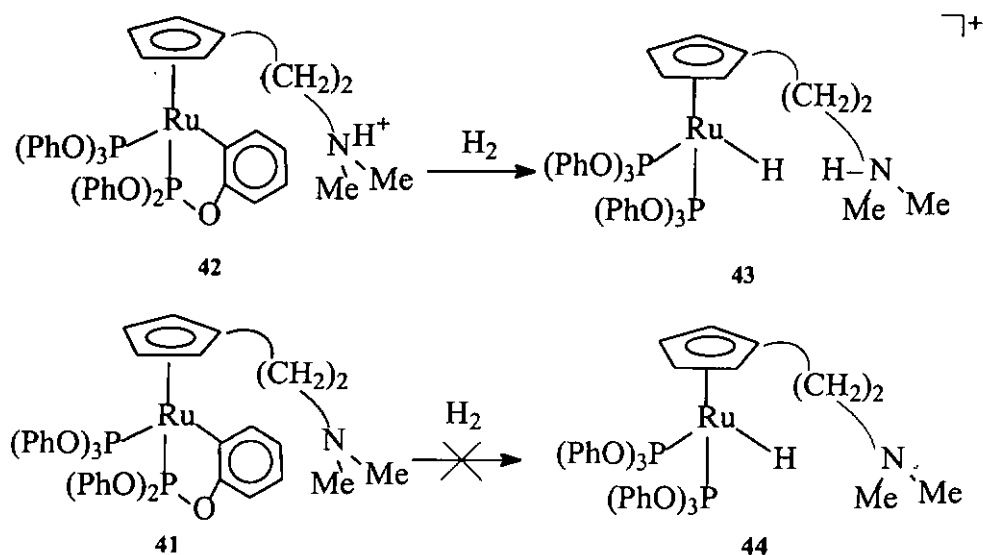
hydrogens, at  $\delta$  1.90 ppm. No N-H signal is observable in the downfield region. Acidification of **41** with tetrafluoroboric acid in etheral solution gives **42** of acceptable purity. Complex **41** can also be prepared by refluxing **40** with sodium methoxide in methanol (Scheme 3.2). Similar ortho-metalation has been achieved for  $(\eta^5\text{-C}_5\text{H}_5)\text{Ru}(\text{P}(\text{OPh})_3)_2\text{Cl}$  by refluxing the complex with methoxide ion in methanol [70]. However, the complexes  $(\eta^5\text{-C}_5\text{H}_5)\text{Ru}(\text{PPh}_3)_2\text{Cl}$  and  $(\eta^5\text{-C}_5\text{H}_5)\text{Ru}(\text{PPh}_3)(\text{P}(\text{OPh})_3)\text{Cl}$  cannot be ortho-metalated under the same experimental conditions [82].



**Scheme 3.2** Reaction pathways for the preparation of ortho-metalated aminocyclopentadienyl ruthenium complexes

### 3.4.2 Synthesis and characterization of hydrido aminocyclopentadienyl ruthenium complexes

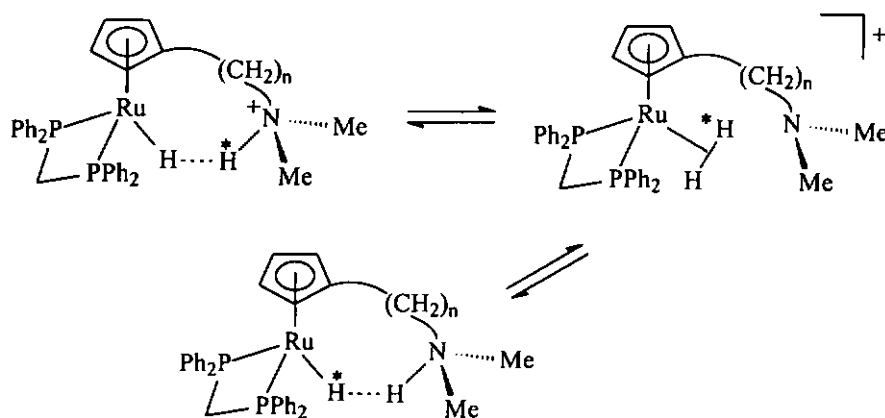
Study of reactivity of **42** and **41** toward pressurized dihydrogen gave interesting results. Complex **42** reacted, as expected, with H<sub>2</sub> (10 atm) in chlorobenzene at room temperature to yield our targeted complex  $[(\eta^5\text{-C}_5\text{H}_4(\text{CH}_2)_2\text{NMe}_2\text{H}^+)\text{Ru}(\text{P}(\text{OPh})_3)_2\text{H}]^+$  (**43**) (Eq. 3.2). Under identical experimental conditions, **41** is, however, inert to H<sub>2</sub>. We expect **41**, in analogous to **42**, to react with H<sub>2</sub>, forming the deprotonated form of **43**, i.e.  $(\eta^5\text{-C}_5\text{H}_4(\text{CH}_2)_2\text{NMe}_2)\text{Ru}(\text{P}(\text{OPh})_3)_2\text{H}$  (**44**). It was later found out that **44** could be obtained by deprotonation of **43** with aqueous KOH in ethanol.



Eq. 3.2

In the <sup>1</sup>H NMR spectrum of **43**, the hydride signal is a sharp triplet (*J*(HP) = 26.0 Hz) at δ -11.83 ppm. Similar to its precursor **42**, complex **43** shows a downfield

shifted signal ( $\delta$  2.61 ppm) for its N-methyl protons, but the signal is a singlet rather than a pair of doublets as observed for the N-methyl protons of **42**. The N-H of **43**, which does not split the N-methyl signal, appears as a broad peak at  $\delta$  8.47 ppm. The  $^{31}\text{P}\{^1\text{H}\}$  NMR spectrum of **43** shows a singlet at  $\delta$  149.7 ppm, indicating that the two phosphorous atoms are equivalent. Several attempts to obtain single crystals of **43** for x-ray structural determination have not been successful; in fact, this complex, and other phosphite complexes reported in this work, are sticky solids, they all resist single crystal formation.



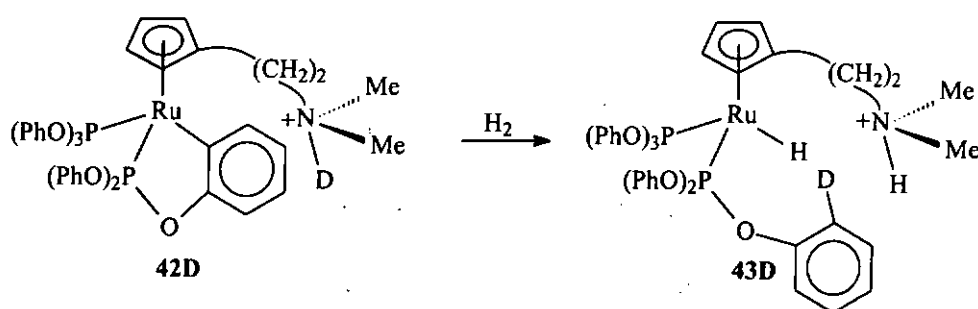
**Scheme 3.3** Proposed mechanism for the rapid and reversible hydride proton exchange via  $\eta^2$ -tautomer in  $[(\eta^5:\eta^1\text{-C}_5\text{H}_4(\text{CH}_2)_2\text{NMe}_2)\text{Ru}(\text{dppm})]^+$

Sharpness of the hydride signal of **43** indicates that  $\text{H}\cdots\text{H}$  interaction between the hydride ligand and N-H on the pendant amine arm is very weak, if exists at all. On the contrary, complex **31**, the dppm analogue of **43**, which shows a broad hydride signal, exhibits considerably strong  $\text{Ru-H}\cdots\text{H-N}$  dihydrogen-bonding interaction, the two hydrogen atoms undergo rapid exchange via the intermediacy of a  $\eta^2$ -dihydrogen species [79] (Scheme 3.3). Broadening of the hydride signal of  $\text{WH}(\text{CO})_2(\text{NO})(\text{PMe}_3)_2$  was

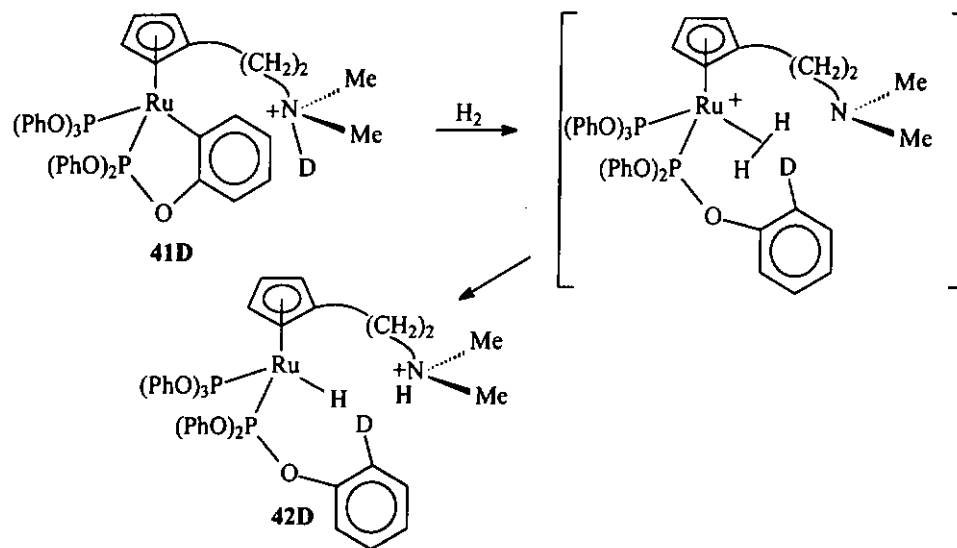
observed in the presence of acidic alcohol, due to the formation of intermolecular M-H...H-OR dihydrogen bond [25]. Significant broadening of the hydride signals of both *cis* and *trans* isomers of RuH<sub>2</sub>(dppm)<sub>2</sub> were also observed upon addition of excess phenol [32]. Lack of Ru-H...H-N dihydrogen-bonding interaction in **43** was also supported by the fact that practically no NOE was detected between Ru-H and N-H. Variable temperature  $T_1$  measurements for the hydride ligand of **43** yielded a  $T_1$ (min) of 890 ms (at 400 MHz and 290 K), this value is very similar to that of the hydride ligand of **44** ( $T_1$ (min) = 900 ms at 400 MHz and 248 K); similarity of  $T_1$ (min) values of the hydride ligands of **43** and **44** lends further support to the notion that intramolecular dihydrogen-bonding interaction in the former is minimal. It is obviously true that the less donating triphenylphosphite ligands lower the basicity of the metal center in **43**, which, in turn decreases the hydricity of the hydride ligand to such an extent that the Ru-H...H-N dihydrogen bond is no longer stable. M-H...H-X dihydrogen bond is a hydride-proton interaction, and its bond strength can be modulated by tuning the nucleophilicity of M-H and/or electrophilicity of H-X [39, 40, 46, 84]. Epstein, Berke, and co-workers have reported that the strengths of the dihydrogen bonds in the tungsten hydride-alcohol complexes W(CO)<sub>2</sub>(NO)(L)<sub>2</sub>H...HOR increase with the donor abilities of the ligand L (PPh<sub>3</sub> < P(<sup>*i*</sup>Pr)<sub>3</sub> < PEt<sub>3</sub> < PMe<sub>3</sub>) [25].

Unlike the dppm analogue **31**, **43** is stable towards H<sub>2</sub> loss even after reflux in THF or heating at 90 °C in chlorobenzene for 2 days. This is not unexpected since lack of Ru-H...H-N dihydrogen bonding in **43** precludes the possibility of eliminating H<sub>2</sub> via the intermediacy of a  $\eta^2$ -H<sub>2</sub> species.

To learn more about the reaction of **42** with H<sub>2</sub>, we reacted  $[(\eta^5\text{-C}_5\text{H}_4(\text{CH}_2)_2\text{NMe}_2\text{D}^+)\text{Ru}(\text{P}(\text{OPh})_3)(\text{P}(\text{OPh})_2\text{OC}_6\text{H}_4)]^+\text{OTf}^-$  (**42D**), the deuterated form of **42** in which the amine sidearm was deuterated, with H<sub>2</sub> and studied the distribution of deuterium in the product. A combination of <sup>1</sup>H and <sup>2</sup>H NMR spectroscopic studies clearly indicated that all the deuterium atoms had been transferred to the triphenylphosphite ligand, and the Ru-H and N-H groups were deuterium-free (Eq. 3.3).



The result of the labeling experiment is in consonance with the proposed reaction mechanism depicted in Scheme 3.4. The crucial step of the hydrogenolysis of **42** with H<sub>2</sub> seems to be protonation of the ortho-carbon in Ru-C by the ammonium proton. It is therefore not surprising to find that **41**, which is devoid of an ammonium proton, is unreactive towards H<sub>2</sub>.



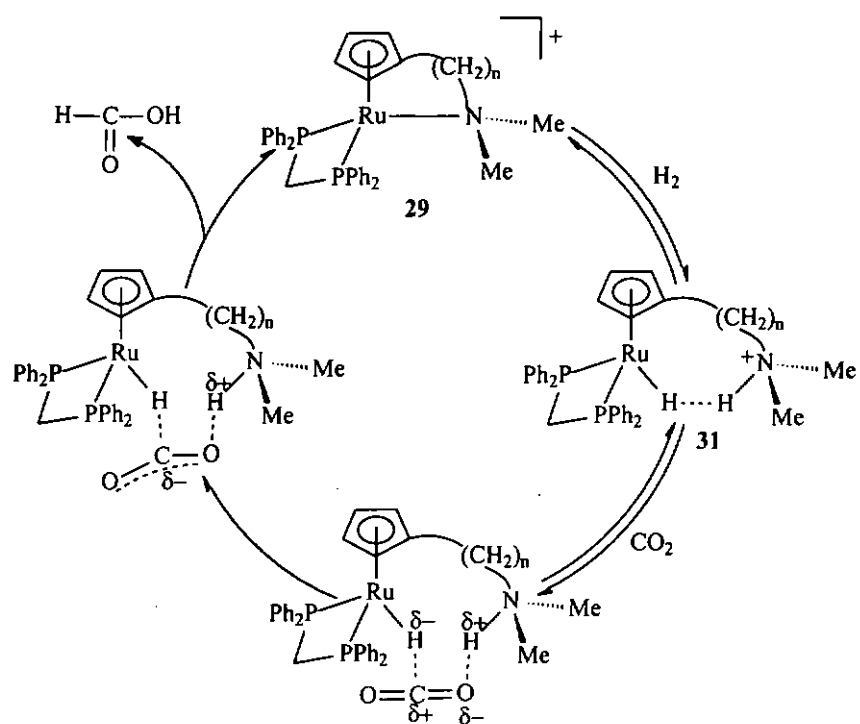
**Scheme 3.4** Proposed reaction pathway of the deuterium labeling experiment

As expected, the  $^1\text{H}$  NMR spectrum of **44** shows a relatively upfield singlet signal for its non-protonated amine group ( $\delta$  2.29 ppm), and no N-H signal is observable in the downfield region. The two equivalent phosphite ligands of **44** appear as a singlet at  $\delta$  143.7 ppm in the  $^{31}\text{P}\{^1\text{H}\}$  NMR spectrum.

### 3.4.3 Reactivities of $[(\eta^5\text{-C}_5\text{H}_4(\text{CH}_2)_2\text{NMe}_2\text{H})\text{Ru}(\text{P}(\text{OPh})_3)_2\text{H}]^+$ towards $\text{H}_2/\text{CO}_2$ .

Since complex **31**, the dppm analogue of **43**, is believed to play a crucial role in reduction of  $\text{CO}_2$  to formic acid catalyzed by its precursor complex **29** (Scheme 3.5), we are thus interested in studying the catalytic activity of **43** (or its precursor **42**) in  $\text{CO}_2$  hydrogenation. No catalytic activity was, however, found. Lack of activity in **43** is attributable to low hydricity of the hydride ligand. In **43**, although the protonated amine

sidearm, like that of 31, can H-bond with one of the oxygen atoms of an incoming CO<sub>2</sub> molecule and thus enhancing the electrophilicity at the carbon, the hydride ligand is unfortunately not hydridic enough to allow its abstraction by the electrophilic carbon center.



**Scheme 3.5** Proposed mechanism for the hydrogenation of carbon dioxide by  $[(\eta^5\text{:}\eta^1\text{-C}_5\text{H}_4(\text{CH}_2)_2\text{NMe}_2)\text{Ru}(\text{dppm})]^+$

## 4. Conclusion

Intermolecular and intramolecular hydrogen bonding is crucial in many chemical reactions including proton transfer reactions. The hydrogen bond strength depends on the proton donating ability of the proton donor and the proton accepting ability of the proton acceptor. Choosing different proton donors or acceptors can vary the strength of the hydrogen bond. The proton transfer reaction between different acidic alcohols; trifluoroethanol (TFE), hexafluoroisopropanol (HFIP) and *per-tert*-fluorobutanol (PFTB) and ruthenium complexes;  $\text{TpRu}(\text{PPh}_3)_2\text{H}$  and  $[\text{TpmRu}(\text{PPh}_3)_2\text{H}](\text{BF}_4)$  were investigated. Intermolecular hydrogen bonded species was detected in variable temperature  $^1\text{H}$  NMR spectra when  $\text{TpRu}(\text{PPh}_3)_2\text{H}$  reacted with acidic alcohol only. Moreover, with HFIP the intermolecularly hydrogen-bonded intermediate was in equilibrium with the  $\eta^2\text{-H}_2$  complex, the product of proton transfer reaction. The stability of the intermolecular hydrogen bond depends on both the proton accepting power of the metal hydride and also the proton donating ability of the acidic alcohols.

For the reaction of TFE with  $\text{TpRu}(\text{PPh}_3)_2\text{H}$ , the low acidity of TFE led to the formation of hydrogen bonded species as the only product. The product of complete proton transfer, the dihydrogen complex was not detected. When a more acidic alcohol, HFIP was employed, variable temperature  $^1\text{H}$  NMR experiment showed an equilibrium between the hydrogen bonded species and the  $\eta^2\text{-H}_2$  complex. Unfortunately,  $T_1(\text{min})$  of the hydrogen-bonded hydride ligand cannot be measured since it broadened into the baseline at temperature lower than 263 K. For the reaction of the most acidic alcohol PFTB



with  $\text{TpRu}(\text{PPh}_3)_2\text{H}$ , the high acidity of PFTB ensured complete proton transfer yielding the  $\eta^2\text{-H}_2$  complex as the only species detected throughout the variable temperature  $^1\text{H}$  NMR experiment.

Changing from the neutral ruthenium complex  $\text{TpRu}(\text{PPh}_3)_2\text{H}$ , to the mono-cationic complex,  $[\text{TpmRu}(\text{PPh}_3)_2\text{H}](\text{BF}_4)$ , no intermolecular hydrogen bonding interaction with any acidic alcohol was observed. The reason of the absence of such interaction with acidic alcohol is attributable to diminished hydricity of the hydride ligand in the complex. The net positive charge of the metal center is responsible for the low hydricity.

Intramolecular  $\text{Ru-H}\cdots\text{H-N}$  dihydrogen bond was previously detected in  $\text{CpNH}^+\text{Ru}(\text{dppm})\text{H}$  (**31**) ( $\text{CpN} = [2\text{-}(\text{N,N-Dimethylamino})\text{ethyl}]\text{cyclopentadienyl}$ ) by our group, in continuing our studies of dihydrogen bonding in aminocyclopentadienyl ruthenium hydride complexes and catalytic activity of these complexes in  $\text{CO}_2$  hydrogenation, I have studied the effect of decreased the basicity of the metal center on the strength of the  $\text{Ru-H}\cdots\text{H-N}$  dihydrogen bond. The basicity of the metal center in the aminocyclopentadienyl ruthenium complex was decreased by replacement of the dppm ligand in **31** or **29** with triphenylphosphite.

The complex  $\text{CpNRu}(\text{P}(\text{OPh})_3)_2\text{Cl}$  was synthesized by refluxing its precursor  $\text{CpNRu}(\text{PPh}_3)_2\text{Cl}$  with triphenylphosphite in toluene. Treatment of  $\text{CpNRu}(\text{P}(\text{OPh})_3)_2\text{Cl}$  with silver triflate yielded the ortho-metalated complex,  $[(\eta^5\text{-C}_5\text{H}_4(\text{CH}_2)_2\text{NMe}_2\text{H}^+)\text{Ru}(\text{P}(\text{OPh})_3)(\text{P}(\text{OPh})_2\text{OC}_6\text{H}_4)]^+\text{OTf}$  (**42-OTf**) with the side arm

protonated. This complex was obtained in impure form due to difficulty in completely removing the silver salts for the product. Eluting a sample of **42-OTf** through neutral alumina yielded the deprotonated ortho-metalated complex, ( $\eta^5$ -C<sub>5</sub>H<sub>4</sub>(CH<sub>2</sub>)<sub>2</sub>NMe<sub>2</sub>)Ru(P(OPh)<sub>3</sub>)(P(OPh)<sub>2</sub>OC<sub>6</sub>H<sub>4</sub>), (**41**). Acidification of **41** by HBF<sub>4</sub>·Et<sub>2</sub>O yielded pure  $[(\eta^5\text{-C}_5\text{H}_4(\text{CH}_2)_2\text{NMe}_2\text{H}^+)\text{Ru}(\text{P}(\text{OPh})_3)(\text{P}(\text{OPh})_2\text{OC}_6\text{H}_4)]^+(\text{BF}_4)^-$  (**42**). Application of hydrogen pressure (25 atm) to **41** and **42** yielded different results, **42** reacted with hydrogen to yield the hydride complex,  $[(\eta^5\text{-C}_5\text{H}_4(\text{CH}_2)_2\text{NMe}_2\text{H}^+)\text{Ru}(\text{P}(\text{OPh})_3)_2\text{H}](\text{BF}_4)$  (**43**), which is analogous to **31** while **41** did not react with hydrogen gas. The amine sidearm deprotonated hydride, ( $\eta^5$ -C<sub>5</sub>H<sub>4</sub>(CH<sub>2</sub>)<sub>2</sub>NMe<sub>2</sub>)Ru(P(OPh)<sub>3</sub>)<sub>2</sub>H (**44**) was synthesized by stirring **43** with KOH in ethanol. NOE experiments for **43** were carried out but no Ru-H···H-N dihydrogen-bonding interaction was detected between the protonated amine sidearm and the ruthenium hydride. It is obviously true that the less donating triphenylphosphite ligands lower the basicity of the metal center in **43**, which, in turn decreases the hydricity of the hydride ligand to such an extent that the Ru-H···H-N dihydrogen bond is no longer stable.

Finally, catalytic activity of **43** towards catalytic hydrogenation of carbon dioxide to formic acid was examined. However, no catalytic activity was detected. Lack of activity is attributed to the low hydricity of the hydride ligand in **43**. Though the protonated amine sidearm can H-bond with one of the oxygen atoms of an incoming CO<sub>2</sub> molecule and thus enhancing the electrophilicity at the carbon, the hydride ligand is unfortunately not hydridic enough to allow its abstraction by the electrophilic carbon center.

## Reference

1. Jeffery, G.A. and W. Saenger, *Hydrogen bonding in biological structures*. 1991, Berlin: Springer-Verlag.
2. Shubina, E.S., N.V. Belkova, and L.M. Epstein, *Novel types of hydrogen bonding with transition metal  $\pi$ -complexes and hydrides*. *Journal of Organometallic Chemistry*, 1997. **536-537**: p. 17-29.
3. Lokshin, B.V., A. Ginzburg, and S.G. Kazaryan, *Infrared spectra of  $[\text{CpRu}(\text{CO})_2]_2$  in liquid xenon solution in the presence of proton donors*. *Journal of Organometallic Chemistry*, 1990. **397**: p. 203-208.
4. Hamley, P.A., S.G. Kazarian, and M. Poliakoff, *Hydrogen bonding and photochemistry of organometallics in liquid xenon solution in the presence of proton donors: A low temperature infrared study of the interaction of  $(\text{CF}_3)_3\text{COH}$  with  $(\text{C}_5\text{Me}_5)\text{M}(\text{CO})_2\text{L}$  ( $\text{M} = \text{Mn}$  and  $\text{Re}$ ;  $\text{L} = \text{CO}$ ,  $\text{N}_2$ , and  $\text{H}_2$ ) and with  $(\text{C}_5\text{Me}_5)\text{V}(\text{CO})_4$* . *Organometallics*, 1994. **13**: p. 1767-1774.
5. Braga, D., F. Grepioni, P. Sabatino, and G.R. Desiraju, *Hydrogen bonding in organometallic crystals. 1. From carboxylic acids and alcohols to carbonyl complexes*. *Organometallics*, 1994. **13**: p. 3532-3543.
6. Braga, D., F. Grepioni, K. Biradha, V.R. Pedireddi, and G.R. Desiraju, *Hydrogen bonding in organometallic crystals. 2. C-H...O hydrogen bonds in bridged and terminal*. *Journal of the American Chemical Society*, 1995. **117**: p. 3156-3166.

7. Kubas, G.J., R.R. Ryan, B.I. Swanson, P.J. Vergamini, and H.J. Wasserman, *Characterization of the First Examples of Isolable Molecular Hydrogen Complexes,  $M(\text{CO})_3(\text{PR}_3)_2(\text{H}_2)$  ( $M = \text{Mo}, \text{W}$ ;  $R = \text{Cy}, i\text{-Pr}$ ). Evidence for a Side-on Bonded  $\text{H}_2$  Ligand.* Journal of American Chemical Society, 1984. **106**: p. 451-452.
8. Kubas, G.J., *Molecular Hydrogen Complexes: Coordination of a  $\sigma$  Bond to Transition Metals.* Accounts of Chemical Research, 1988. **21**: p. 120-128.
9. Heinekey, D.M. and W.J.J. Oldham, *Coordination Chemistry of Dihydrogen.* Chemistry Reviews, 1993. **93**: p. 913-926.
10. Jessop, P.G. and R.H. Morris, *Reactions of transition metal dihydrogen complexes.* Coordination Chemistry Reviews, 1992. **121**: p. 155-284.
11. Crabtree, R.H., *Dihydrogen Complexes: Some Structural and Chemical Studies.* Accounts of Chemical Research, 1990. **23**: p. 95-101.
12. Calderazzo, F., G. Fachinetti, and F. Marchetti, *Preparation and crystal and molecular structure of two trialkylamine adducts of  $\text{HCo}(\text{CO})_4$  showing a preferential  $\text{NR}_3\text{H}^+\cdots[(\text{OC})_3\text{Co}(\text{CO})^-]$  interaction.* Chemical Communications, 1981: p. 181-183.
13. Brammer, L., J.M. Charnock, P.L. Goggin, R.J. Goodfellow, T.F. Koetzle, and A.G. Orpen, *Hydrogen bonding by cisplatin derivatives: Evidence for the formation of  $\text{N}\cdots\text{H}\cdots\text{Cl}$  and  $\text{N}\cdots\text{H}\cdots\text{Pt}$  bonds in  $[\text{NPr}^n_4]_2\{[\text{PtCl}_4]\cdot\text{cis}-[\text{PtCl}_2(\text{NH}_2\text{Me})_2]\}$ .* Chemical Communications, 1987: p. 443-445.
14. Brammer, L., J.M. Charnock, P.L. Goggin, R.J. Goodfellow, A.G. Orpen, and T.F. Koetzle, *The role of transition metal atoms as hydrogen bond acceptors: a neutron*

- diffraction study of  $[NPr^n_4]_2[PtCl_4] \cdot cis-[PtCl_2(NH_2Me)_2]$  at 20 K.* Dalton Transactions, 1991: p. 1789-1798.
15. Brammer, L., M.C. McCann, R.M. Bullock, R.K. McMullan, and P. Sherwood,  *$Et_3NH^+Co(CO)_4^-$ : Hydrogen-bonded adduct or simple ion pair? Single-crystal neutron diffraction study at 15K.* Organometallics, 1992. 11: p. 2339-2341.
  16. Kazarian, S.G., P.A. Hamley, and M. Poliakoff, *Intermolecular Hydrogen Bonding to Transition Metal Centres; Infrared Spectroscopic Evidence for O-H...Ir Bonding between  $[(\eta^5-C_5Me_5)Ir(CO)_2]$  and Fluoroalcohols in Solution at Room Temperature.* Chemical Communications, 1992: p. 994-997.
  17. Shubina, E.S., A.N. Krylov, A.Z. Kreindin, M.I. Rybinskaya, and L.M. Epstein, *Hydrogen-bonded complexes involving the metal atom and protonation of metallocenes of the iron subgroup.* Journal of Organometallic Chemistry, 1994. 465: p. 259-262.
  18. Shubina, E.S., A.N. Krylov, N.V. Belkova, L.M. Epstein, A.P. Borisov, and V.D. Mahaev, *The role of hydrogen bonds involving the metal atom in protonation of polyhydrides of molybdenum and tungsten of  $MH_4(dppe)_2$ .* Journal of Organometallic Chemistry, 1995. 493: p. 275-277.
  19. Hedden, D., D.M. Roundhill, W.C. Fultz, and A.L. Rheingold, *Reaction chemistry of some new hybrid phosphine amide complexes of platinum (II) and palladium (II). Isolation and x-ray structure determination of an ortho-metalated platinum(II) complex derived from a chelated phosphine amide complex of platinum(II).* Organometallics, 1986. 5: p. 336-343.

20. Shubina, E.S., A.N. Krylov, T.V. Timofeeva, Y.T. Struchkov, A.G. Ginzburg, N.M. Loim, and L.M. Epstein, *Hydrogen bonds and conformations of  $\alpha$ -carbinol derivatives of cyclopentadienyltricarbonyls of manganese and rhenium*. Journal of Organometallic Chemistry, 1992. 434: p. 329-339.
21. Kegley, S.E., C.J. Schaverien, J.H. Freudenberger, and R.G. Bergman, *Rhodium alkoxide complexes: Formation of an unusually strong intermolecular hydrogen bond in  $(PMe_3)_3Rh-Otol(HOtol)$* . Journal of the American Chemical Society, 1987. 109: p. 6563-6565.
22. Kim, Y.J., K. Osakada, A. Takenaka, and A. Yamamoto, *Allylnickel and -palladium alkoxides associated with alcohols through hydrogen bonding*. Journal of the American Chemical Society, 1990. 112: p. 1096-1104.
23. Alsters, P.L., P.J. Basejou, M.D. Janssen, H. Kooijman, A. Sicherer-Roetman, A.L. Spek, and G. van Kotén, *Palladium and platinum diphenoxide and aryl phenoxide complexes with amine donors: Effect of hydrogen bonding on structure and properties*. Organometallics, 1992. 11: p. 4124-4135.
24. Yandulov, D.V., K.G. Caulton, N.V. Belkova, E.S. Shubina, L.M. Epstein, D.V. Khoroshun, D.G. Musaev, and K. Morokuma, *Dimishing  $\pi$ -Stabilization of an Unsaturated Metal Center: Hydrogen Bonding to  $OsHCl(CO)(P^tBu_2Me)_2$* . Journal of the American Chemical Society, 1998. 120: p. 12553-12563.
25. Shubina, E.S., N.V. Belkova, A.N. Krylov, E.V. Vorontsov, L.M. Epstein, D.G. Gusev, M. Niedermann, and H. Berke, *Spectroscopic Evidence for Intermolecular M-H $\cdots$ H-OR Hydrogen Bonding: Interaction of  $WH(CO)_2(NO)L_2$  Hydrides with*

- Acidic Alcohols*. Journal of the American Chemical Society, 1996. **118**: p. 1105-1112.
26. Belkova, N.V., E.S. Shubina, A.V. Ionidis, L.M. Epstein, H. Jacobsen, A. Messmer, and H. Berke, *Intermolecular Hydrogen Bonding of  $ReH_2(CO)(NO)L_2$  Hydrides with Perfluoro-tert-butyl Alcohol. Competition between  $M-H\cdots H-OR$  and  $M-NO\cdots H-OR$  Interactions*. Inorganic Chemistry, 1997. **36**: p. 1522-1525.
27. Messmer, A., H. Jacobsen, and H. Berke, *Probing Regioselective Intermolecular Hydrogen Bonding to  $[Re(CO)H_2(NO)(PR_3)_2]$  Complexes by NMR Titration and Equilibrium NMR Methodologies*. Chemistry - A European Journal, 1999. **5**(11): p. 3341-3349.
28. Belkova, N.V., E.S. Shubina, E.I. Gutsul, L.M. Epstein, I.L. Eremenko, and S.E. Nefedov, *Structural and energetic aspects of hydrogen bonding and proton transfer to  $ReH_2(CO)(NO)(PR_3)_2$  and  $ReHCl(CO)(NO)(PMe_3)_2$  by IR and X-ray studies*. Journal of Organometallic Chemistry, 2000. **610**: p. 58-70.
29. Shubina, E.S., et al., *In situ IR and NMR study of the interactions between proton donors and the Re(I) hydride complex  $[(MeC(CH_2PPh_2)_3)Re(CO)_2H]$ .  $ReH\cdots H$  bonding and proton transfer pathways*. Inorganic Chimica Acta, 1998. **280**: p. 302-307.
30. Belkova, N.V., E.V. Bakhmutova, E.S. Shubina, C. Bianchini, M. Peruzzini, V.I. Bakhmutov, and L.M. Epstein, *The Energy Profile of Proton Transfer from Bronsted Acids to Terminal Hydrides in Transition Metal Complexes Can Be Estimated by Combining in situ IR and NMR Spectroscopy*. European Journal of Inorganic Chemistry, 2000: p. 2163-2165.

31. Belkova, N.V., A.V. Ionidis, L.M. Epstein, E.S. Shubina, S. Gruendemann, N.S. Golubev, and H.H. Limbach, *Proton Transfer to CpRuH(CO)(PCy<sub>3</sub>) Studied by Low-Temperature IR and NMR Spectroscopy*. *European Journal of Inorganic Chemistry*, 2001: p. 1753-1761.
32. Ayllon, J.A., C. Gervaux, S. Sabo-Etienne, and B. Chaudret, *First NMR Observation of the Intermolecular Dynamic Proton Transfer Equilibrium between a Hydride and Coordinated Dihydrogen:  $(dppm)_2HRuH \cdots H-OR = [(dppm)_2HRu(H_2)]^+(OR)^-$* . *Organometallics*, 1997. **16**: p. 2000-2002.
33. Ayllon, J.A., S. Sabo-Etienne, B. Chaudret, S. Ulrich, and H.H. Limbach, *Modulation of quantum mechanical exchange couplings in transition metal hydrides through hydrogen bonding*. *Inorganica Chimica Acta*, 1997. **259**: p. 1-4.
34. Grundemann, S., S. Ulrich, H.H. Limbach, N.S. Golubev, G.S. Denisov, L.M. Epstein, S. Sabo-Etienne, and B. Chaudret, *Solvent-Assisted Reversible Proton Transfer within an Intermolecular Dihydrogen Bond and Characterization of an Unstable Dihydrogen Complex*. *Inorganic Chemistry*, 1999. **38**: p. 2550-2551.
35. Crabtree, R.H., *Transition metal complexation of  $\sigma$  bonds*. *Angewandte Chemie - International Edition*, 1993. **32**: p. 789-805.
36. Wessel, J., et al., *An unconventional intermolecular three-center N-H $\cdots$ H<sub>2</sub>Re hydrogen bond in crystalline  $[ReH_5(PPh_3)_3] \cdot indole \cdot C_6H_6$* . *Angewandte Chemie - International Edition*, 1995. **34**(22): p. 2507-2509.



37. Peris, E., J. Wessel, B.P. Patel, and R.H. Crabtree, *d<sup>0</sup> and d<sup>2</sup> Polyhydrides as Unconventional Proton Acceptors in Intermolecular Hydrogen Bonding*. Chemical Communications, 1995: p. 2175-2176.
38. Patel, B.P., W. Yao, G.P.A. Yap, A.L. Rheingold, and R.H. Crabtree, *Re-H...H-N interactions in the second-coordination sphere of crystalline [ReH<sub>5</sub>(PPh<sub>3</sub>)<sub>2</sub>(imidazole)]*. Chemical Communications, 1996: p. 991-992.
39. Abdur-Rashid, K., D.G. Gusev, A.J. Lough, and R.H. Morris, *Intermolecular Proton-Hydride Bonding in Ion Pairs: Synthesis and Structural Properties of [K(Q)][MH<sub>5</sub>(P<sup>i</sup>Pr<sub>3</sub>)<sub>2</sub>] (M = Os, Ru; Q = 18-crown-6, 1-aza-18-crown-6, 1,10-diaza-18-crown-6)*. Organometallics, 2000. 19: p. 834-843.
40. Chu, H.S., Z. Xu, S.M. Ng, C.P. Lau, and Z. Lin, *Protonation of [tpmRu(PPh<sub>3</sub>)<sub>2</sub>H]BF<sub>4</sub> [tpm = Tris(pyrazolyl)methane]-Formation of Unusual Hydrogen-Bonded Species*. European Journal of Inorganic Chemistry, 2000: p. 993-1000.
41. Stevens, R.C., R. Bau, D. Milstein, O. Blum, and T.F. Koetzle, *Concept of the H(δ<sup>+</sup>)...H(δ<sup>-</sup>) interaction. A low-temperature neutron diffraction study of cis-[IrH(OH)(PMe<sub>3</sub>)<sub>4</sub>]PF<sub>6</sub>*. Dalton Transactions, 1990: p. 1429-1432.
42. Lee, J.C., Jr., A.L. Rheingold, B. Muller, P.S. Pregosin, and R.H. Crabtree, *Complexation of an Amide to Iridium via an Iminol Tautomer and Evidence for an Ir-H...H-O Hydrogen bond*. Chemical Communications, 1994: p. 1021-1022.
43. Peris, E., J.C. Lee, and R.H. Crabtree, *Intramolecular N-H...X-Ir (X = H, F) hydrogen bonding in metal complexes*. Chemical Communications, 1994: p. 2573.

44. Lee, J.C., Jr., E. Peris, A.L. Rheingold, and R.H. Crabtree, *An Unusual Type of H···H Interaction: Ir-H···H-O and Ir-H···H-N Hydrogen Bonding and Its Involvement in  $\sigma$ -Bond Metathesis*. Journal of the American Chemical Society, 1994. **116**: p. 11014-11019.
45. Yao, W. and R.H. Crabtree, *An  $\eta^1$ -aldehyde complex and the role of hydrogen bonding in its conversion to an  $\eta^1$ -imine complex*. Inorganic Chemistry, 1996. **35**: p. 3007-3011.
46. Peris, E., J.C. Lee Jr., J.R. Rambo, O. Eisenstein, and R.H. Crabtree, *Factors affecting the strength of X-H···H-M hydrogen bonds*. Journal of the American Chemical Society, 1995. **117**: p. 3485-3491.
47. Lee, D.H., B.P. Patel, E. Clot, O. Eisenstein, and R.H. Crabtree, *Heterolytic dihydrogen activation in an iridium complex with a pendant basic group*. Chemical Communications, 1999: p. 297-298.
48. Lee, D.H., H.J. Kwon, B.P. Patel, L.M. Liable-Sands, A.L. Rheingold, and R.H. Crabtree, *Effects of a Nonligating Pendant Hydrogen-Bonding Group in a Metal complex: Stabilization of an HF Complex*. Organometallics, 1999. **18**: p. 1615-1621.
49. Gruet, K., R.H. Crabtree, D.H. Lee, L. Liable-Sands, and A.L. Rheingold, *Two-Point Cooperative Binding of Ketones by a Metal and by a Neighboring Pendant NH Group*. Organometallics, 2000. **19**: p. 2228-2232.
50. Park, S., R. Ramachandran, A.J. Lough, and R.H. Morris, *A new type of Intramolecular H···H···H interaction involving N-H···H(Ir)···H-N atoms*. Crystal and molecular structure of  $[\text{IrH}\{\eta^1\text{-SC}_5\text{H}_4\text{NH}\}_2(\eta^2\text{-$

- $SC_5H_4N)(PCy_3)]BF_4 \cdot 0.72CH_2Cl_2$ . *Chemical Communications*, 1994: p. 2201-2202.
51. Lough, A.J., S. Park, R. Ramachandran, and R.H. Morris, *Switching on and off a new intramolecular hydrogen-hydrogen interaction and the heterolytic splitting of dihydrogen. Crystal and molecular structure of  $[Ir\{H(\eta^1-SC_5H_4NH)\}_2(PCy_3)_2]BF_4 \cdot 2.7CH_2Cl_2$* . *Journal of the American Chemical Society*, 1994. **116**: p. 8356-8357.
  52. Liu, Q. and R. Hoffmann, *Theoretical aspects of a novel mode of hydrogen-hydrogen bonding*. *Journal of the American Chemical Society*, 1995. **117**: p. 10108-10112.
  53. Xu, W., A.J. Lough, and R.H. Morris, *Competition between  $NH \cdots HIr$  intramolecular proton-hydride interactions and  $NH \cdots FBF_3^-$  or  $NH \cdots O$  intermolecular hydrogen bonds involving  $[IrH(2-thiazolidinethione)_4(PCy_3)](BF_4)_2$  and related complexes*. *Inorganic Chemistry*, 1996. **35**: p. 1549-1555.
  54. Park, S., A.J. Lough, and R.H. Morris, *Iridium(III) complex containing a unique bifurcated hydrogen bond interaction involving  $Ir-H \cdots H(N) \cdots F-B$  atoms. Crystal and molecular structure of  $[IrH(\eta^1-SC_5H_4NH)(\eta^2-SC_5H_4N)(PPh_3)_2](BF_4) \cdot 0.5C_6H_6$* . *Inorganic Chemistry*, 1996. **35**: p. 3001-3006.
  55. Chu, H.S., C.P. Lau, K.Y. Wong, and W.T. Wong, *Intramolecular  $N-H \cdots H-Ru$  proton-hydride interaction in ruthenium complexes with (2-(dimethylamino)ethyl)cyclopentadienyl and (3-*

- (dimethylamino)propyl)cyclopentadienyl ligands. Hydrogenation of CO<sub>2</sub> to formic acid via the N-H···H-Ru hydrogen-bonded complexes. *Organometallics*, 1998. **17**: p. 2768-2777.
56. Ayllon, J.A., S.F. Sayers, S. Sabo-Etienne, B. Donnadieu, and B. Chaudret, *Proton transfer in Aminocyclopentadienyl ruthenium hydride complexes*. *Organometallics*, 1999. **18**(20): p. 3981-3990.
57. Aime, S., M. Ferriz, R. Gobetto, and E. Valls, *Coordination of an Imine ligand on an Os<sub>3</sub> Cluster stabilized by intramolecular Os-H···H-N hydrogen bonding*. *Organometallics*, 1999. **18**: p. 2030-2032.
58. Slone, C.S., D.A. Weinberger, and C.A. Mirkin, *The transition metal coordination chemistry of hemilabile ligands*, in *Progress in inorganic chemistry*, K.D. Karlin, Editor. 1999, John Wiley & Sons, Inc. p. 233-350.
59. Jutzi, P. and T. Redeker, *Aminoethyl-Functionalized Cyclopentadienyl Complexes of d-Block Elements*. *European Journal of Inorganic Chemistry*, 1998: p. 663-674.
60. Jutzi, P. and U. Siemeling, *Cyclopentadienyl compounds with nitrogen donors in the side-chain*. *Journal of Organometallic Chemistry*, 1995. **500**: p. 175-185.
61. Schumann, H., F. Erbstein, J. Demtschuk, and R. Weimann, *Organometallic Compounds of the Lanthanides. 133 Synthesis and Characterization of donor-functionalized ansa-Metallocenes of Yttrium, Neodymium, Samarium, Erbium, and Lutetium*. *Zeitschrift Fur Anorganische Und Allegemeine Chemie*, 1999. **625**: p. 1457-1465.

62. Flores, J.C., J.C.W. Chien, and M.D. Rausch, *{[2-(Dimethylamino)ethyl]cyclopentadienyl}trichlorotitanium: A new type of olefin polymerization catalyst*. *Organometallics*, 1994. **13**: p. 4140-4142.
63. Jutzi, P., T. Redeker, B. Neumann, and H. Stammler, *Halbsandwich-komplexe der elemente titan und zirconium mit dem (Diisopropylaminoethyl) cyclopentadienyl-ligand: molekulstruktur von  $[(C_5H_4CH_2CH_2N(H)^iPr_2)ZrCl_3]^+Cl^- \cdot 2CH_3OH$* . *Journal of Organometallic Chemistry*, 1997. **533**: p. 237-245.
64. Beckhaus, R., J. Oster, B. Ganter, and U. Englert, *Vinyltitanium complexes containing [2-(N,N-Dimethylamino)ethyl]tetramethylcyclopentadienyl ligand  $Cp^*N$ : Generation and reactivity of the vinylidene intermediate  $[(Cp^*N)(Cp^*)Ti=C=CH_2]$  ( $Cp^*N = \eta^5-C_5Me_4(CH_2)_2NMe_2$ ,  $Cp^* = \eta^5-C_5Me_5$ )*. *Organometallics*, 1997. **16**: p. 3902-3909.
65. Jutzi, P., C. Muller, B. Neumann, and H. Stammler, *Dialkylaminoethyl-functionalized ansa-zirconocene dichlorides: synthesis, structure, and polymerization properties*. *Journal of Organometallic Chemistry*, 2001. **625**: p. 180-185.
66. Muller, C., D. Lilge, M.O. Kristen, and P. Jutzi, *Dialkylaminoethyl-functionalized ansa-zirconocene dichlorides: Precatalysts for the regulation of the molecular weight distribution of polyethylene*. *Angewandte Chemie - International Edition*, 2000. **39**(4): p. 789-792.
67. Bertuleit, A., C. Fritze, G. Erker, and R. Frohlich, *Uncovering alternative reaction pathways taken by group 4 metallocene cations: Facile intramolecular CH*

- activation of Cp-(dimethylamino)alkyl substituents by a methylzirconocene cation. Organometallics, 1997. 16: p. 2891-2899.*
68. Jutzi, P., M.O. Kristen, J. Dahlhaus, B. Neumann, and H. Stammler, *Cobalt complexes with the 1-[2-(N,N-Dimethylamino)ethyl]-2,3,4,5-tetramethylcyclopentadienyl ligand. Organometallics, 1993. 12: p. 2980-2985.*
  69. Jutzi, P., M.O. Kristen, B. Neumann, and H. Stammler, *Rhodium and iridium complexes with the 1-(2-(dimethylamino)ethyl)-2,3,4,5-tetramethylcyclopentadienyl ligand. Organometallics, 1994. 13: p. 3854-3861.*
  70. Wang, T., T. Lee, J. Chou, and C. Ong, *Half-sandwich complex with intramolecular amino group coordination: synthesis of molybdenum iodide complexes. Journal of Organometallic Chemistry, 1992. 423: p. 31-38.*
  71. Wang, T. and Y. Wen, *Half-sandwich complexes with intramolecular amino group coordination: synthesis and structure of cationic molybdenum dienyl complexes. Journal of Organometallic Chemistry, 1992. 439: p. 155-162.*
  72. Wang, T., C. Lai, and Y. Wen, *Preparation and reactions of half-sandwich rhenium nitrosyl complexes containing a tethered amino ligand. Journal of Organometallic Chemistry, 1996. 523: p. 187-195.*
  73. Wang, T., C. Lai, C. Hwu, and Y. Wen, *Half-Sandwich Aminorhenium Complexes: Preparation and Regioselective N-versus Re-Alkylations. Organometallics, 1997. 16: p. 1218-1223.*
  74. Nlate, S., E. Herdtweck, and R.A. Fischer, *An intermolecularly donor-stabilized silanediyl(silyl)nickel complex: Combined Si-Si bond cleavage and methyl*

- migration between silicon centers.* *Angewandte Chemie - International Edition*, 1996. **35**: p. 1861-1863.
75. Dedieu, A., ed. *Transition metal hydrides*. . 1991, VCH Publishers, Inc.
  76. Stephenson, T.A., *Inorganic synthesis*. Vol. 12. 1971. 238.
  77. Hallman, P.S., T.A. Stephenson, and G. Wilkinson, *Inorganic Synthesis*. Vol. 12. 1970. 237.
  78. Chan, W.C., C.P. Lau, Y.Z. Chen, Y.Q. Fang, S.M. Ng, and G. Jia, *Syntheses and Characterization of Hydrotris(1-pyrazolyl)borate Dihydrogen complexes of Ruthenium and their roles in Catalytic Hydrogenation reactions*. *Organometallics*, 1997. **16**: p. 34.
  79. Chu, H.S., *Syntheses and reactivities of ruthenium complexes with pendant amino sidearms and biphasic catalytic hydrogenation reactions with trispyrazolylmethane ruthenium complexes*, in *Applied Biology and Chemical Technology*. 1998, The Hong Kong Polytechnic University: Hong Kong. p. 22.
  80. Abel, E.W., F.G.A. Stone, and G. Wilkinson, eds. *Comprehensive Organometallic Chemistry II*. . Vol. 7. 1995, Pergamon.
  81. Alt, H.G., M. Jung, and W. Milius, *Verbrückte indenyliden-cyclopentadienylidenkomplexe des typs  $(C_9H_5CH_2Ph-X-C_5H_4)MCl_2$  ( $X = CMe_2, SiMe_2$ ;  $M = Zr, Hf$ ) als metallocenkatalysatoren für die ethylenpolymerisation. Die molekülstrukturen von  $(C_9H_5CH_2Ph-CMe_2-C_5H_4)MCl_2$  ( $M = Zr, Hf$ )*. *Journal of Organometallic Chemistry*, 1998. **558**: p. 111-121.
  82. Cooper, A.C., J.C. Huffman, and K. Caulton, *A case of C-H activation (Ortho Metalation) which is reversible at 25°C*. *Organometallics*, 1997. **16**: p. 1974-1978.

83. Philippopoulos, A.I., N. Hadjiliadis, C.E. Hart, B. Donnadieu, P.C. McGowan, and R. Poilblanc, *Transition-metal derivatives of a functionalized cyclopentadienyl ligand. 156. Synthesis and structures of amino cyclopentadienyl derivatives of rhodium(I) and rhodium(III) including water-soluble compounds*. *Inorganic Chemistry*, 1997. 36: p. 1842-1849.
84. Buil, M.L., M.A. Esterulas, E. Onate, and N. Ruiz, *H...H Interaction in Four-Membered P-H...H-M (M = Osmium, Ruthenium) Rings*. *Organometallics*, 1998. 17: p. 3346-3355.



## Appendix

Current Data Parameters  
 NAME Test  
 EPRNO B1  
 PROCNO 1

F2 - Acquisition Parameters  
 Date\_ 20010221  
 Time 15.41  
 INSTRUM DDV400  
 PROBN 5 m QNP 1H  
 PULPROG zgpg30  
 TD 4930  
 SOLVENT CUC13  
 NS 64  
 DS 6  
 SWH 11890.407 MHz  
 FIDRES 0.366918 MHz  
 AQ 1.2664768 sec  
 RG 256  
 DA 41.700 usec  
 DE 4.50 usec  
 TE 300.2 K  
 D1 2.0000000 sec

===== CHANNEL f1 =====  
 NUC1 1H  
 P1 9.50 usec  
 PL -6.00 dB  
 SF01 400.1487880 MHz

F2 - Process/ps parameters  
 SI 16384  
 SF 400.1300050 MHz  
 MDV EM  
 SSB 0  
 LB 0.30 MHz  
 GB 0  
 PC 1.00

3D NMR plot parameters  
 CX 20.00 GHz  
 FIP 10.000 GHz  
 F1 4001.30 MHz  
 F2P 0.000 GHz  
 F2 0.00 MHz  
 PRACH 0.000000 GHz  
 HZCH 200.000000 MHz

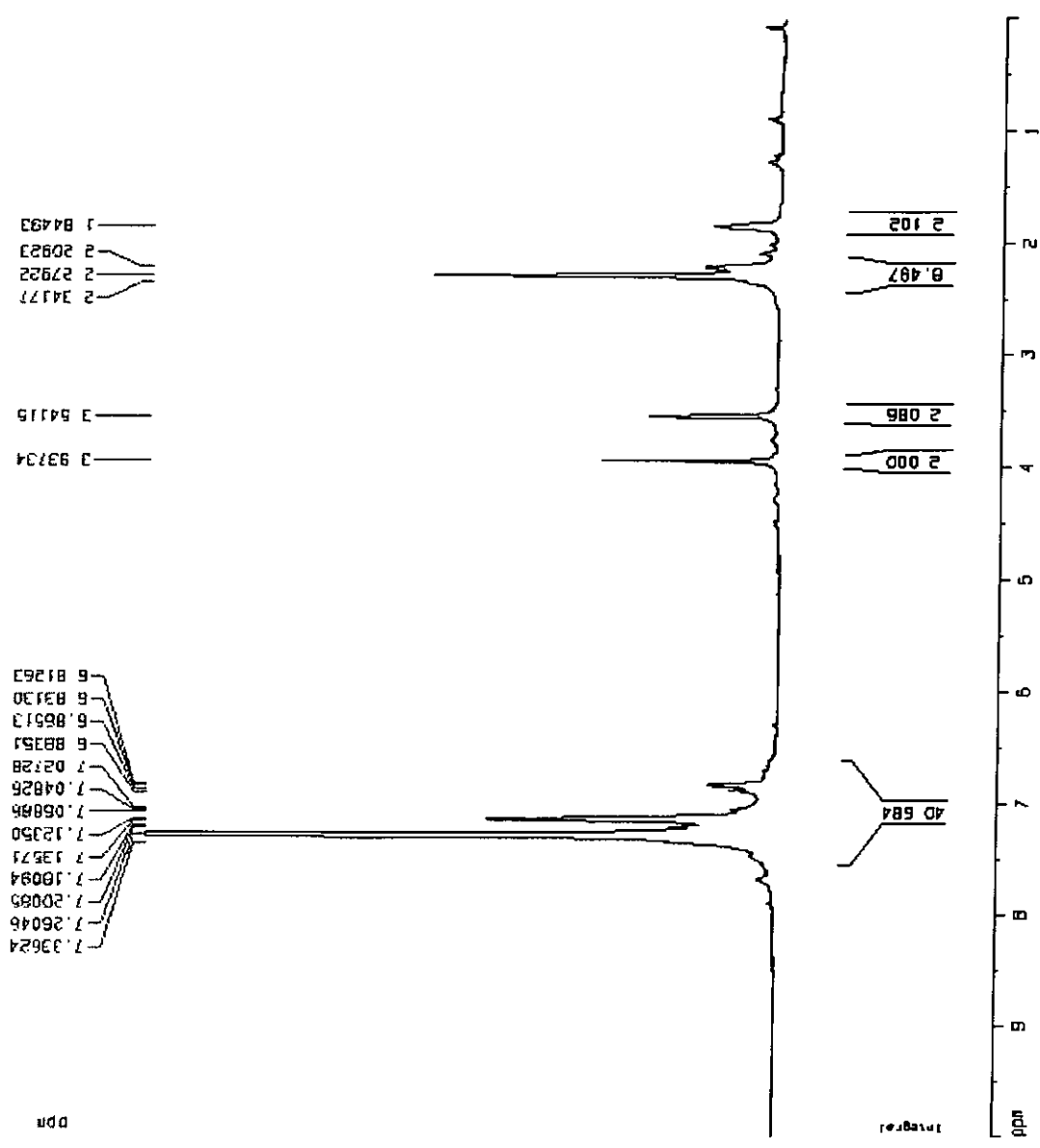


Figure 3.1 400 MHz <sup>1</sup>H NMR spectrum of CpNRu[P(OPh)<sub>3</sub>]<sub>2</sub>Cl (40)



```

Current Data Parameters
NAME: Test
EXPNO: 59
PROCNO: 1

F2 - Acquisition Parameters
Date_ 20101117
Time 21:29
INSTRUM gpc400
PROBHD 5 mm QNP 1H
PULPROG zgpg30
TD 32768
SOLVENT acetone
NS 64
DS 0
SWH 11880.407 MHz
FIDRES 0.356818 MHz
AQ 1.3654705 sec
RG 114
DM 41.700 usec
DE 4.60 usec
TE 300.2 K
D1 2.0000000 sec

===== CHANNEL f1 =====
NUC1 1H
P1 9.50 usec
PL1 -6.00 dB
SFO1 400.1261800 MHz

F2 - Processing parameters
SI 16384
SF 400.1261864 MHz
WDW EM
SSB 0
LB 0.30 Hz
GB 0
PC 1.00

3D NMR plot parameters
D 20.00 cm
F1P 10.000 cm
F1 4001.20 MHz
F2P 0.000 cm
F2 0.00 MHz
PRCH 0.00000000 cm
AQDN 200.00487 MHz/cm

```

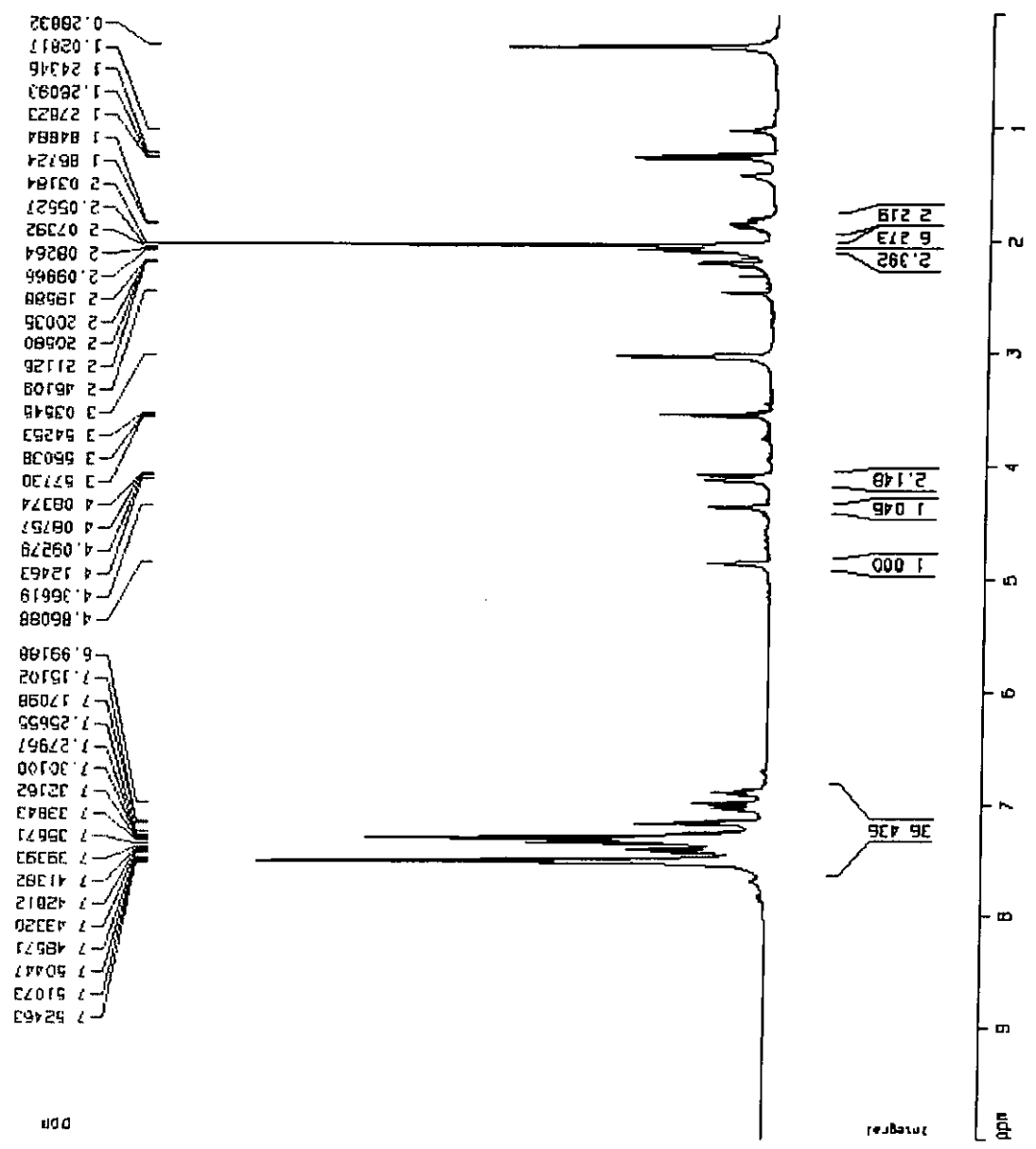


Figure 3.3 400 MHz <sup>1</sup>H NMR spectrum of CpNRu[P(OPh)<sub>3</sub>][(OPh)<sub>2</sub>P(OC<sub>6</sub>H<sub>4</sub>)] (41)

```

Current Data Parameters
NAME          F31Acad
EXPNO        65
PROCNO       1

F2 - Acquisition Parameters
Date_        20010117
Time         21.24
INSTRUM     spect
PROBHD      5 mm QNP 1H
PULPROG     zgpg30
TD           65536
SOLVENT     ACETOP
NS           32
DS           0
SWH          64935.065 MHz
FIDRES      0.800830 MHz
AQ           0.3046772 sec
RG           8192
DN           7.700 usec
DE           4.50 usec
TE           300.0 K
DQ           2.0000000 sec
DD           0.03000000 sec

***** CHANNEL F1 *****
NUC1         31P
P1           7.20 usec
RG1          -6.00 dB
SFO1        161.873732 MHz

***** CHANNEL F2 *****
CPDPRG2     MVEL216
NUC2         1H
PULPROG     zgpg30
RG2          120.00 dB
SFO2        400.1463600 MHz

F2 - Processing Parameters
SI           32768
SF           161.8750045 MHz
AQ           0
GB           0
PC           1.40

3D NMR PLOT PARAMETERS
D            20.00 cm
FIDRES      200.000000 ppm
F1           32395.17 MHz
F2           0.000000 ppm
FREQH       10.000000 MHz
NBDN       1618.750010 MHz/cm

```

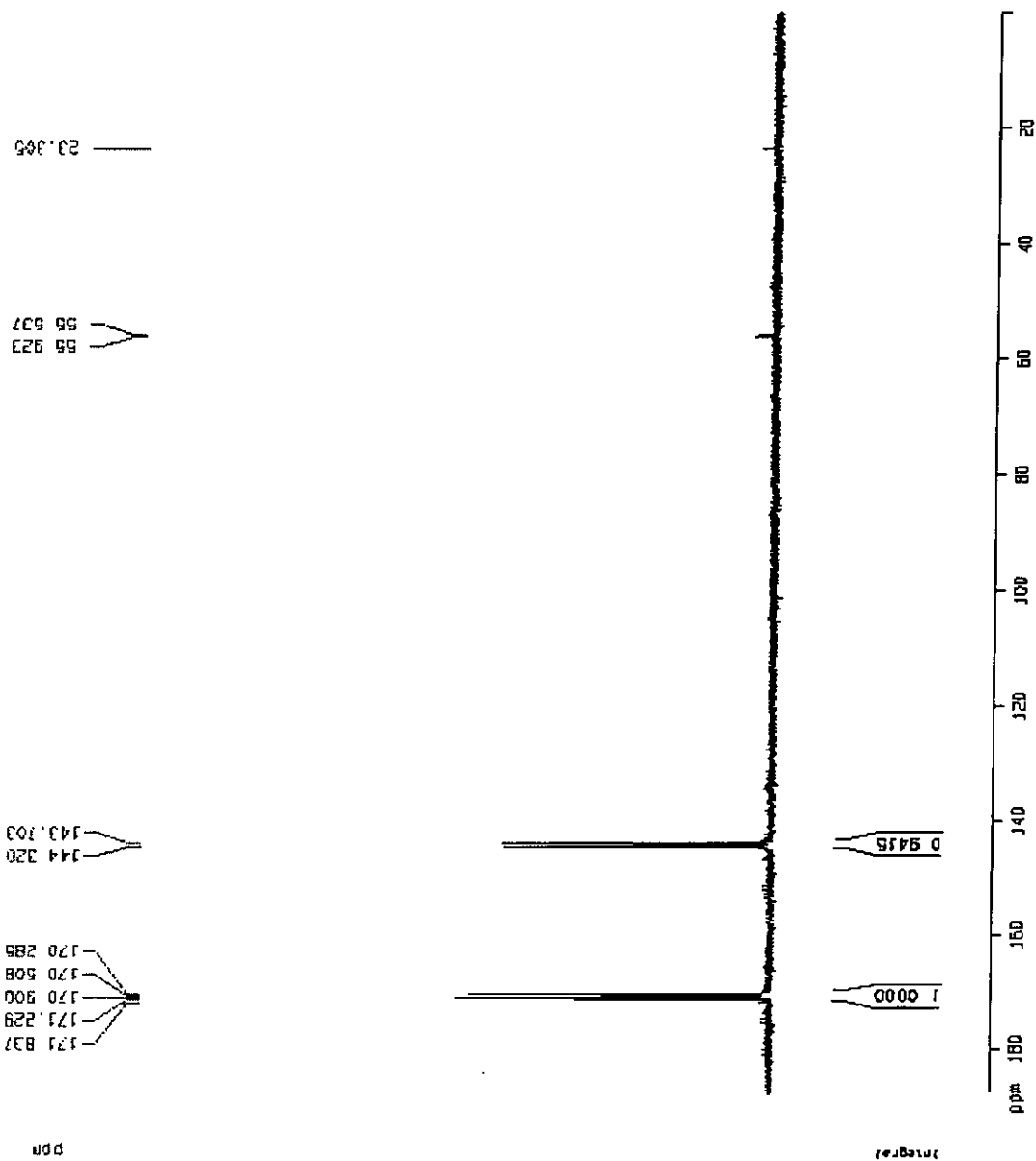


Figure 3.4  $161.7 \text{ MHz } ^{31}\text{P}\{^1\text{H}\}$  NMR spectrum of  $\text{CpNRu}[\text{P}(\text{OPh})_3][(\text{OPh})_2\text{P}(\text{OC}_6\text{H}_4)]$  (41)

```

Current Data Parameters
NAME      C13-019
EXPNO    9
PROCNO   1

F2 - Acquisition Parameters
Date_    20010604
Time     8:48
INSTRUM  gpc-400
PROBHD   5 mm QNP 1H
PULPROG  zgpg30
TO       65638
SOLVENT  THF
RG       18432
DS       0
ENH      40404.939 Hz
FILTERS  0.616017 Hz
AQ       0.6110560 SEC
RG       6459.8
DN       12.375 uSEC
DE       4.50 uSEC
TE       300.0 K
D1       2.00000000 SEC
D11      0.63000000 SEC

***** CHANNEL F1 *****
NUC1      13C
P1       5.00 uSEC
PL1      -6.00 dB
SFO1     100.617986 MHz

***** CHANNEL F2 *****
CPDPRG2  NUC1L18
NUC2      1H
P2       71.00 uSEC
PL2      130.00 dB
PL12     17.00 dB
SFO2     400.1315003 MHz

F2 - Processing Parameters
SI       32768
SF       100.617986 MHz
WDW      EM
SSB      0
LB       1.00 Hz
GB       0
PC       1.40

1D NMR plot parameters
DI       20.00 cm
F1P      151.900 ppm
F1       12073.62 Hz
F2P      100.900 ppm
F2       10061.27 Hz
PRACH    1.00000 ppm/cm
HZDN     100.61270 Hz/cm

```

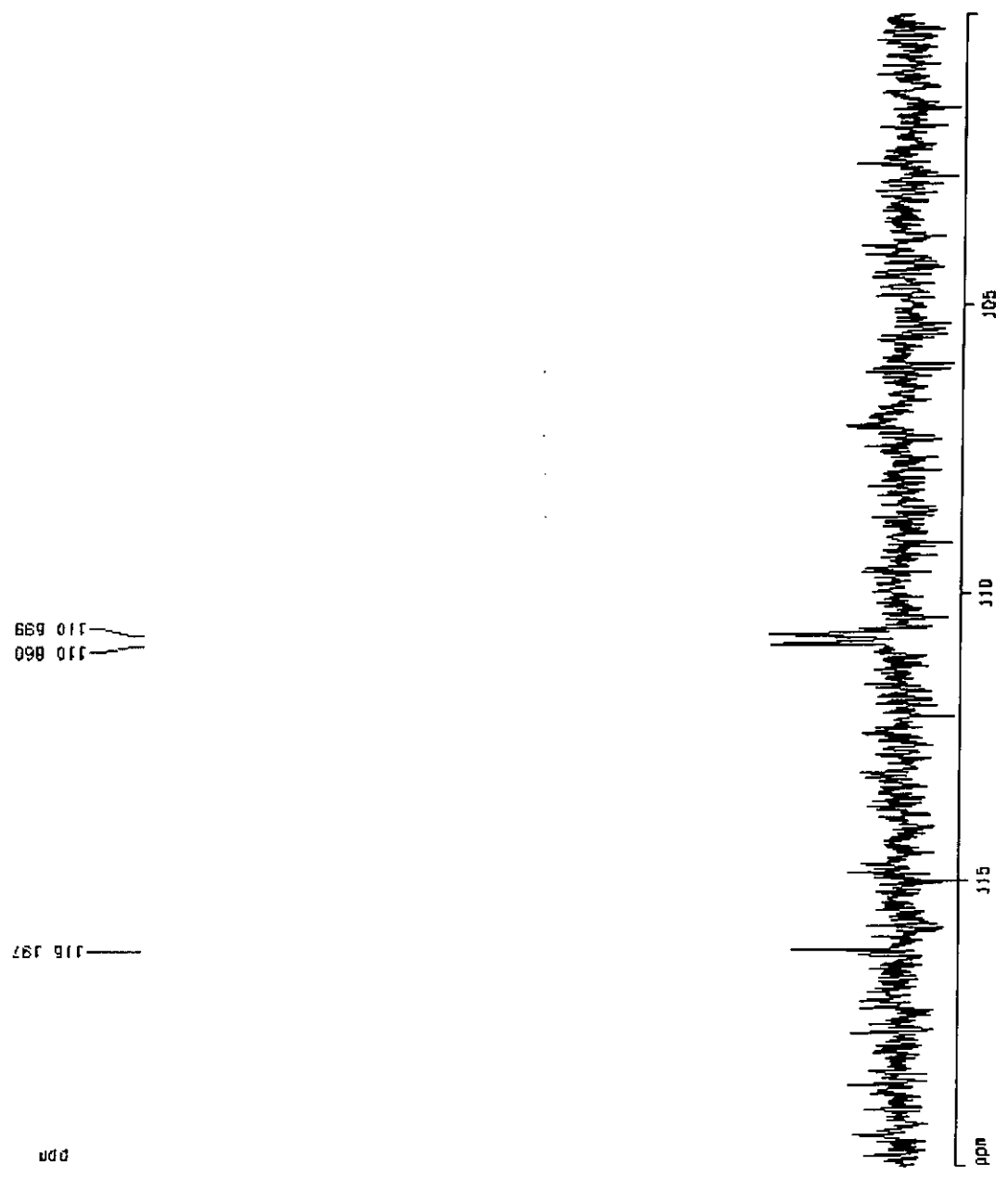


Figure 3.5 100.6 MHz  $^{13}\text{C}\{^1\text{H}\}$  NMR spectrum of  $\text{CpNRu}[\text{P}(\text{OPh})_3][(\text{OPh})_2\text{P}(\text{OC}_6\text{H}_4)]$  (41)

```

Current Data Parameters
NAME      Test
EXPNO    171
PROCNO   1

F2 - Acquisition Parameters
Date_    20070903
Time     18 13
INSTRUM  gpc400
PROBHD   5 mm QNP 1H
PULPROG  zg30
TD        32768
SOLVENT  CDCl3
NS        128
DS        4
SFO      11880 407 MHz
FIDRES   0.316818 MHz
AQ        1.3664766 sec
RG         302
DA        41 700 USEC
DE         4 60 USEC
TE        300.0 K
DQ        2.0000000 sec

===== CHANNEL f1 =====
NUC1      1H
P1        9.60 USEC
PL1       -6.00 DB
SFO1     400.1287888 MHz

F2 - Processing parameters
SI        16384
SF        400.1288866 MHz
WDW       EM
SSB       0
LB        0.30 MHz
GB        0
PC        1.00

ID NMR plot parameters
D         20.00 cm
F1P       10 000 cm/s
F1        4001.30 MHz
F2P       0.000 ppm
F2        0.00 MHz
PPMCH    0 60000 cm/s
HZCM     200 06488 MHz/cm

```

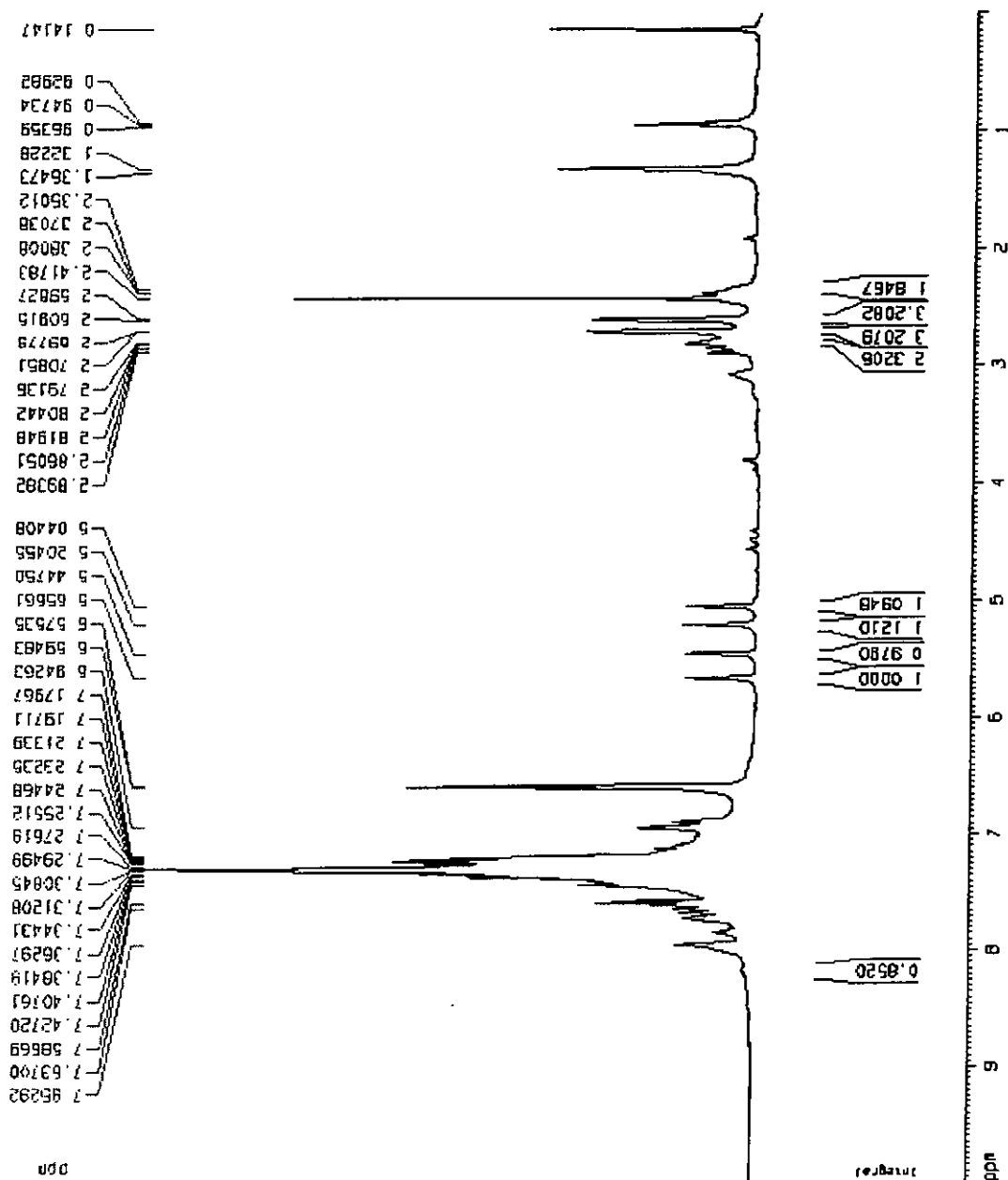


Figure 3.6 400 MHz  $^1\text{H}$  NMR spectrum of  $[\text{CpNH}^+\text{Ru}[\text{P}(\text{OPh})_3][(\text{OPh})_2\text{P}(\text{OC}_6\text{H}_4)]](\text{BF}_4)$  (42)





```

Current Data Parameters
NAME      1,2-propylene
EXPNO    1
PROCNO   1

F2 - Acquisition Parameters
Date_    20010210
Time     14.32
INSTRUM  zgpg30
PROBHD   5 mm QNP 1H
PULPROG  zgpg30
TD       65536
SOLVENT  CDCl3
NS       1438
DS       0
SWH      40404.518 Hz
FIDRES   0.1616017 Hz
AQ       0.6110680 sec
RG       7298.2
DN       12.375 usec
DE       4.20 usec
TE       300.0 K
D1       2.00000000 sec
D11      0.03000000 sec

***** CHANNEL f1 *****
NUC1      13C
P1        5.80 usec
PL1       -6.00 dB
SFO1     100.617586 MHz

***** CHANNEL f2 *****
DEPRG2   zgpg30
NUC2      1H
P2        71.00 usec
PL2       120.00 dB
SFO2     400.1415003 MHz

F2 - Processing parameters
SI        32768
SF        100.6185738 MHz
NUC1      13C
NUC2      1H
LB        1.00 Hz
GB        0
PC        1.40

3D NMR plot parameters
DI        20.00 cm
F1P       120.000 cmh
F1        12072.62 Hz
F2P       100.000 cmh
F2        10061.27 Hz
PRACH     1 00000 pph/cm
ROACH     100 51267 Hz/cm

```

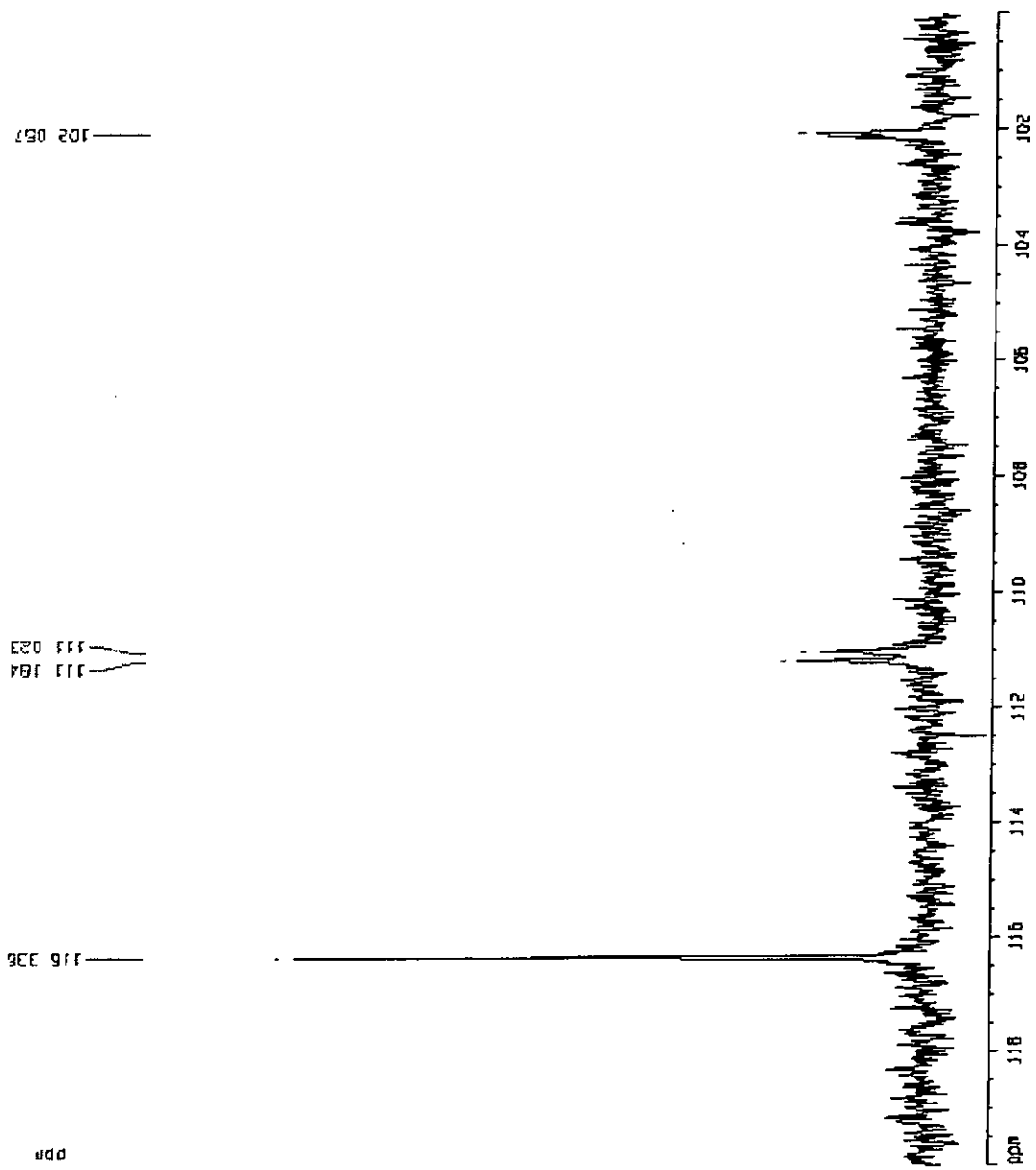


Figure 3.8 100.6 MHz  $^{13}\text{C}\{^1\text{H}\}$  NMR spectrum of  $\{\text{CpNH}^+\text{Ru}[\text{P}(\text{O}^i\text{Pr})_3][\{(\text{O}^i\text{Pr})_2\text{P}(\text{OC}_6\text{H}_4)\}]\}(\text{BF}_4)$  (42)

```

Current Data Parameters
NAME      Test
EXPNO    110
PROCNO   1

F2 - Acquisition Parameters
Date_    20101007
Time     15.07
INSTRUM  cp1-400
PROBHD   5 mm QNP 1H
PULPROG  zgpg30
TD        65536
SOLVENT  CDCl3
NS        64
DS        4
SWH       10000.000 MHz
FIDRES    0.305175 MHz
AQ         1.6304500 sec
RG         256
CH        50.000 usec
DE         4.50 usec
TE        300.0 K
D1         2.00000000 sec
d12        0.00000000 sec

===== CHANNEL f1 =====
NUC1      1H
P1        9.50 usec
PL1       -6.00 dB
SFO1     400.1267899 MHz

===== CHANNEL f2 =====
NUC2      1H
P2        120.00 dB
PL2       120.00 dB
SFO2     400.1311193 MHz

F2 - Processing parameters
SI        16384
SF        400.1259418 MHz
WDW       EM
SSB       0
LB        0.20 Hz
GB        0
PC        1.00

1D NMR Data Parameters
SI        20.00 cm
FIDRES    10.000 ppm
F1         400.130 MHz
F2        -15.000 ppm
F3        -5001.85 MHz
PULPROG   zgpg30
PC        1.25000 ppm/cp
NUC1       1H
NUC2       1H
  
```

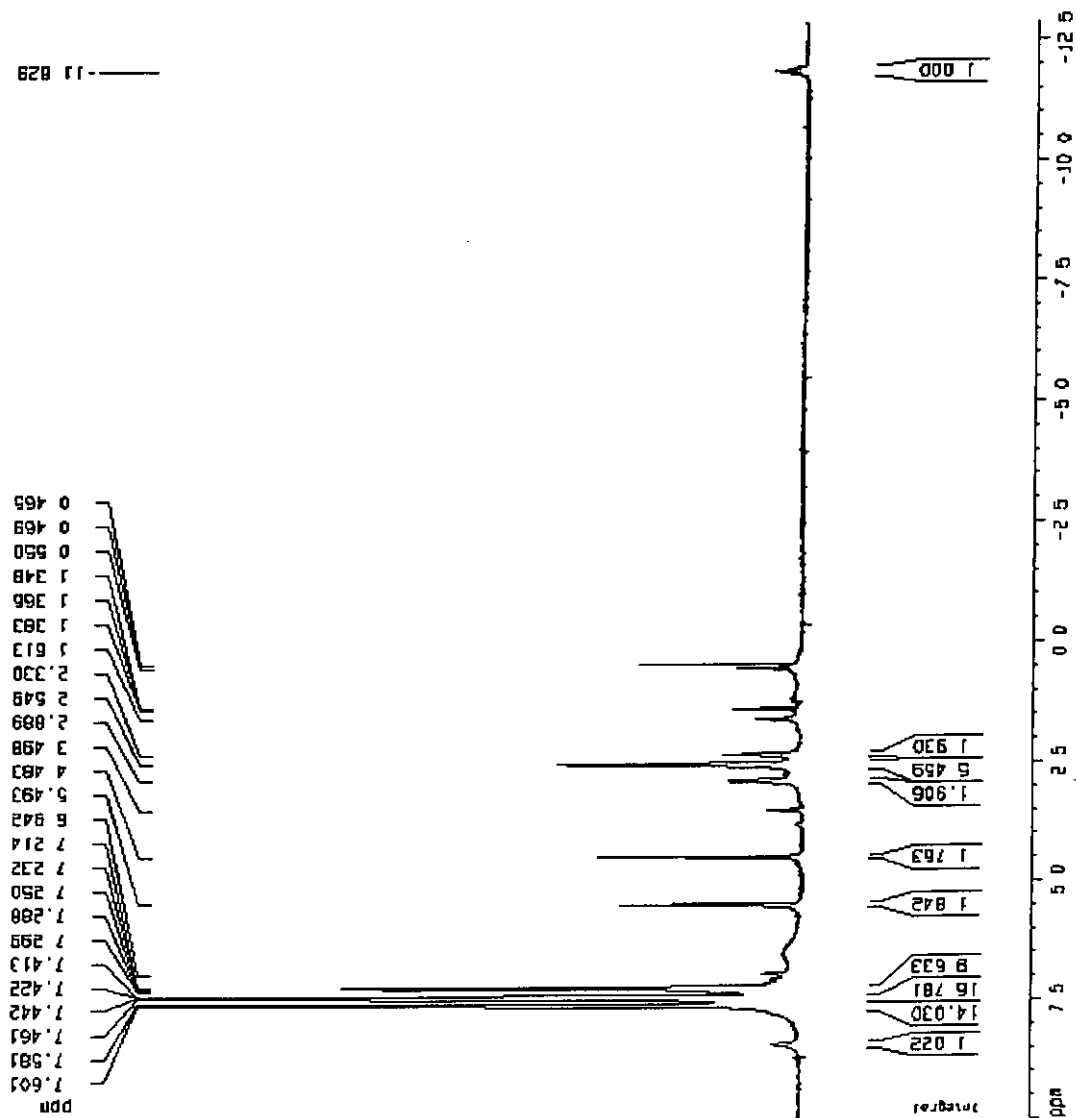


Figure 3.9 400 MHz  $^1\text{H}$  NMR spectrum of  $\{\text{CpNH}^+\text{Ru}[\text{P}(\text{OPh})_3]_2\text{H}\}(\text{BF}_4)$  (43)

```

Current Data Parameters
NAME          P310004
EXPNO        132
PROCNO       1

F2 - Acquisition Parameters
Date_        20010320
Time         10.24
INSTRUM     dp-400
PROBHD      5 mm QNP 1H
PULPROG     zgpg30
TD           65536
SOLVENT     CDCl3
NS           128
DS           0
SWH          64838.065 Hz
FIDRES      0.8908310 Hz
AQ           0.3046772 sec
RG           11688.2
DN           7.700 uS/cyc
DE           4.50 uS/cyc
TE           300.0 K
D1           2.00000000 sec
d11          0.03000000 sec

***** CHANNEL F1 *****
NUC1          31P
P1           7.20 uS/cyc
PL1          -6.00 dB
SFO1         161.872732 MHz

***** CHANNEL F2 *****
CPDPRG2      zgpg30
NUC2          1H
PCPD2        71.00 uS/cyc
PL2          120.00 dB
PL12         17.00 dB
SFO2         400.1435000 MHz

F2 - Processing Parameters
SI           32768
SF           161.8727355 MHz
NUC1         31P
NUC2         1H
LB           3.00 Hz
GB           0
PC           1.40

3D NMR Plot Parameters
D            20.00 um
F1P          200.000 DSS
F1           32384.87 Hz
F2P          160.000 ppm
F2           16197.44 Hz
PRNCH1      5 00000 ppm/cp
NUC1        609 87183 Hz/cp

```

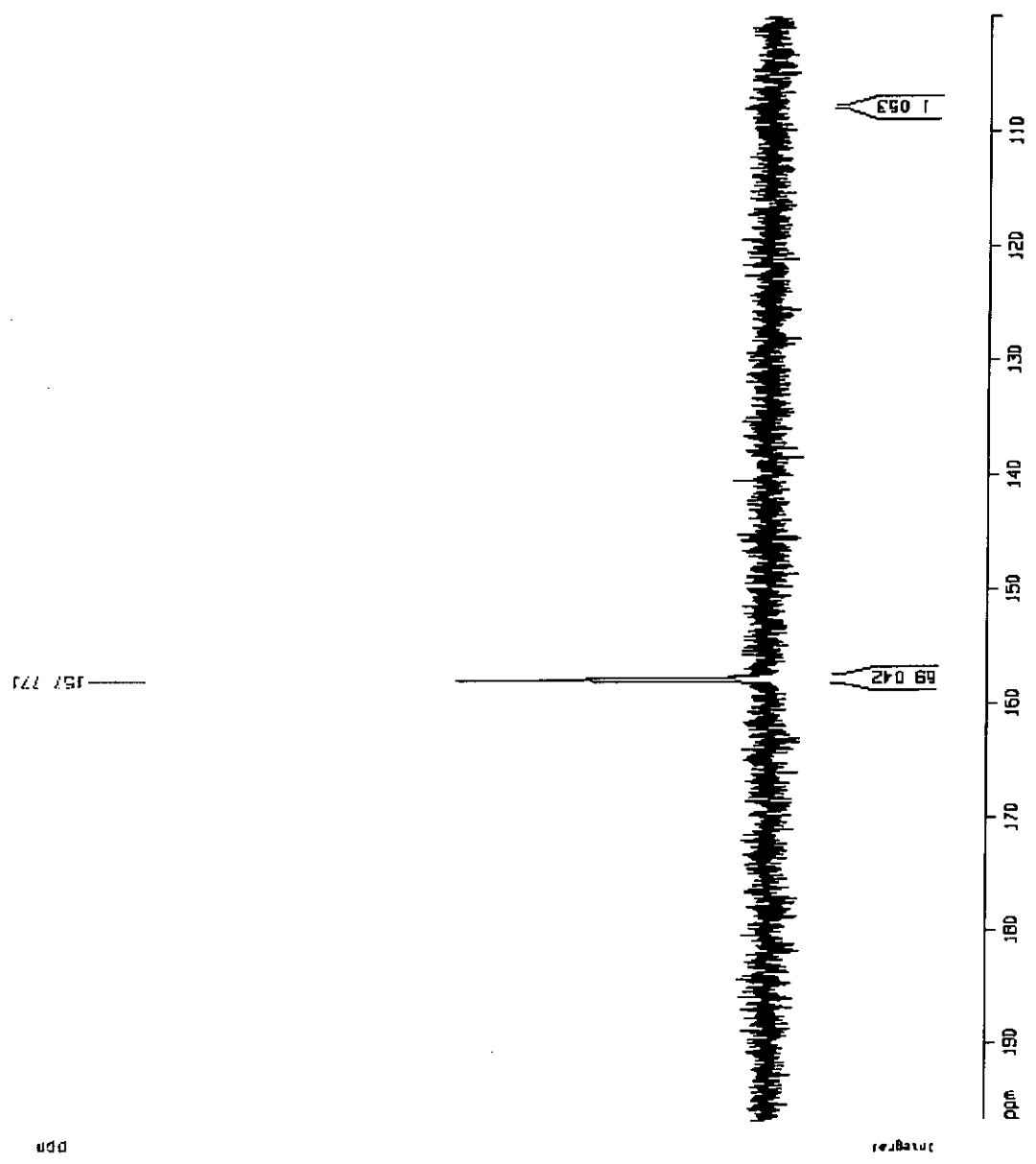


Figure 3.10 161.7 MHz  $^{31}\text{P}\{^1\text{H}\}$  NMR spectrum of  $\{\text{CpNH}^+\text{Ru}[\text{P}(\text{OPh})_3]_2\text{H}\}(\text{BF}_4)$  (43)

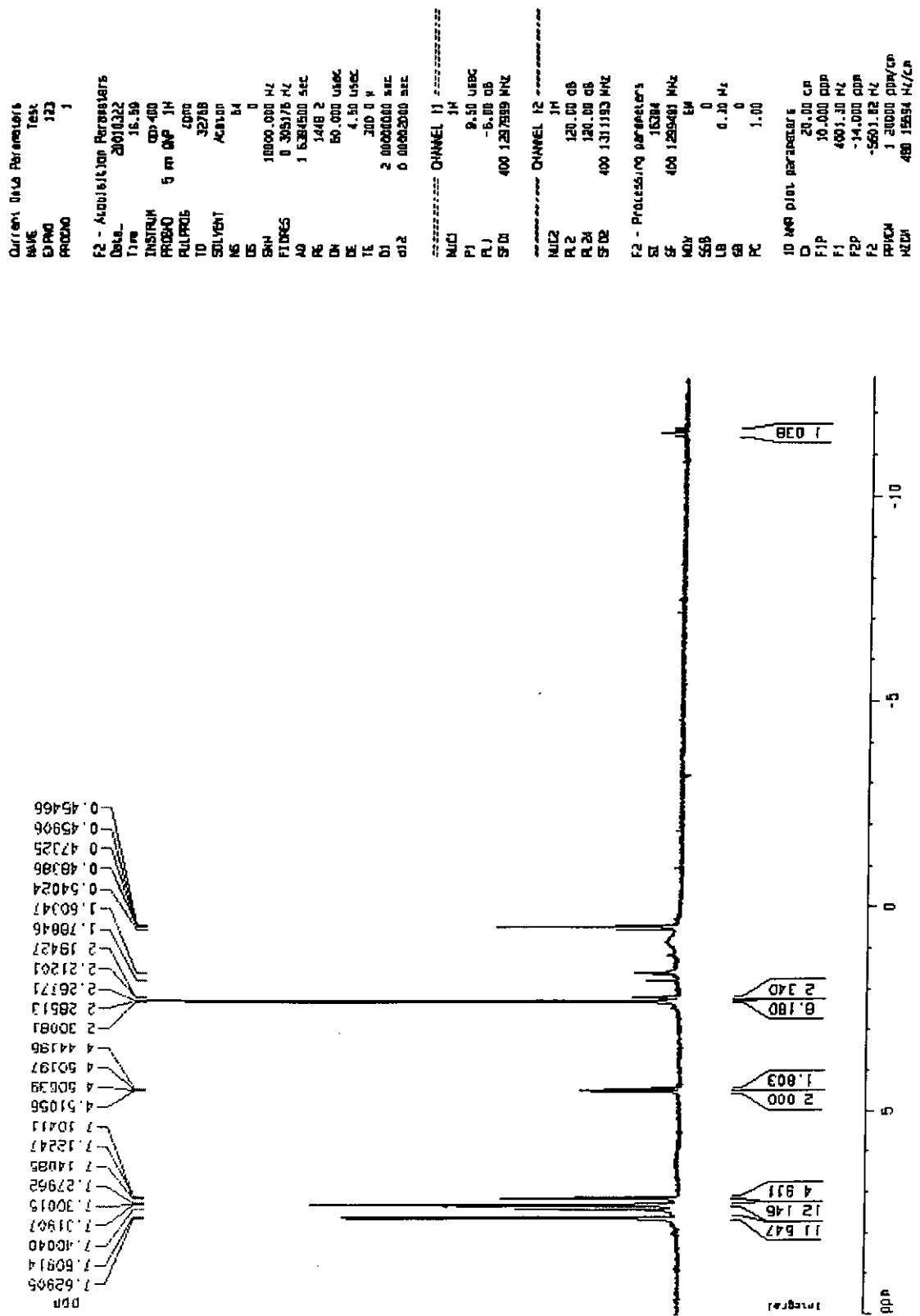


Figure 3.11 400 MHz <sup>1</sup>H NMR spectrum of CpNRu[P(OPh)<sub>3</sub>]<sub>2</sub>H (44)

```

Current Data Parameters
NAME          P31MMS1
EXPNO        135
PROCNO        1

F2 - Acquisition Parameters
Date_         20010322
Time          15.47
INSTRUM      spect
PROBHD       5 mm BBO 1H
PULPROG      zgpg30
TD           65536
SOLVENT      DMSO
NS           204
DS           0
SWH           64035.955 MHz
FIDRES       0.0000319 MHz
AQ           0.0046372 sec
RG           31665.2
OR           7.700 deg
DE           4.50 deg
TE           300.0 K
D1           2.00000000 sec
D11          0.03000000 sec

----- CHANNEL f1 -----
NUC1          31P
P1           7.20 usec
PL1          -6.00 dB
SFO1         161.873325 MHz

----- CHANNEL f2 -----
CDEPRG2      hb1h1h1h
NUC2          1H
PULPROG      zgpg30
F2           71.00 MHz
PL2          120.00 dB
PL12         17.00 dB
SFO2         400.1326000 MHz

F2 - Processing parameters
SI           32768
SF           161.977325 MHz
WDW          EM
SSB          0
LB           3.00 Hz
GB           0
PC           1.40

ID NMR plot parameters
C            20.00 CF
F1F          200.000 MHz
F1           32395.48 MHz
F2          0.500 ppm
F2          0.60 MHz
PPMCH       10.00000 ppm/Hz
RZLN        1619.77319 MHz/cm

```

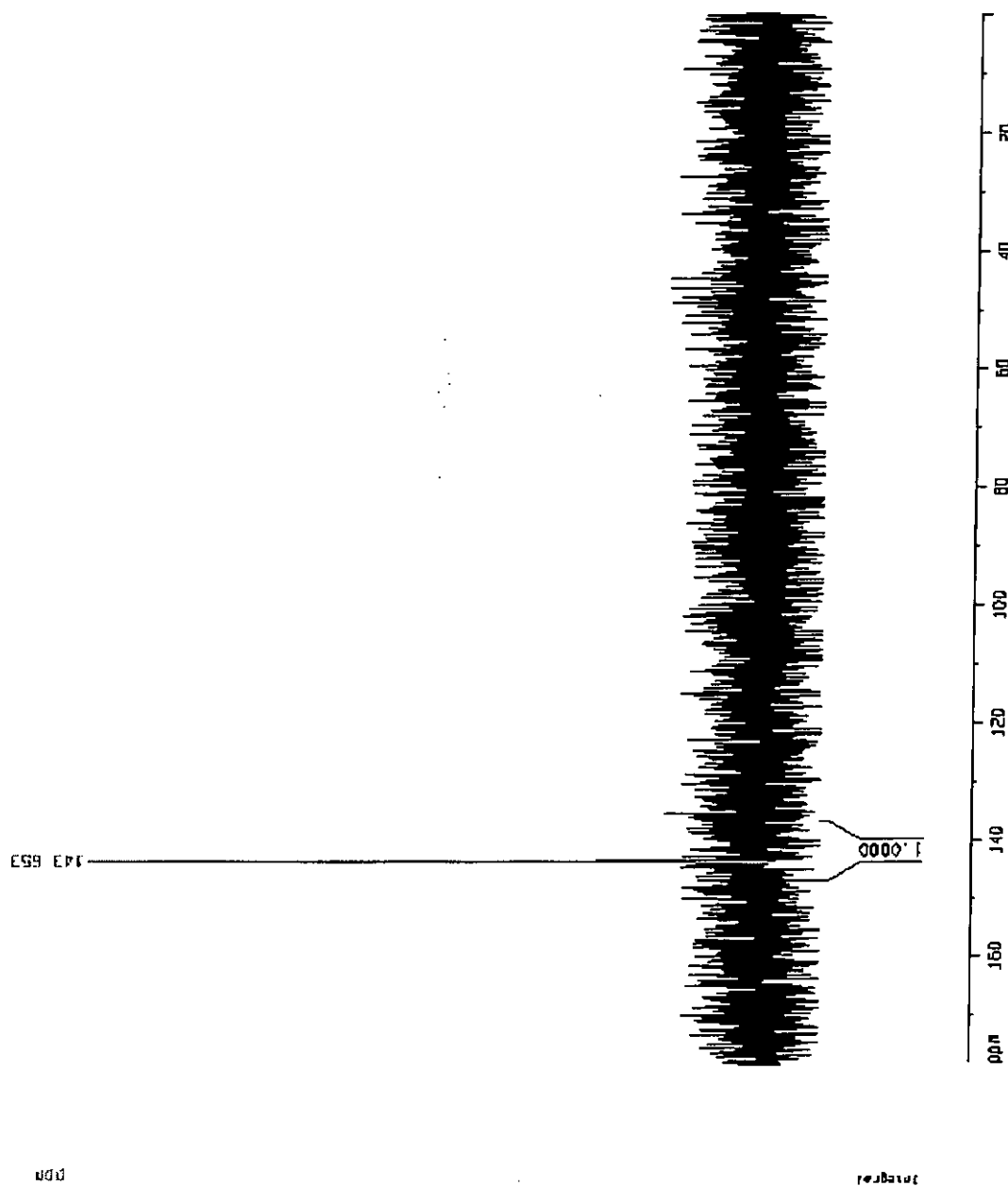


Figure 3.12 161.7 MHz  $^{31}\text{P}\{^1\text{H}\}$  NMR spectrum of  $\text{CpNRu}[\text{P}(\text{OPh})_3]_2\text{H}$  (44)